DESIGN AND DEVELOPMENT OF A PYROLYSIS PROBE FOR SHORT PATH THERMAL DESORPTION

by

HAO FAN

A Thesis submitted to the

Graduate School-New Brunswick

Rutgers, The State University of New Jersey

in partial fulfillment of the requirements

for the degree of

Master of Science

Graduate Program in Food Science

written under the direction of

Professor Thomas G. Hartman

and approved by

_____

_____

_____

New Brunswick, New Jersey

[May, 2010]

ABSTRACT OF THE THESIS

Design and Development of a Pyrolysis Probe for Short Path Thermal Desorption

By HAO FAN

Thesis Director:
Professor Thomas G. Hartman, Ph.D

Pyrolysis is the process of heating a substance to high temperature in the absence of oxygen so it does not burn but rather the thermal energy causes dissociation of chemical bonds. It has been widely employed as an analytical tool where it is combined with gas chromatography (GC) and its ancillary techniques (Mass Spectrometry, Fourier transform infrared spectroscopy, etc.). Analytical pyrolysis has been applied in a variety of areas such as microbial classification, protein identification, food packaging material identification, and forensics.

State of the art commercial pyrolysis instruments have intrinsic disadvantages that undermine widespread application. Most pyrolysis systems are dedicated attachments to a GC which preclude using the system for other injection techniques. Furthermore, commercial pyrolysis instruments are essentially probes inserted into the GC injector or are extensions to the GC injector. Pyrolysis releases high molecular weight, non-volatile residues into the GC injector which can foul the system and lead to sample to sample cross contamination problems.

The objective of this research is to design and develop a pyrolysis probe attachment for Short Path Thermal Desorption which would remedy the disadvantages of current

commercial systems. Specifically, the new pyrolysis probe should combine the features of Short Path Thermal Desorption, have a quick setup, not be prone to injector contamination, be easily moveable and transferable, accurate and precise.

A prototype has been built in our laboratory and subjected to mechanical and engineering tests. In the first demonstration of the new pyrolysis probe, virgin high density polyethylene (HDPE) was analyzed by pyrolysis-direct thermal desorption (DTD)-GC-MS. A very strong peak of ethylene (primary pyrolysis product) was evolved in the pyrogram followed by a homologous series of oligomers up to C_{40} thereby validating the instrument. Pyrolysis studies on other model polymers such as polystyrene (PS), ethylene vinyl alcohol (EVOH), ethylene vinyl acetate (EVA), and polyethylene terephthalate (PET) were also proved successful in revealing their monomers, oligomers, important decomposition products, and additives. The pyrolysis chamber and sample tube was very clean after each run and no cross contamination was detected between injections, proving the superiority of this novel pyrolysis system over existing commercial instruments.

ACKNOWLEDGEMENT

I would like first to extend my greatest thanks and regards to my advisor Dr. Thomas Hartman, for offering me the opportunity to work on this project. His extensive support and guidance makes this accomplishment possible.

I would like to specially thank Dr. Chi-Tang Ho and Dr. Henryk Daun for having consented to be a part of my defense committee. I also sincerely appreciate their valuable time and inputs.

I would like to thank the lab specialists Dr. Bin Khong Khoo and Joseph Lech for their guidance and assistance. I would like to mention my special appreciation to Dr. Bin Khong Khoo for having guided me thought the time I have worked in the Mass Spectrometry lab with his patience and eagerness to help students.

Finally I would like to thank my parents for their constant support and encouragements on my project that leads to this thesis. Their beliefs in me are the source of my determination and endeavor.

TABLE OF CONTENTS

LIST OF FIGURES

LIST OF TABLES

I. INTRODUCTION

Polymer characterization using pyrolysis analysis followed by gas chromatography (GC) is currently one of the most dynamic fields in applied analytical research (Liebman and Levy, 1984). Synthetic polymer chemists count on detailed microstructural analysis to improve material performance and efficiency while process control specialists need instrumental and computer aides to monitor product quality in large scale production. During researchers' efforts to tailor materials for today's sophisticated needs, gas chromatography and its ancillary techniques (MS, FTIR, *etc*.) have been extensively taken advantage of and are continually gaining popularity throughout the polymer industry (Liebman *et al.*, 1982).

However, the pace of pyrolysis instrumentation development failed to keep up with the ever growing sophistication of polymer investigation requirements, in that (1) most of the current pyrolyzers are dedicated attachments to GC injector thus difficult to move or transfer, and (2) high molecular weight and non-volatile residues released from pyrolysis tend to accumulate within injection port or GC interface and lead to sample to sample cross contamination. Therefore an advancement of pyrolysis instrumentation that can alleviate aforementioned problems is not only desirable but imperative.

Short Path Thermal Desorption system (SPTD, Hartman *et al.*, 1991) has successfully proved itself as an excellent technique for the analysis of volatile and semi-volatile organics which can be easily purged from various sample matrices. Setup of the system on GC is easy and sample to sample cross contamination does not exist due to changing sample tube from sample to sample. These features grant Short Path Thermal

Desorption system an amenable device for pyrolysates study and thereby a potential remedy for pyrolysis instrumentation.

The objective of this research is to first integrate a pyrolysis probe into Short Path Thermal Desorption system, which would be expected to eliminate the disadvantages of current commercial pyrolysis units, then to use model polymers to evaluate the performance of the new pyrolysis unit in analytical pyrolysis study.

II. LITERATURE REVIEW

A. Pyrolysis Introduction

1. General Information

Pyrolysis is the process of heating a substance to a high temperature (300-1000°C) in the absence of oxygen so it does not burn (oxidize) but rather the thermal energy directed towards the dissociation of chemical bonds. The word "pyrolysis" is coined from the Greek-derived element pyro "fire" and lysis "decomposition". Pyrolysis has been widely employed as an analytical tool for synthetic and natural polymers where it is combined with GC (PGC) and its hyphenated techniques such as GC-MS, GC-FTIR, GC-Flame Ionization Detector (GC-FID) to produce a chromatogram known as a "Pyrogram". A pyrogram is a very complicated but reproducible chromatogram that can be thought of as a "chemical fingerprint" of a substance under investigation.

Analytical pyrolysis has been applied in different areas within food science such as food born pathogen classification (Stern *et al.*, 1980), meat adulteration detection (Raghavan, 1985), packaging polymer material characterization (Liebman *et al.*, 1982), and food forensics (Steward *et al.*, 1974). Pyrolysis is often superior to traditional chemical decomposition methods for its convenience and rapidity in obtaining results (Liebman and Levy, 1984).

In most cases the subjects of pyrolysis are polymers, either biopolymers or synthetic resins. After thermal decomposition the most reasonable products are monomers plus low molecular oligomers of the polymer building blocks. The pyrolysis products of polystyrene are, not surprisingly, styrene monomer, dimer and trimer. However, more

complicated pyrolysis mechanisms also exist: random chain scission, depolymerization, cabonization, and side group reactions are the four dominating mechanisms that take place successively or concurrently in pyrolysis process (Liebman and Levy, 1984). Figure 1 listed some representative mechanisms for illustration.

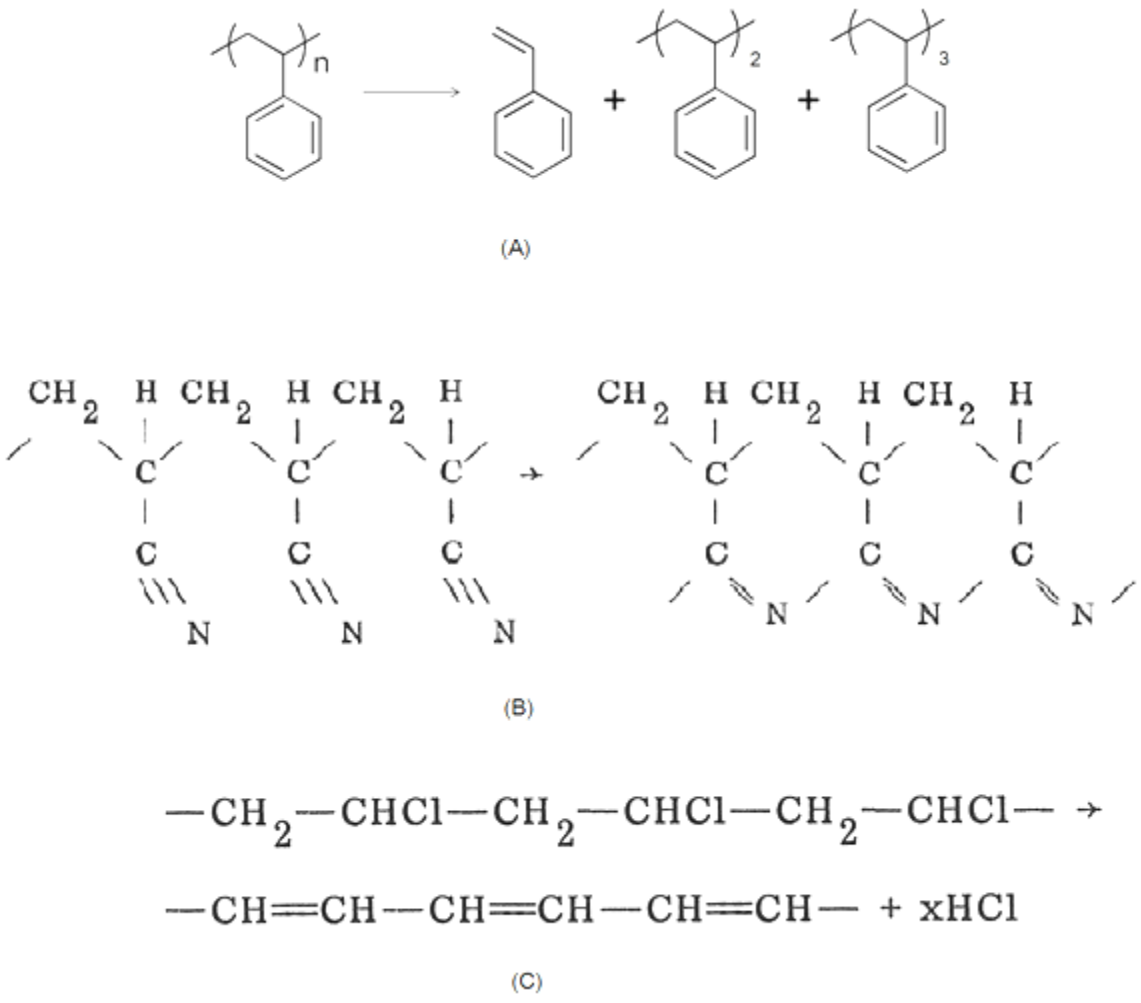

Figure 1. Pyrolysis mechanisms

(A) Polystyrene, chain cleavage (B) Polyacrylonitrile, side group cyclization (C) Polyvinyl chloride (PVC), side group elimination (Liebman and Levy, 1984)

2. Flash Pyrolysis and Programmed Pyrolysis

Pyrolysis can be divided in two major categories: pulse (flash) pyrolysis and programmed pyrolysis. Flash pyrolysis is usually completed within seconds by quickly heating a polymer under investigation to final temperature and is mostly carried out with the purpose of compositional study or trace additive identification. Programmed pyrolysis (also known as "time-resolved PGC"), on the other hand, could range from minutes to hours under a programmed temperature control (linear or multi-step) and allows for studies of detailed degradation mechanisms.

For instance Stern *et al.* in 1980 used analytical flash pyrolysis (detailed information provided in section II-C-1-3) of whole *Yersinia enterocolitica* bacteria for virulence prediction (Figure 2), computerized statistical analysis (SLDA, stepwise linear discriminate analysis) was involved in pyrogram interpretation. Ballisteri *et al.* in 1980 used programmed heating to investigate polyethylene-containing polymer under different atmosphere (helium or air) and revealed a remarkable difference in the pyrograms shown in Figure 3—the diene/monoene/*n*-alkane ratios sensitively reflected the thermal influence on the decay mechanisms for this polymer.

Current analytical pyrolysis research is primarily focused on polymer chemical structure, micro-structure details, as well as the qualitative and quantitative determination of residues, additives, and trace impurities. In order to obtain such comprehensive information, assistance from instrumentations which are versed in separation and identification with properly developed methodologies are required. GC, among those instrumentations, has already been proved for its capability in providing details in

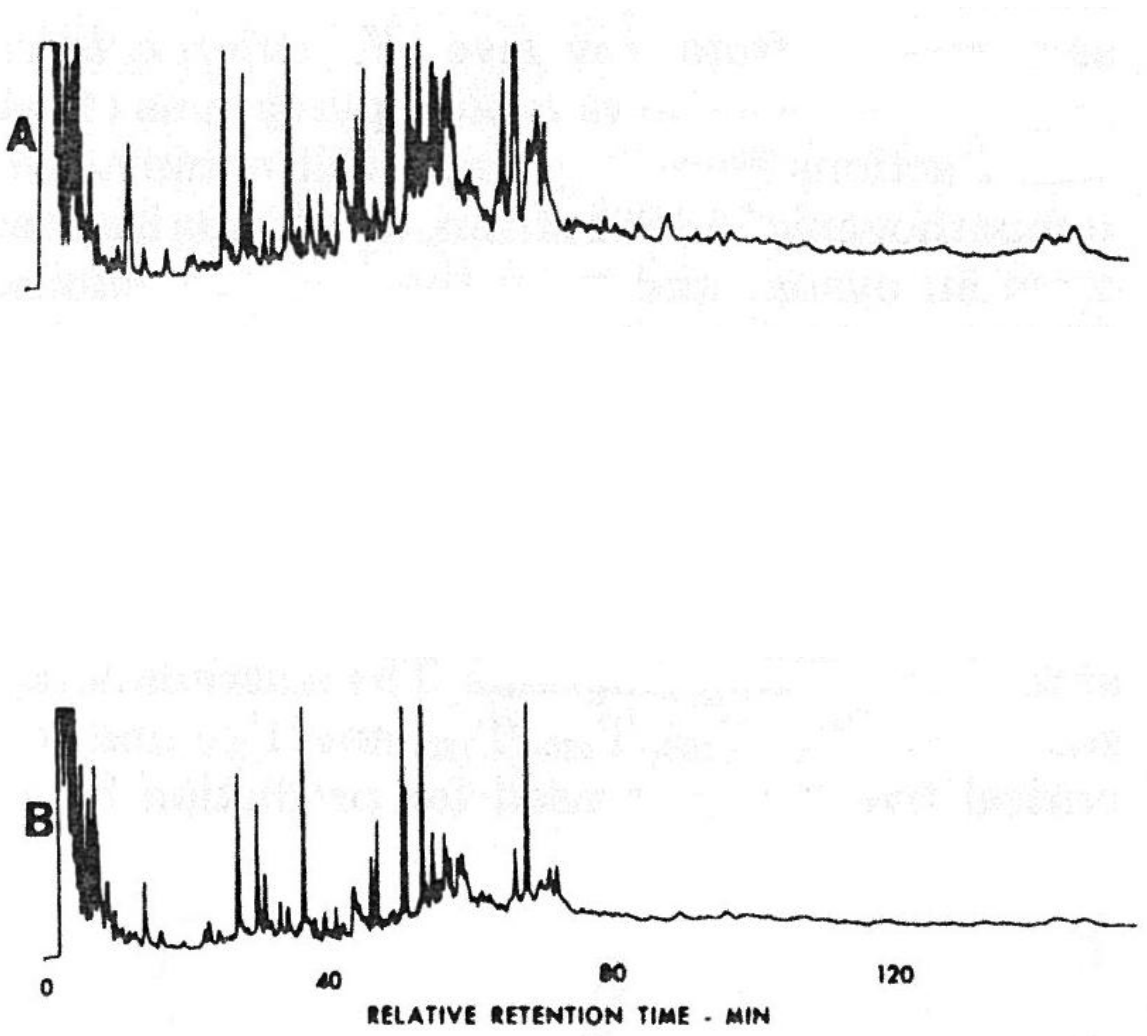

Figure 2. PGC pyrogram of *Yersinia enterocolitica* whole cell preparation

Flash pyrolysis at 900°C for 20 s via CDS Pyroprobe® 100. (A) HeLa cell noninvasive Y. *enterocolitica* strain 78 1994 (B) HeLa cell invasive *Y. enterocolitica* strain IP 161, interpretation and discrimination was done by stepwise linear discriminate analysis (Stern *et al.*, 1980)

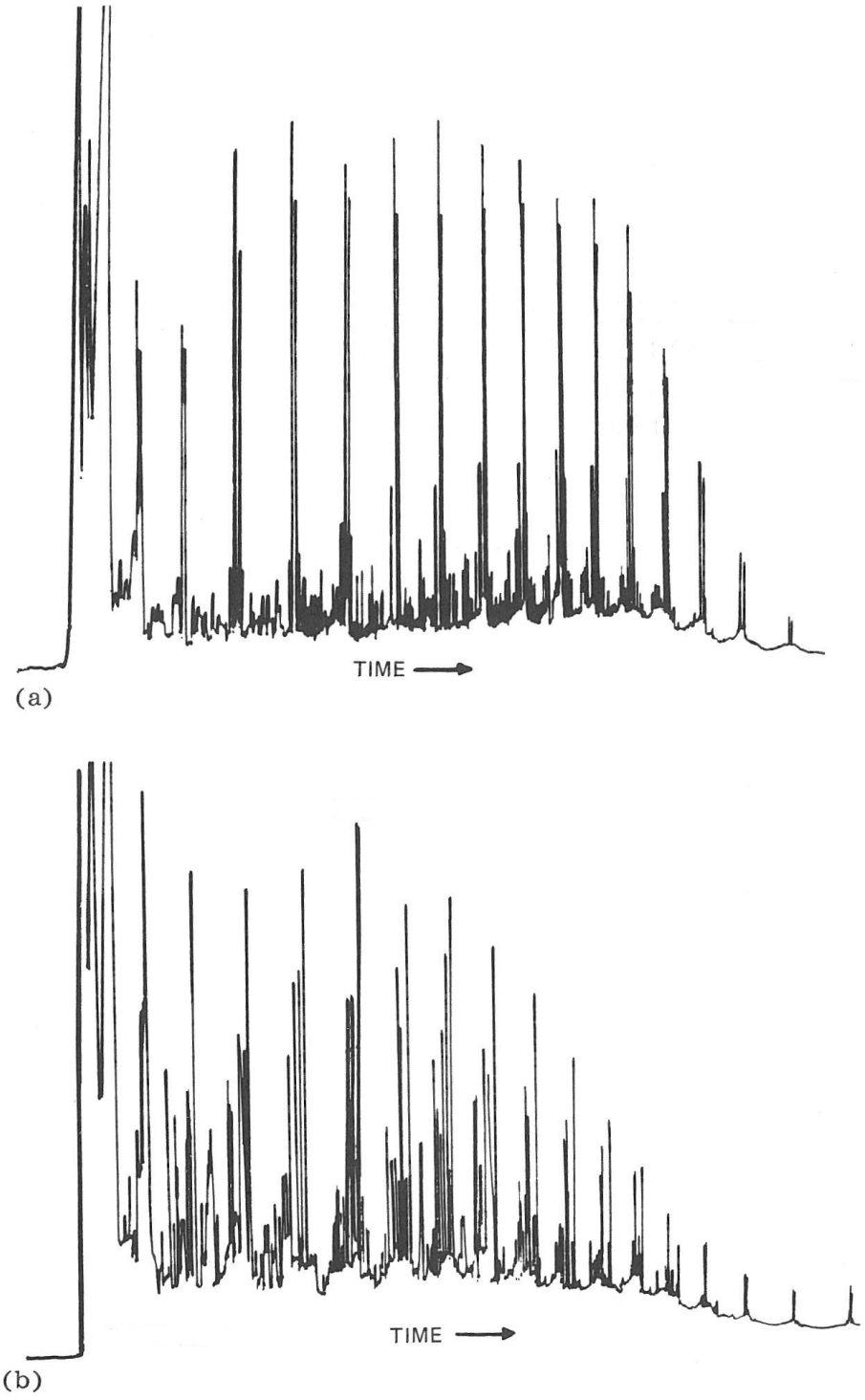

Figure 3. Ethylene-vinyl acetate copolymer pyrogram

Column: 60m x 0.25mm fused silica column chemically bonded DB-5. Column temperature control: 50°C, 2min, 5°C.min to 250°C, 2min. (a) Programmed 30°C/minute from 80°C to 650°C in helium (b) Same temperature program in air (Ballisteri *et al.*, 1980)

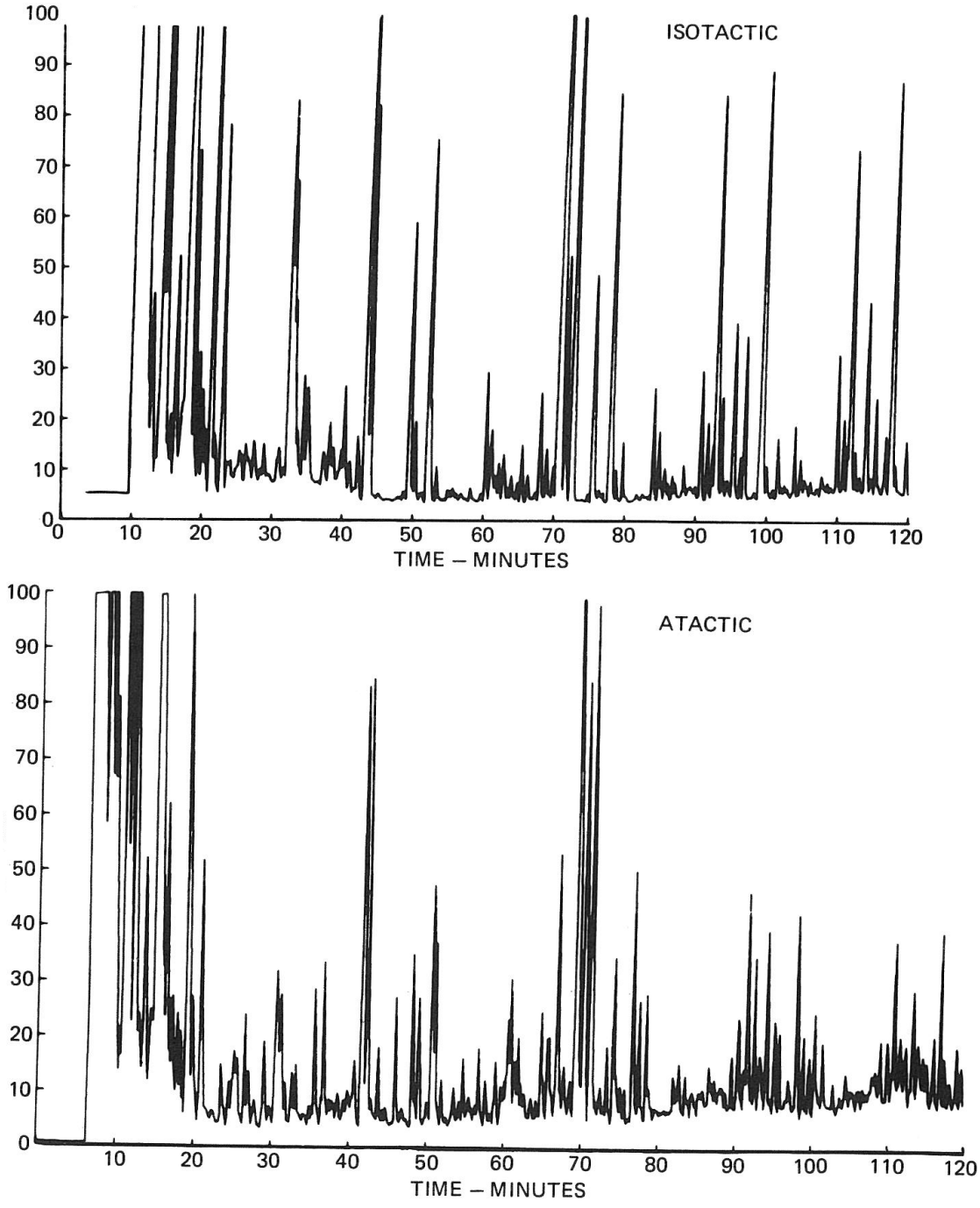

Figure 4. Comparison of isotactic and atatic polypropylene pyrogram

Flash pyrolysis at 750°C for 10 seconds. (Liebman and Levy, 1984)

composition, impurities, copolymer sequence and will permit understanding of polymers to predict, control, and optimize their applications. For example, pulse pyrolysis when combined with high-resolution capillary column GC-FID was able to generate distinguishable pyrograms (Figure 4, Liebman and Levy, 1984) for characterization of isotactic and atactic (different stereochemical structure arrangements of adjacent chiral centers within macromolecules) polypropylene (PP) samples.

B. Pyrolysis Instrumentation—Pyrolyzers

Pyrolysis gas chromatography (PGC), as evidenced by the increasing number of publications in the field, is a full-fledged analytical tool. It has been widely applicable to analysis of polymers, plastics, fibers, and many organic substances. Decades ago there were numerous types of pyrolyzers that were constructed in laboratories and lack of standardization. Nowadays most of the pyrolyzers in service are commercialized equipments that can be directly purchased from manufacturers like CDS (Chemical Data Systems, Inc.). The two most common designs are (1) resistively-heated devices, and (2) inductively-heated devices.

1. Resistively-Heated Pyrolyzers

1) General Information

Resistively-heated units were among the earliest pyrolyzers. The commercial advancement of a self-sensing pyrolyzer (CDS Pyroprobe®) made this type the most popular system in laboratories throughout the world (Figure 5, from CDS website). Its versatility and capability were demonstrated by the full range of experimental modes and samples: pulse pyrolysis (Stern *et al.*, 1980; Liebman and Levy, 1984) or programmed pyrolysis (Ballisteri *et al.*, 1980); varied atmospheres (inert and reductive) (Ballisteri *et al.*,

1980); powdered, semi-solid (Stern *et al.*, 1979) or liquid sample; and interfaced to required analytical systems (GC, MS, FTIR, *etc*.). Platinum filament (coil, Figure 6) or ribbon is chosen for its high melting point (1768°C) and inertness, but the potential catalytic effects of Pt under pyrolysis temperature must be accounted for (Anderson *et al.*, 1980).

Though through decades the CDS Pyroprobe® has evolved from Model 100 to the state of the art Model 5000, the basic configuration of the units remain unchanged: control module, pyrolysis probe, and GC interface. On the probe a quartz tube is used to hold solid polymer sample and heated from the Pt coil surrounding it. Typical loading amount of 50μg is recommended. The Pyroprobe® is provided with an interface that serves as an extension to the GC injection port. On the control module the rate of temperature rise (ramp control), the final pyrolysis temperature and the pyrolysis interval (total duration of heating time including ramp time) can be readily changed to accommodate pyrolysis study of a wide variety of substances. All models have linear rates of 20, 10, 5, 2, 1, 0.5, 0.2 and 0.1°C/msec (typically used for programmed pyrolysis) and an "off" ramp which gives a non-linear but reproducible rate at least 75°C/msec (typically used for pulse pyrolysis). Selectable time intervals are 20, 50, 100, 200 and 500 msec and 1, 2, 5, 10, and 20 sec. A general guide for PGC method development is shown in Figure 7 from a CDS manual, the best method selected should be practical in use and conform to the nature of the information needed from the experiment.

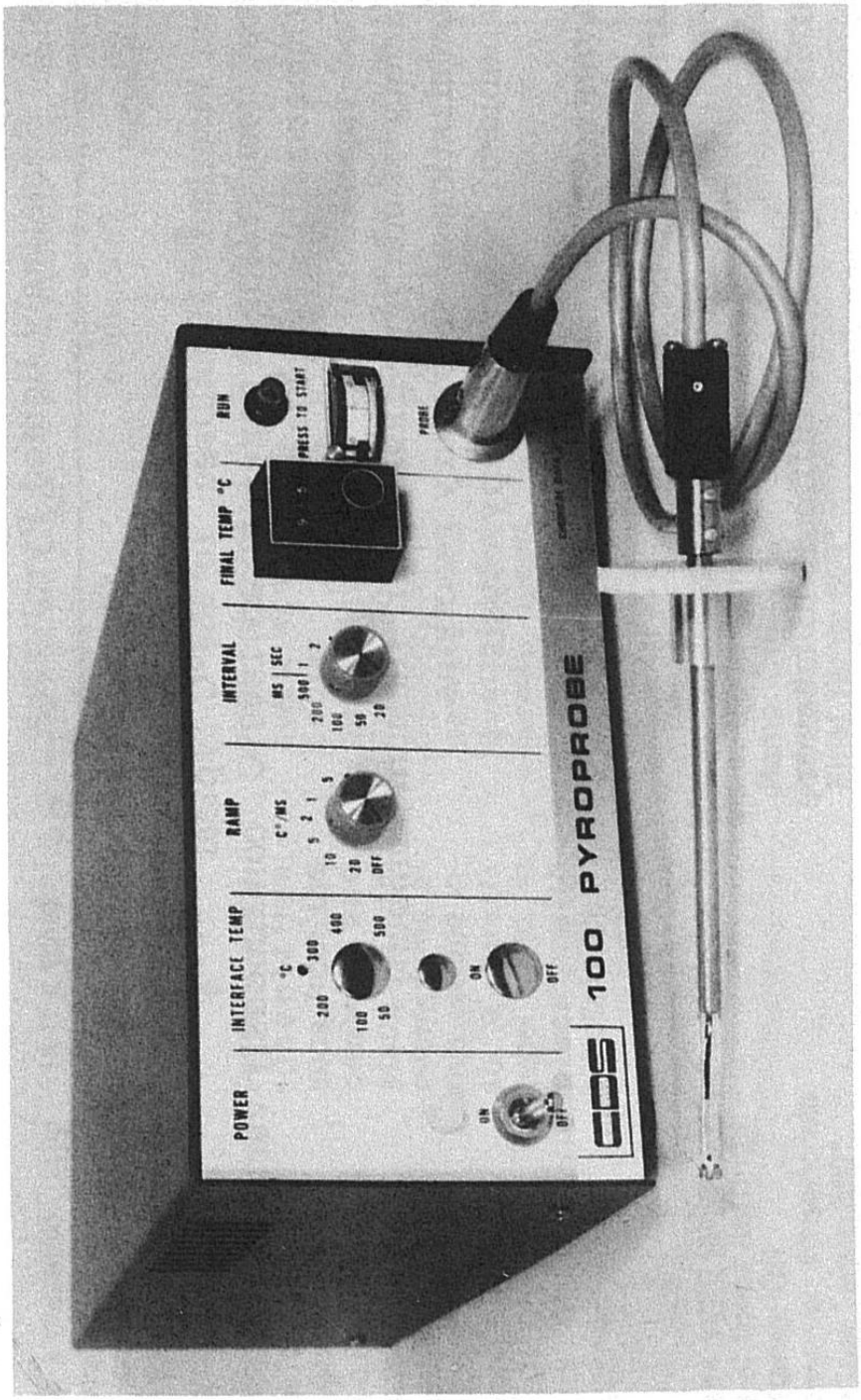

Figure 5. Control Module and Probe of CDS Model 100 Pyroprobe® (from CDS website)

Figure 6. Platinum coil on CDS Pyroprobe® 100

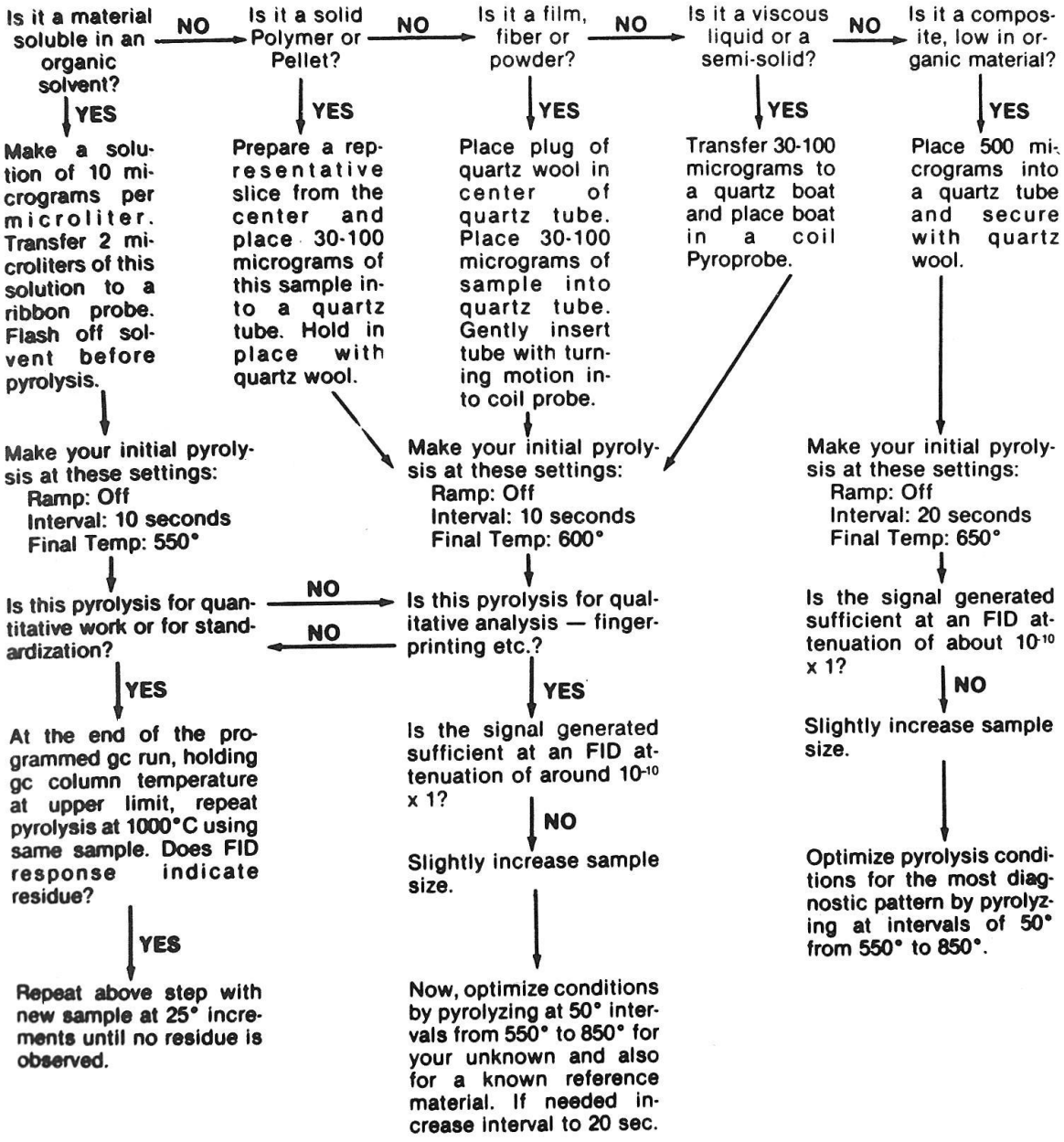

Figure 7. Guide for PGC method development (from CDS Pyroprobe® 100 manual)

2) Theory of Operation

The platinum element on Pyroprobe® serves simultaneously as a heater and sensor. The use of feedback makes the system independent of line voltage and ambient temperature. Figure 8 showed the basic Wheatstone bridge circuit used for control. The bridge output (V_1-V_2) goes to zero when $\frac{R1}{R2+R3} = \frac{R4}{R5}$. R_1 is the pyrolysis element (coil) and has a cold resistance of approximately 0.25 ohms. Potentiometer R_3 is set proportional to this cold resistance. Resistor R_4 is approximately 0.1 ohms with a low temperature coefficient. Potentiometer R_2 is the final temperature control and potentiometer R_5 is used

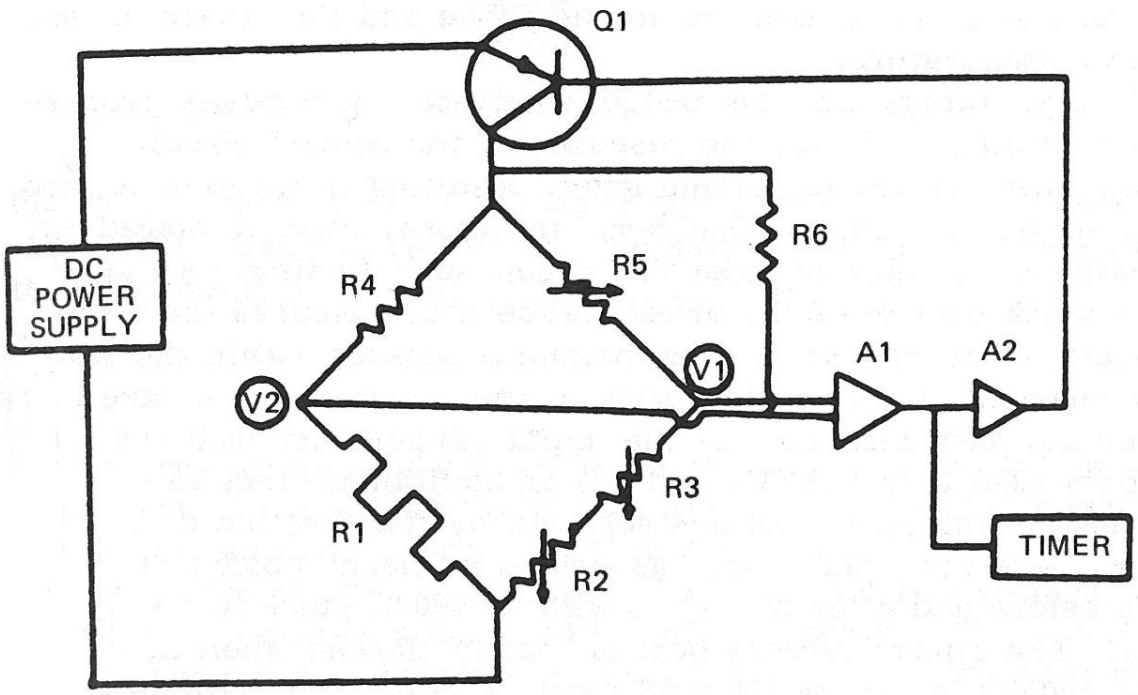

Figure 8. Basic schematic for CDS Pyroprobe® 100 control circuit (from CDS Pyroprobe® 100 manual)

to calibrate R_2. The operational amplifier (A_1) and the power amplifier (A_2) supply base current to the power transistor (Q_1) to provide current to the entire bridge. The timer can block the base current to Q_1 to control the starting time and then length of time at the final temperature. The response of the control circuit diminishes with the bridge voltage level, resulting in inaction at zero volts (description cited from CDS Pyroprobe® 100 manual).

When submitting a pyrolysis command, the run switch is depressed, starting the timer, and allowing the biased operational amplifier to provide base current to the power transistor Q_1. Q_1 becomes conducting and the full voltage of the power supply loads across the bridge. Passing high current through the element (R_1), heating it rapidly. As the temperature of R_1 increase, its resistance increases, and the bridge approaches balance. The operational amplifier then lowers the base current to Q_1 which lowers the bridge current. As the set temperature is approached, Q_1 controls the current to maintain the element temperature. At the end of the time interval, the timer cuts off the base current to Q_1 and thus shuts down the circuit (description cited from CDS Pyroprobe® 100 manual).

One of the major advancement in Pyroprobe® history is the incorporation of microprocessor and computerization. Now the Model 5000 Pyroprobe® (Figure 9), with the aid of microprocessor, features precision, reproducibility, ease of operation and allows graphic user interface software, multiple ramp and interval combinations that are comprehensive enough to satisfy the most sophisticated pyrolysis studies.

Figure 9. CDS Pyroprobe® 5000 (from CDS website)

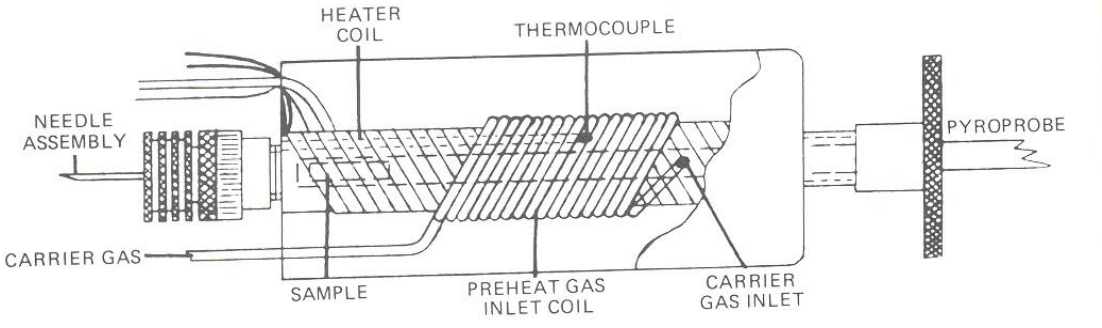

Figure 10. GC interface in CDS Pyroprobe® 100 (Liebman and Levy, 1984)

3) Disadvantages

Like all other instrumentations, the Pyroprobe® pyrolyzers have intrinsic disadvantages that undermine their widespread application.

- Dedicated to GC injection port, need screws and bolts to keep in position and difficult to unload.
- High boiling point oligomers and non-volatiles tend to accumulate within interface, causing carry over from previous run or sample to sample cross contamination (Figure 10).
- Large dead volume within interface, causing sample lose and compromising sensitivity and peak shape.

Overall, resistively-heated pyrolyzers appear to be the simplest, most versatile, and least costly systems for pyrolysis study. The availability of such a full range of capabilities from the simple pulse mode to the advanced microprocessor-based multimode systems would indicate a promising future for these pyrolyzers. But in the meantime, the aforementioned drawbacks is intimidating researchers from adopting it and should be eliminated to accommodate the more detailed and sophisticated studies nowadays.

2. Inductively-Heated Pyrolyzers

1) General Information

Inductively-heated pyrolyzers depend on a unique property of certain metals known as ferromagnetism. Ferromagnetic metals and alloys absorb radio frequency energy under an electromagnetic field and heat up rapidly. Energy absorption stops at a fixed temperature for each material (Curie point) and the temperature stabilizes (Liebman and

Levy, 1984) (Table 1, Walker *et al.*, 1972). The final temperature and heating time can be affected by a list of factors such as wire alloy composition, RF-generating power oscillator, the position of the wire in the high frequency coil, mass and diameter of wire (Liebman and Levy, 1984).

Table 1 Comparison of Curie point temperatures from different alloys (Walker *et al.*, 1972)

Temperatures(°C)	Composition		
	%Fe	%Ni	%Co
360	0	100	0
480	52	48	0
600	42	42	0
700	33	33	33
770	100	0	0
980	0	60	40
1130	0	0	100

The common RF oscillators operate at 400 to 600 KHz and have power outputs range from 100 to 1500 watts. Final temperature can range from 300 to 1100°C depending on the alloy composition of the wire element and temperature rise times are between 10 to 100 msec (Liebman and Levy, 1984). Curie point pyrolyzer units are commercially available from manufacturers like Fischer, Japan Analytical Industry Co. Ltd., and Pye Unicam Ltd. from England (Figure 11, Berezkin *et al.*, 1977).

Curie point pyrolyzers, when coupled with other analytical instruments like GC-MS, have found their applications in rubber analysis and biomolecular field (Liebman and Levy, 1984).

2) Advantages and Disadvantages

The most striking advantage of Curie point pyrolyzers is their extremely rapid temperature rise rates. The heating time is usually a few tenth of a second to a second or even shorter. The alloys are inexpensive enough so that several wires may be used for different temperature desired. However, disadvantages that limit its application are noticeable: too many conditions that might compromise reproducibility such as wire alloys, RF generators, and wire positions in RF coil. Additionally, the catalytic effect concern is much greater with Curie point wires consisting of iron, nickel, and cobalt which are not as inert as platinum from resistively-heated pyrolyzers. Lastly but most importantly, Curie point pyrolyzers cannot yield continuously variable temperatures as the resistively-heated pyrolyzers do. Final temperatures are almost predetermined by the natures and compositions of ferromagnetic alloys present in the element and thus discrete, which preclude many potential applications of these units.

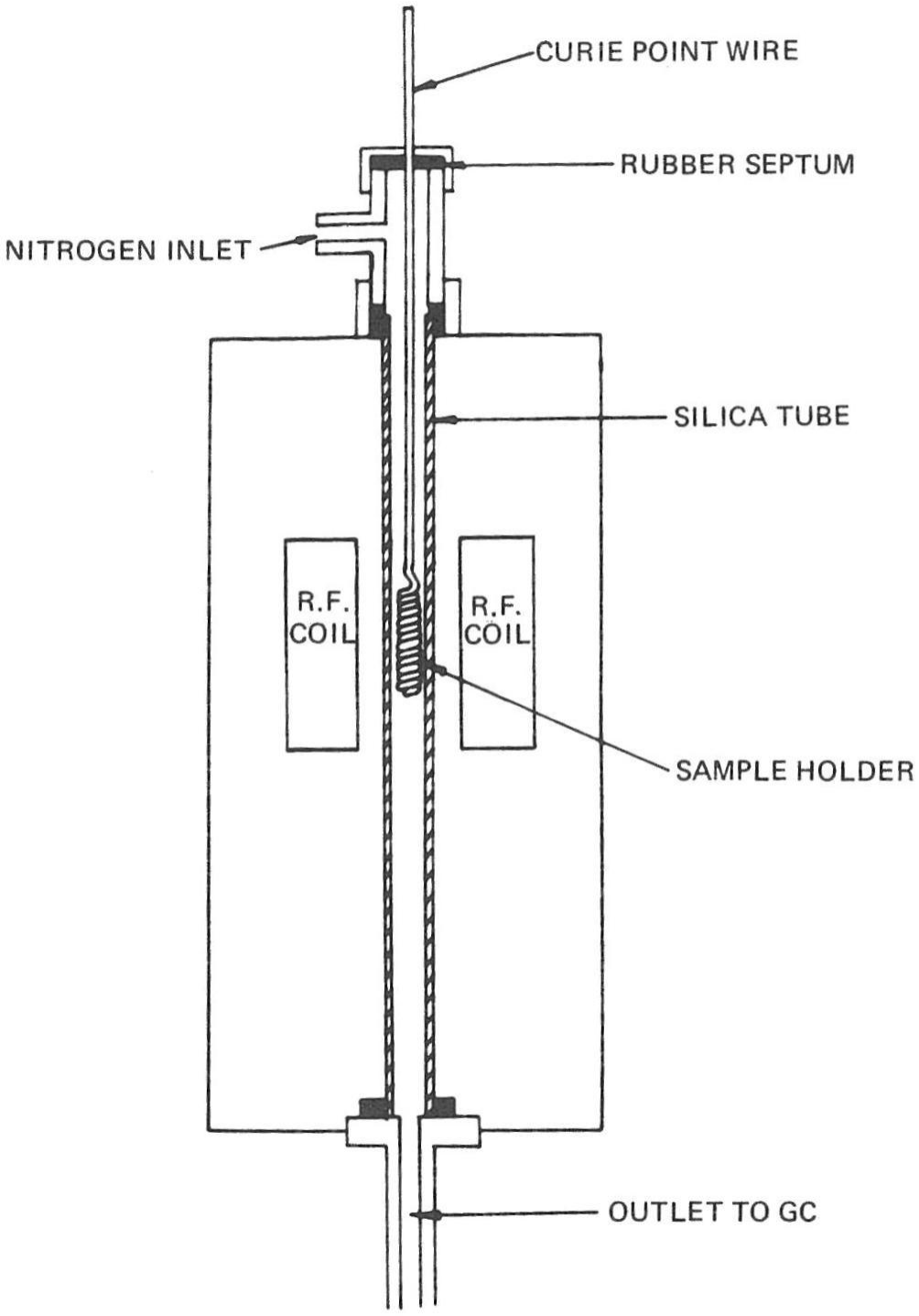

Figure 11. Cross section view of a typical Curie point pyrolyzer (Berezkin *et al.*, 1977)

Other types of commercialized pyrolyzers including radiative-heating pyrolyzer (Hanson *et al.*, 1977) and microfurnaces (Wolf *et al.*, 1972) can be found from manufacturers but will not be discussed here for their limited capabilities and applications.

C. Pyrolysis Applications

1. Analysis of Biopolymers

A significant application of analytical pyrolysis is in the analysis of biopolymers. Biological materials, such as proteins, enzymes, carbohydrates, and microorganisms, are often intractable, thermally labile, and non-volatile. Analytical pyrolysis is perfectly suited for their studies because of its ability to thermally decompose these complex polymers into volatile molecules that can be analyzed on GC. Other conventional chemical biopolymer analysis methods such as hydrolysis and derivatization are usually tedious and time consuming. The direct coupling of analytical pyrolysis to GC allows for rapid volatilization, separation, and detection of characteristic fragments from important biopolymers (Liebman and Levy, 1984).

1) Amino Acids and Peptides

The pyrolysis of amino acids has been extensively studied because of their building block nature for a large variety of peptides, proteins, and enzymes. One of the pioneering studies in this field was from Vollmin, *et al.* (1966), who published the Curie point pyrograms of 17 different amino acids (Figure 12). Another representative study that made one step further is from Merritt and Robertson (1967), who analyzed a different set of 17 amino acids by PGC-MS and indicated in Table 2 that for every amino acid a single

pyrolysate could be found that was either unique to that amino acid or that constituted the major product among those identified.

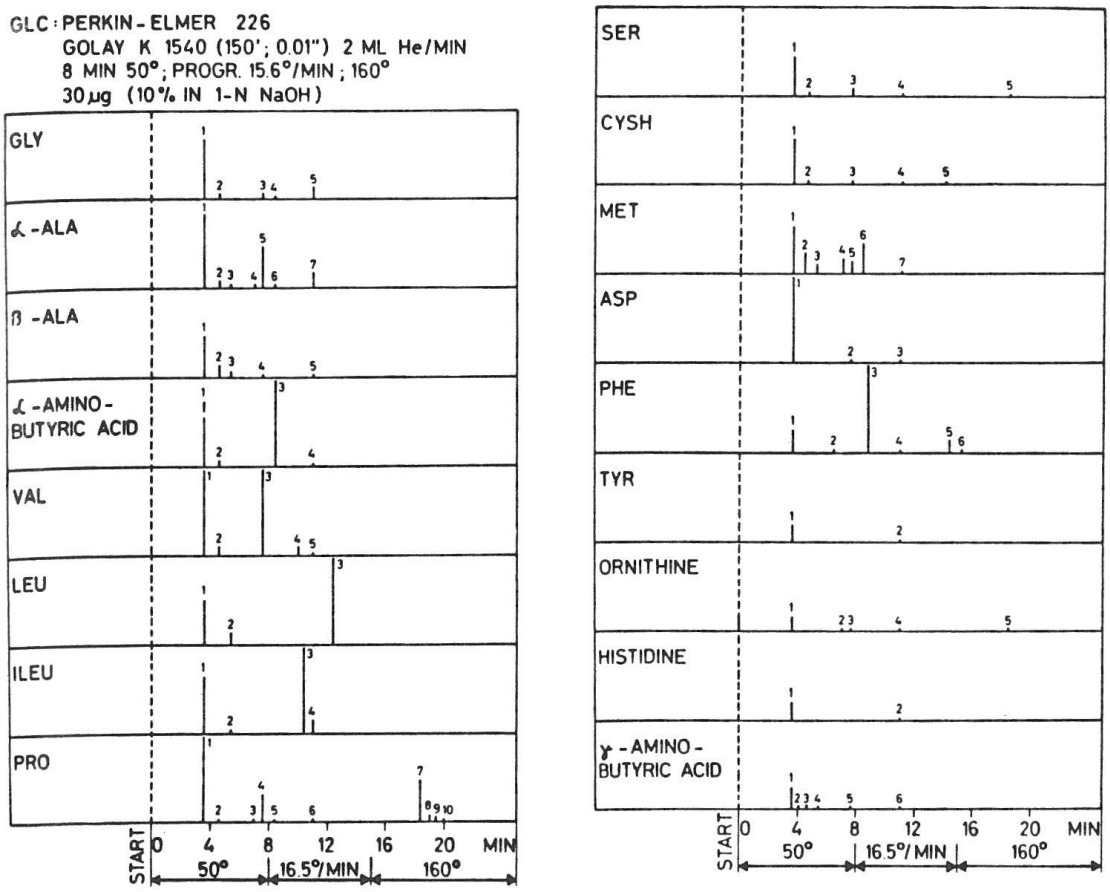

Figure 12. Curie point pyrogram for 17 amino acids

Numbers on the bar graph were peak notations for each amino acid, did not indicate specific pyrolysate. It was possible to identify most of these amino acids by their PGC patterns (except for histidine and tyrosine) (Vollmin, *et al.*, 1966)

Table 2. Unique pyrolysis products from several amino acids (Merritt *et al.*, 1967)

Amino acids	Unique pyrolysis product
Alanine	Acetaldehyde
Beta-alanine	Acetic acid
Cystine	Methyl thiophene
Glycine	Acetone
Hydroxyproline	N-methyl pyrrole
Isoleucine	2-Methyl butanal
Leucine	3-Methyl butanal
Methionine	Methyl propyl sulfide
Norvaline	N-butanal
Phenylalanine	Benzene
Proline	Pyrrole
Serine	Pyrazine
Taurine	Thiopene
Threonine	2-Ethylethyleneimine
Tyrosine	Toluene
Tryptophan	Ammonia, carbon dioxide
Valine	2-methyl propanal

When it comes to peptide pyrolysis studies are not as extensive as in amino acids due to the increased complexity of the biomolecules. Two competing proposals coexist: (1) the pyrolysis of peptides gives pyrogram that are essentially linear combinations of the pyrograms of the constituent amino acids (Simon *et al.*, 1965); and (2) the pyrolysis products of peptides are determined by the amino acid linkage or sequence (Smith *et al.*, 1980). Most of the data tends to support the latter hypothesis and one representative evidence was from the work of Merritt and Robertson (1967), in which dipeptides Gly-Ala and Ala-Gly were pyrolyzed. The Ala-Gly dipeptide produced acetone, acetaldehyde, and ammonia as major pyrolysates whereas Gly-Ala yielded primarily ammonia and 2-methylpyrrole. Furthermore, it was found that the products could be altered by the pH values of solutions under pyrolysis.

2) Proteins

Proteins are naturally occurring polypeptides of high molecular weight that folded into a globular form. It is not very surprising that the relationship between amino acid subunit structure and the resulting pyrogram has not been fully established due to the complexity of proteins. Current studies on protein pyrolysis can be loosely divided into three categories: (1) differentiation of one protein from another, (2) qualitative identification of the presence of protein in a sample matrix, and (3) analysis of the amino acid content of a protein to identify it or to establish the presence of particular residue(s) (Liebman and Levy, 1984). Studies so far have not achieved much beyond the analysis of primary amino acid sequence, let along the elucidation of conformation or three-dimensional structure, which appears unreachable via analytical pyrolysis approach.

PGC of hemoglobins has been studied by a number of investigators. In 1976 Bayer successfully differentiated adult (Hgb A) and fetal (Hgb F) hemoglobins by pyrolysis at 900°C, followed by programmed temperature GC separation of the pyrolysates on a Carbowax® 20M-TPA packed column. Both Hgb A and Hgb F have 572 amino acids but their sequences differ slightly. From Figure 13 one can notice the differences of a shoulder on an early eluting peak and subtle differences in the relative peak heights of the last three eluting peaks. The reproducible differences of the circled area permitted correct identification of Hgb samples.

Another case is the application of PGC to fingerprint the presence of foreign protein in a food matrix. Raghavan, S.K. in 1985 utilized PGC-MS to differentiate muscle protein from lung, spleen, and soy protein which can possibly be used as adulteration. In this case the meat matrix was far more complicated than the 572-amino acid hemoglobins, thus resulting pyrograms were interpreted by, rather than human effort, computerized statistical program for pattern recognition. Quantification work was also carried out through estimation of the amount of a component present in a mixture based on the peak intensity of selected unique compounds.

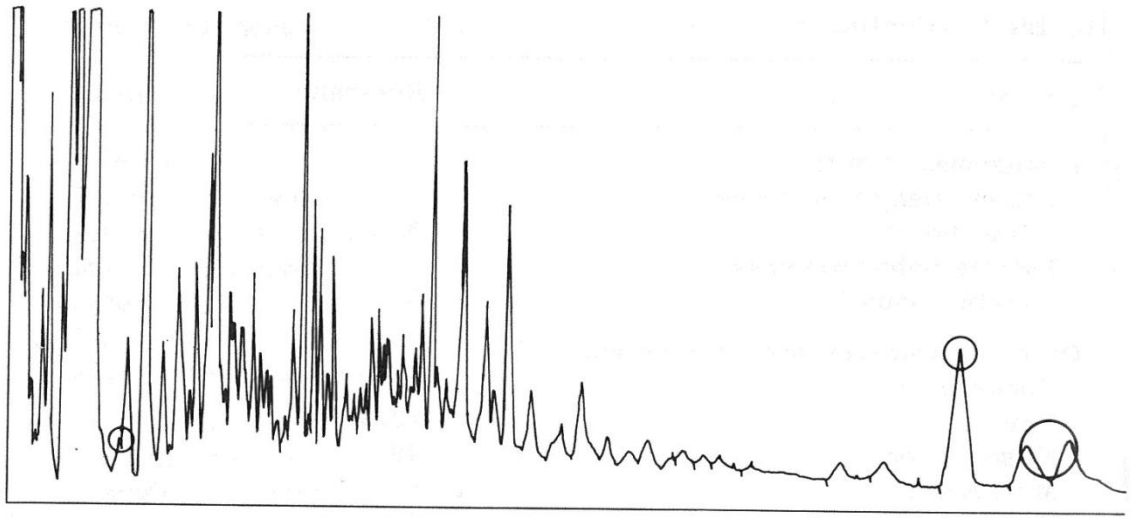

(A)

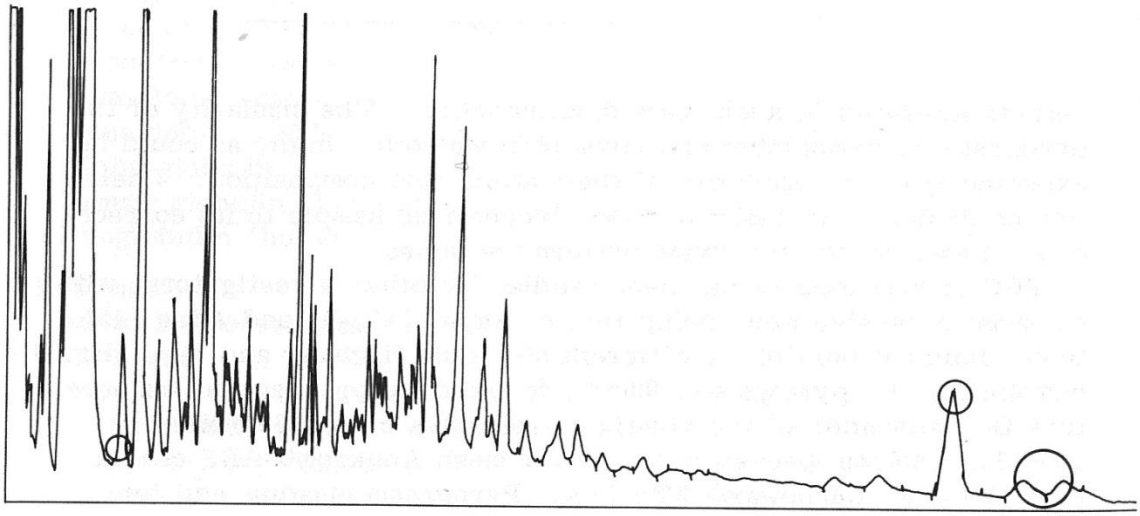

(B)

Figure 13. PGC pyrogram in Hemoglobin identification

(A) fetal (Hgb F) hemoglobin (B) normal adult (Hgb A) hemoglobin (Bayer, 1976)

3) Microorganisms

Conventional taxonomic characterization techniques are through extensive biochemical, serological, and antigenic processes that are often tedious and time-consuming. Some of these techniques require subjective interpretation and may not provide direct chemical structure information (Liebman and Levy, 1984). In response to the craving for objective and reliable diagnostic procedures, analytical pyrolysis has been applied in microorganism classification and identification. Analytical pyrolysis avoided extensive culturing procedure because of its microscale sample requirement and the time needed for pyrolysis GC is usually within an hour or even shorter.

N.J. Stern in 1980 applied PGC in virulence prediction of *Yersinia enterocolitica* (HeLa cell-invasive and noninvasive strains). Whole cell preparation and cell wall fraction were pyrolyzed by CDS Pyroprobe® 100 unit at 900°C for 20s in a continuous stream of helium carrier gas, followed by programmed temperature GC separation of the pyrolysates on a high-resolution Carbowax® coated capillary column. The resulting pyrograms were subjected to stepwise linear discriminant analysis (SLDA) aided by statistical technique termed three nearest-neighbor discriminate analysis (3-NNDA) (Figure 2). The results showed good correlation in prediction of the HeLa cell virulence from invasivity test.

2. Microstructural Study of Synthetic Polymer

Analytical pyrolysis has achieved broad recognition for polymer identification and characterization, particularly in the area of synthetic polymer structure determination. PGC has been applied to the determination of polymer microstructure with considerable success since its inception. The capacity to obtain reproducible pyrograms, coupled with the ability

to separate and identify the peaks resulting from the degradation of a synthetic polymer offers us good opportunity for a thorough understanding of the polymers microstructure.

The pyrolysis of PE proceeds by a radical chain cleavage followed by intramolecular hydrogen abstraction reactions (Wall *et al.*, 1954) to yield a series of hydrocarbon triplets (the α, ω-diolefin, the α-olefin and the corresponding n-alkane). Figure 14 showed the pyrograms of HDPE with and without hydrogenation. Detailed thermal decomposition mechanism for HDPE and other polymers will be discussed in details in result and discussion section V.

3. Forensic Study

Pyrolysis is a powerful analytical tool in forensic cases for its ability to separate and characterize pyrolysates. The combination of pyrolysis and GC is a powerful and sensitive analytical method for discriminating materials belonging to the same group or class (Liebman and Levy, 1984). PGC has become an indispensable tool for the identification and comparison of paints, fibers, plastics, and other polymeric evidences.

Stewart in 1974 successfully employed PGC to distinguish many 1973 model automotive finishes. Using a combination column he successfully associated a variety of acrylic enamel finishes with paint suppliers. Figure 15 showed three pyrograms of blue automotive finishes used by three different manufacturers. All the three finishes can be distinguished both by peak intensity and peak location. Such study would provide valuable information in tracking suspect vehicles in hit and run crime cases.

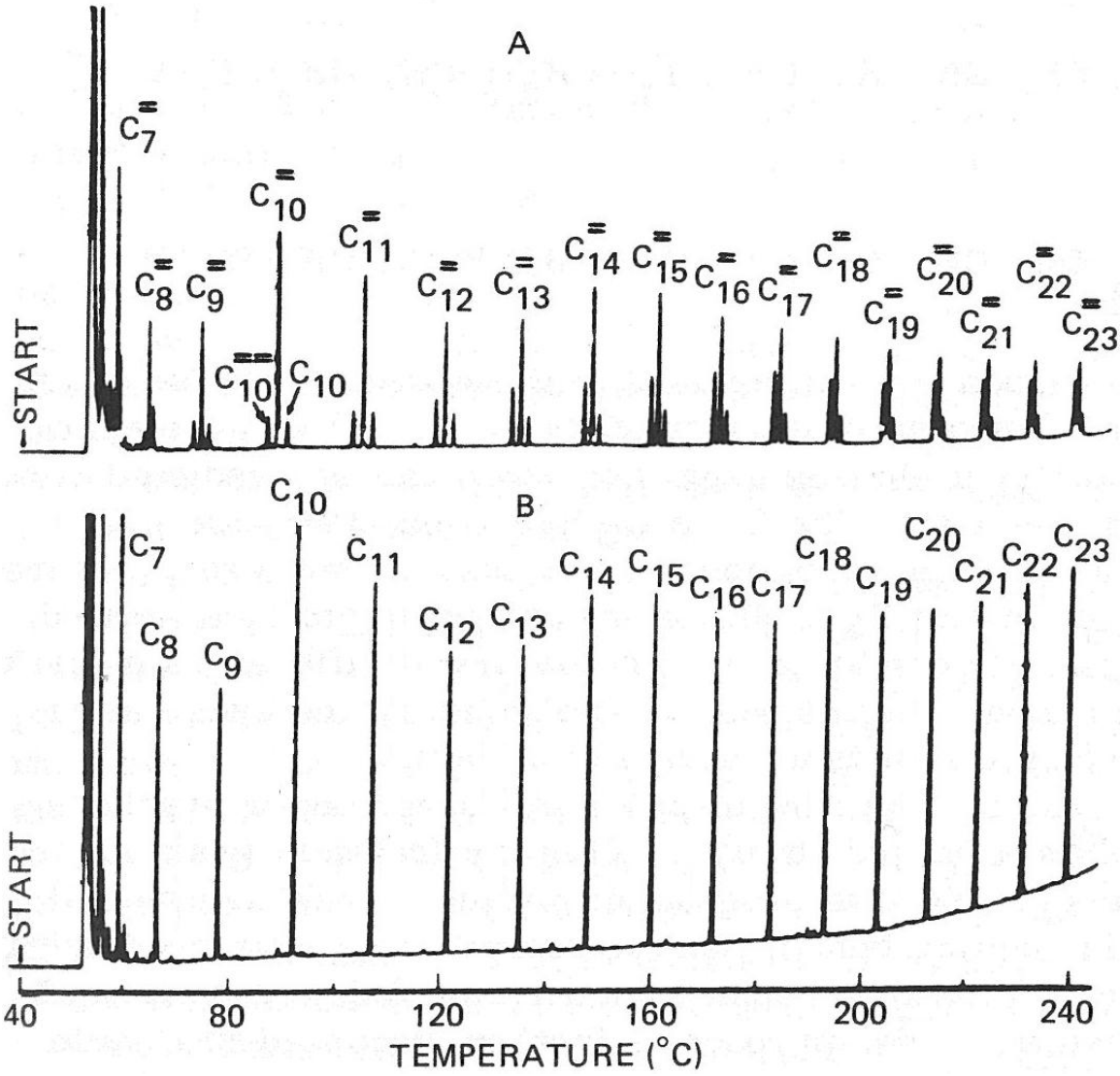

Figure 14. High-resolution pyrograms of HDPE before and after hydrogenation

(A) without hydrogenation (C10:n-alkane; =C10:α-olefin; ==C10:α, ω-diolefin) and (B) after hydrogenation (only n-alkanes) (Sugimura *et al.*, 1979)

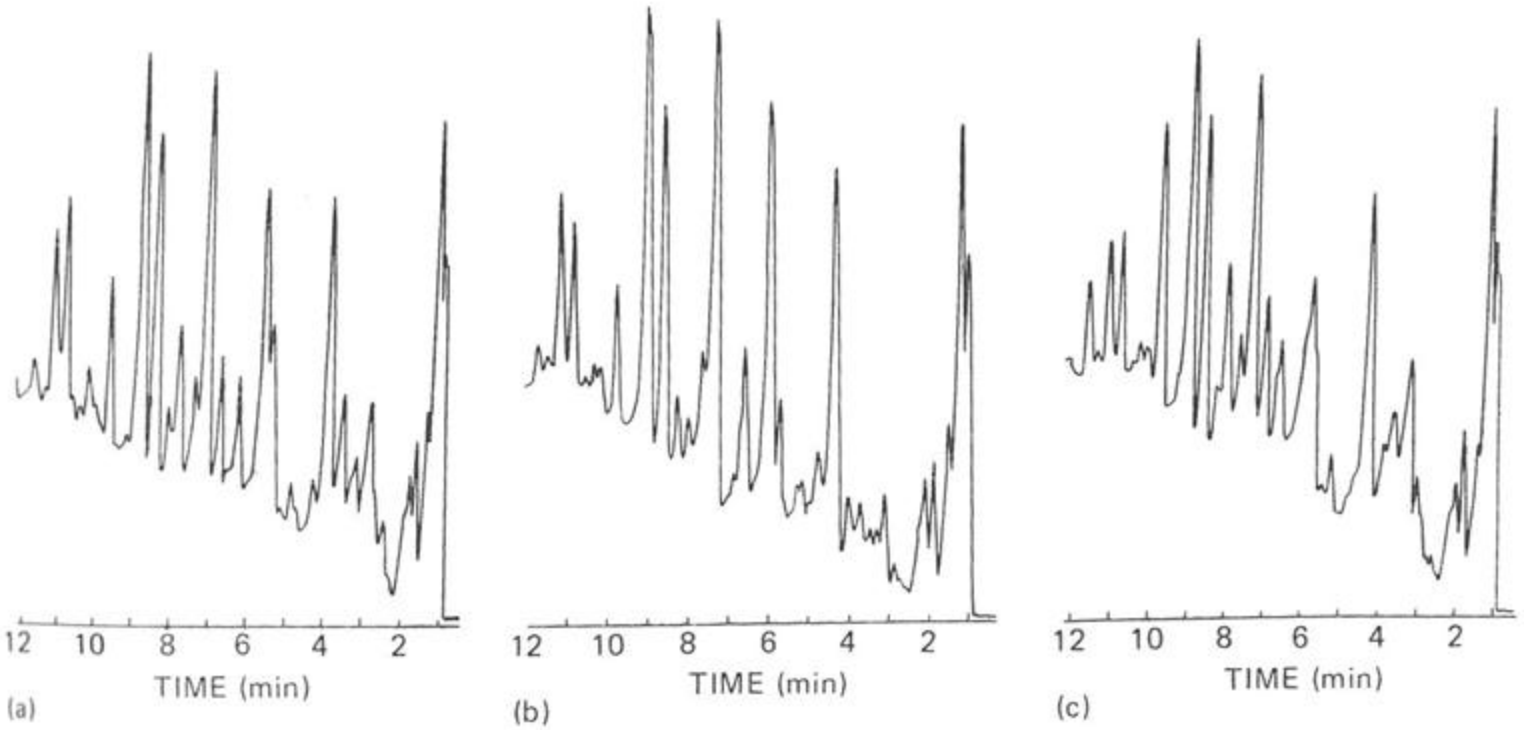

Figure 15. Comparison of similar blue metallic dispersion-type finishes

combination column comprised of 3m x 3mm, 15% Carbowax® 20M column and 1m x 3mm, 10% PC-200 column
(a) Ford Motor Company, (b) Chrysler Corp., (c) American Motors Corp. (Steward *et al.*, 1974)

D. Short Path Thermal Desorption

1. General Information

The technique of Short Path Thermal Desorption has been developed to permit the analysis of organic compounds present in air or compounds which can be easily purged from solid and liquid matrices. Samples such as volatile organics in air, flavors and fragrances in foods and cosmetics, manufacturing chemical residues in pharmaceuticals, volatiles in packaging materials and building products, and aromatic residues in forensic arson samples are just a few of the applications to which this technique has been adapted. It has been commercialized by SIS (Scientific Instrument Services, Inc.) in 1991.

The Short Path Thermal Desorption system consists of two modules: an electronic control unit and the desorption unit. The desorption unit is placed directly on top of the injection port of most GC's, where it is utilized for the direct desorption of samples into the GC injection port and column (Figure 16). Figure 17 and 18 provided us closer look and more detailed information. The air powered autoinjector permits the user to inject desorption tube with needle attached into GC injection port. Carrier gas (usually helium) flows through desorption tube and needle continuously when activated and is regulated by a flow controller valve mounted on the top of the desorption unit. The flow can be monitored by either a two ball rotameter mounted on the right side (between 1 and 120ml/min depending on the split/splitless method applied) or a pressure gauge mounted on the left side (between 0 and 60 psi). The front viewport permits the easy viewing of injection port and desorption tube when injected and also provides for cooling of the aluminum heater blocks.

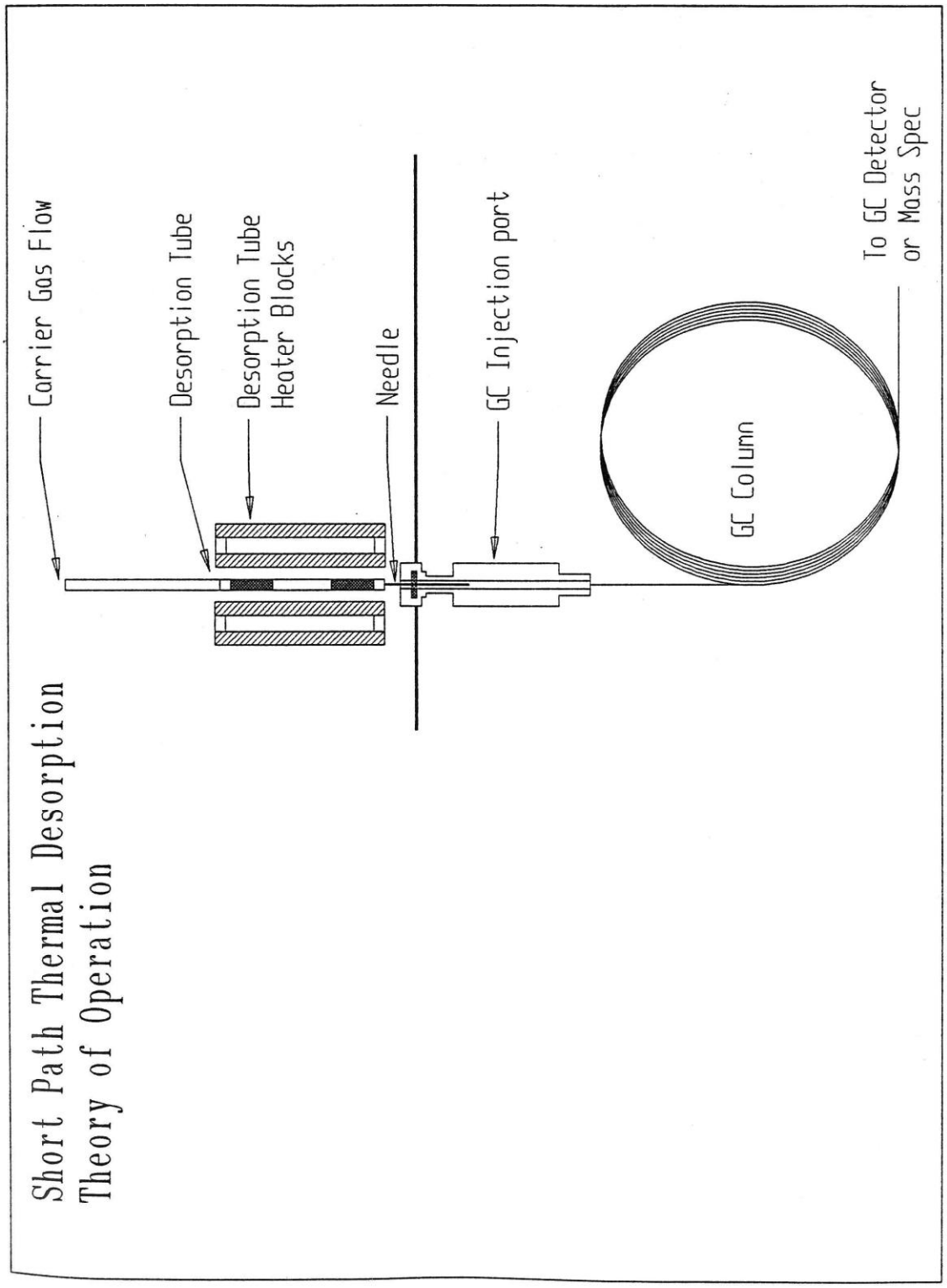

Figure 16. Short Path Thermal Desorption Theory of Operation (from SIS manual)

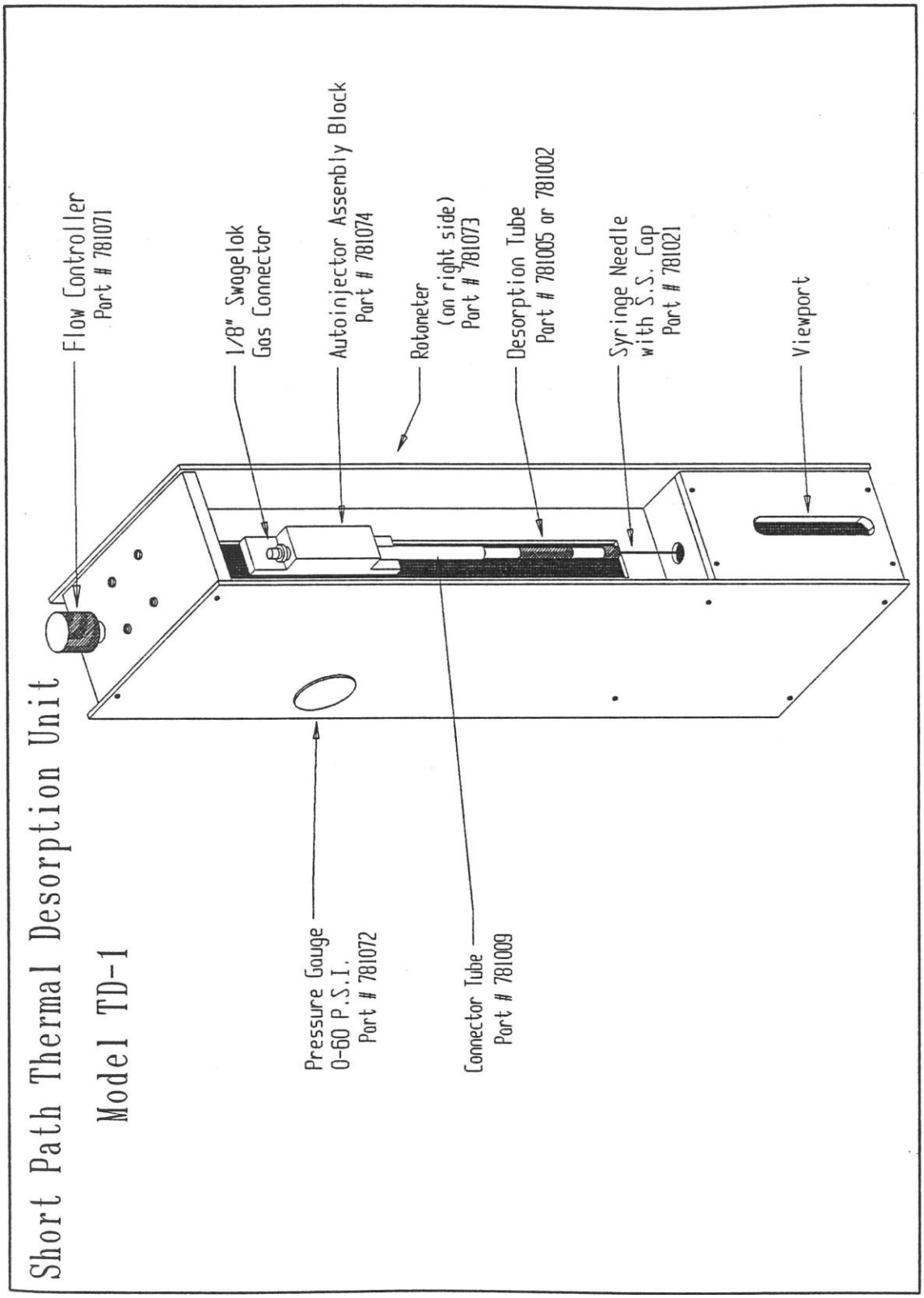

Figure 17. Short Path Thermal Desorption unit (from SIS manual)

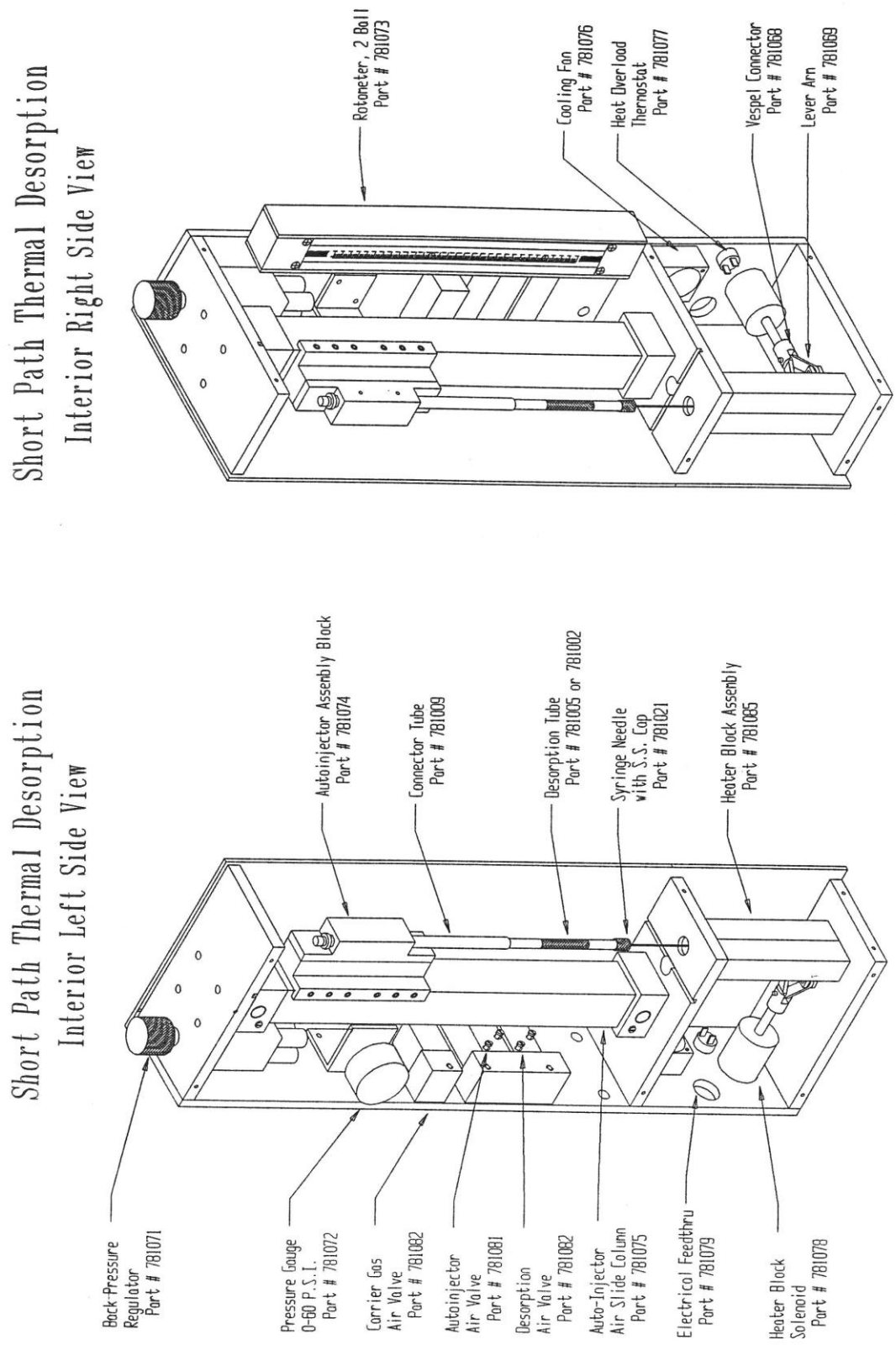

Figure 18. Short Path Thermal Desorption interior view (from SIS manual)

2. Theory of Operation

The drawing in Figure 19 showed a desorption unit with peripheral plates removed to provide a visual representation of the operation procedure. Samples to be analyzed are collected inside the glass lined stainless steel (GLT) desorption tube in the loading position. The carrier gas through desorption unit is turned on and the flow rate is adjusted via the flow controller. The electronic console is activated to inject desorption tube with needle attached into the GC injection port (injecting). When injection is complete (injection complete), the flow is readjusted as required by the method of analysis (spilt or splitless). In this position the sample is not being desorbed into the GC since the heating blocks is not in contact with the desorption tube. Desorption process can then be commenced by activating the desorption switch on the electronics console. This will close the two heating blocks (whose temperature has previously been set on the electronics console, up to 350°C) around the desorption tube which will rapidly be heated up to the set temperature, and the combination of the heat applied and the flow through the desorption tube will drive the desired components into the GC injection port and onto the front of GC column (heat & desorb). A digital timer, built into the electronics console, controls the length of time the sample is to be desorbed and ranges from 1 sec to 100 minutes. When this timer countdown to zero the heating blocks will automatically open and the desorption tube will begin to cool by the cooling fan in the back (description cited from SIS manual). The flow chart in Figure 20 briefly summarized a typical operation cycle.

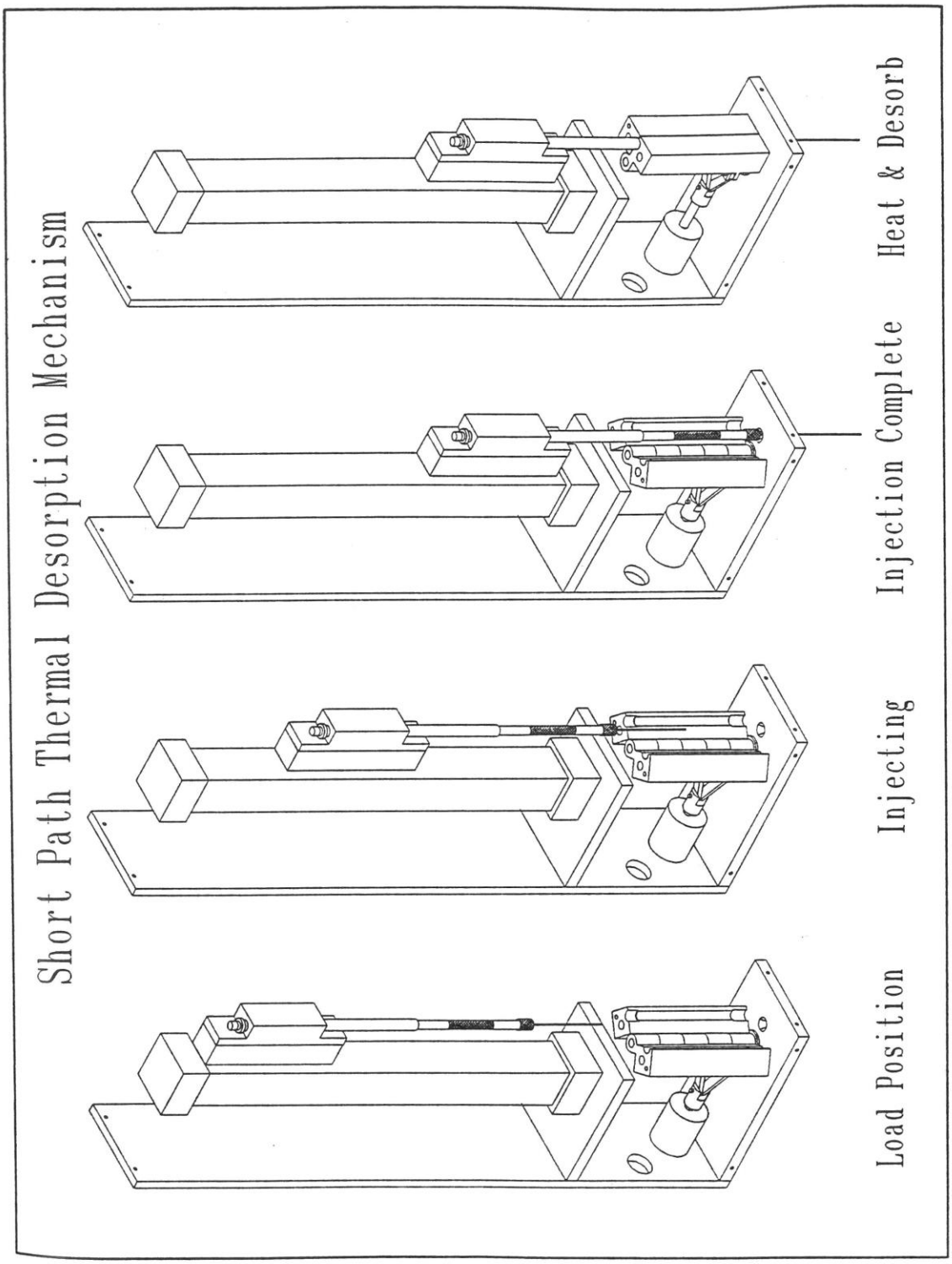

Figure 19. Short Path Thermal Desorption mechanism (from SIS manual)

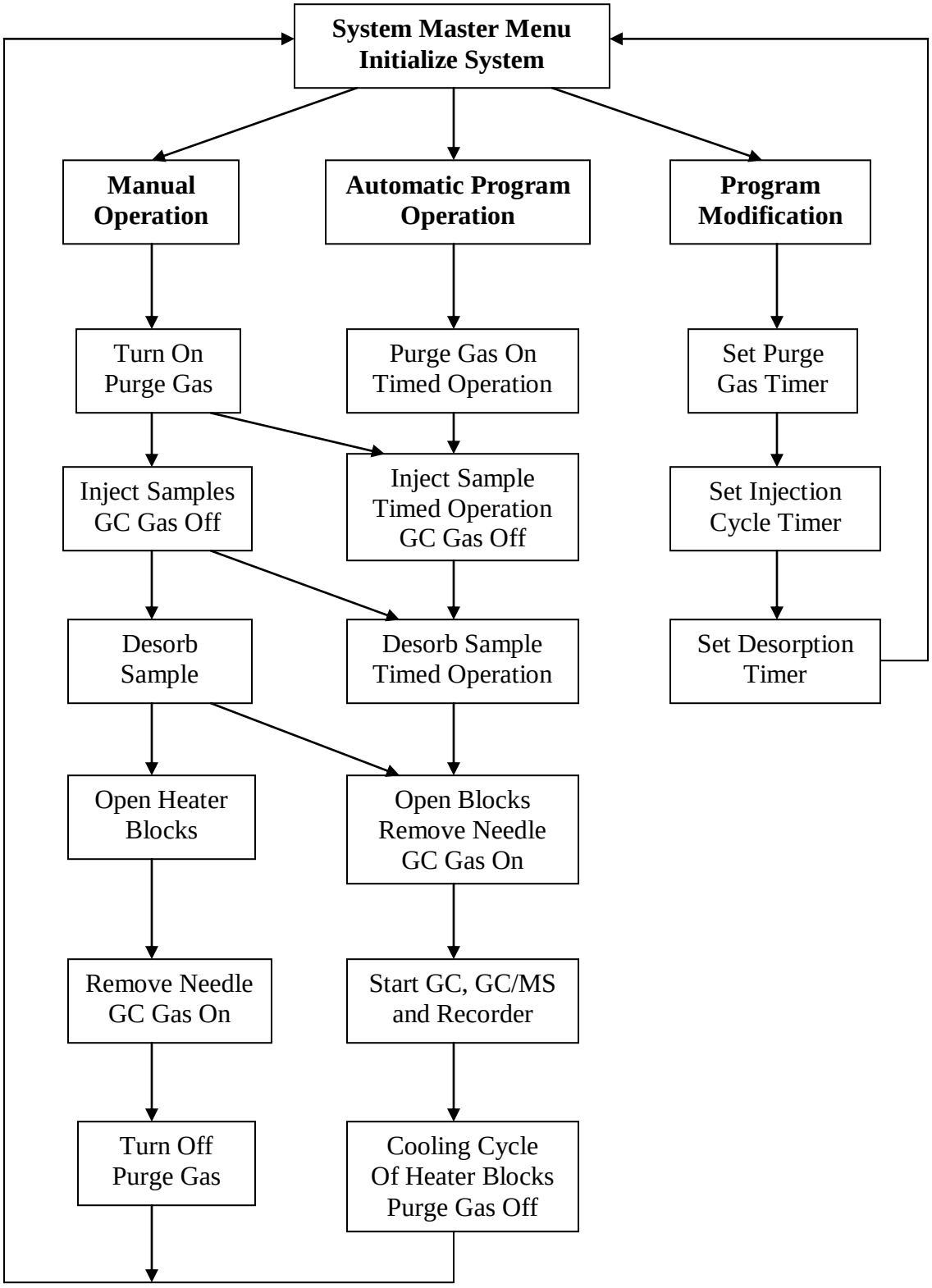

Figure 20. Short Path Thermal Desorption program flow schematic (from SIS manual)

3. The Two Thermal Desorption Approaches

The GLT desorption tube in Short Path Thermal Desorption unit is a multi-functional part serves as sample container, desorption vessel, and carrier gas flow path (Figure 21). Samples to be analyzed are collected on GLT desorption tubes packed with a porous polymer such as Tenax® or activated charcoal or combination which has been previously packed and conditioned in the tube. Desorption tubes are rugged for transportation and use and the glass lining provides an inert inner surface for samples and can be silylated if desired. When ready for analysis, the caps are removed and a stainless steel needle on a cap is attached to the desorption tube. The collected sample can then be desorbed directly in the GC. This analysis method is also known as “desorption tube for thermal desorption”.

An alternative method of analysis using the Short Path Thermal Desorption system is called direct thermal desorption (DTD) analysis, which permits the analysis of low moisture content samples to be placed directly in the GLT desorption tubes. Samples such as spices, paints, and fibers can be analysis using this technique. Water vapor must be minimized by nitrogen flush since it tends to condense at the front of the GC capillary column and thus block the volatiles from passing through.

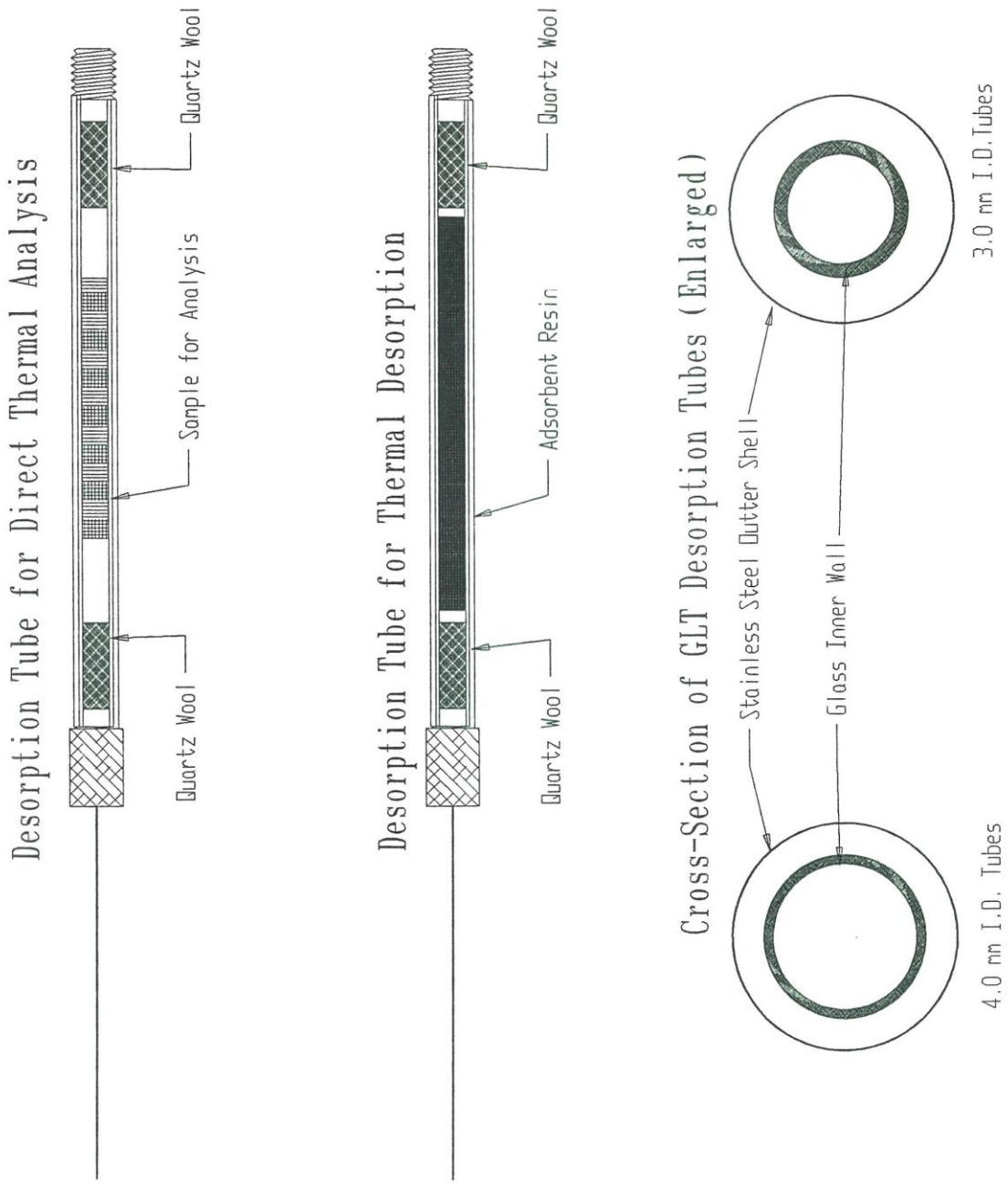

Figure 21. Desorption tube interior and section view (from SIS manual)

4. Advantages

Comparing to other desorption techniques, the Short Path Thermal Desorption system provides following advantages:

- The installation of units onto GC is extremely simplified, no screws and bolts involved, simply slip-in and ready to go. Also desorption units are easily transferrable and removable.
- The "short path" of sample flow provides for the maximum delivery of sample and minimum dead volume to the GC via the inert GLT desorption tube which can be ballistically heated up to 350°C.
- Each sample has its own individual desorption tube and needle to eliminate cross contamination from sample to sample, thus preventing any "memory effects".
- The Tenax® absorbent trap or volatiles rendered the unit excellent sensitivity compared with Solid Phase Microextraction (SPME) and other sampling techniques.
- Two analysis techniques, thermal desorption and direct thermal analysis can be utilized to analyze a wide variety of sample types.

5. Applications

Short Path Thermal Desorption system has found its application and is still gaining popularity in a wide range of analysis. Figure 22 showed GC-MS ion current chromatograms of vanilla bean samples analyzed by DTD-GC-MS to pinpoint geographical origin. The sample composites were subjected to DTD at 220°C for 5 minutes and the desorbed flavor volatiles analyzed by GC-MS (Hartman *et al.*, 1992). Major differences between the two cultivars are readily apparent from the DTD-GC-MS grams.

The volatile flavor profile of a granular dehydrated garlic powder sample is analyzed by Purge&Trap-thermal desorption—GC-MS (P&T-TD—GC-MS analysis). The sample was purged at room temperature for 30 minutes onto a Tenax® trap. Thermal desorption for 5 minutes at 220°C was followed by GC-MS analysis. The resulting chromatogram (Figure 23, Hartman *et al.*, 1991) showed various allylic sulfur compounds peaks corresponding to garlic flavor and aroma.

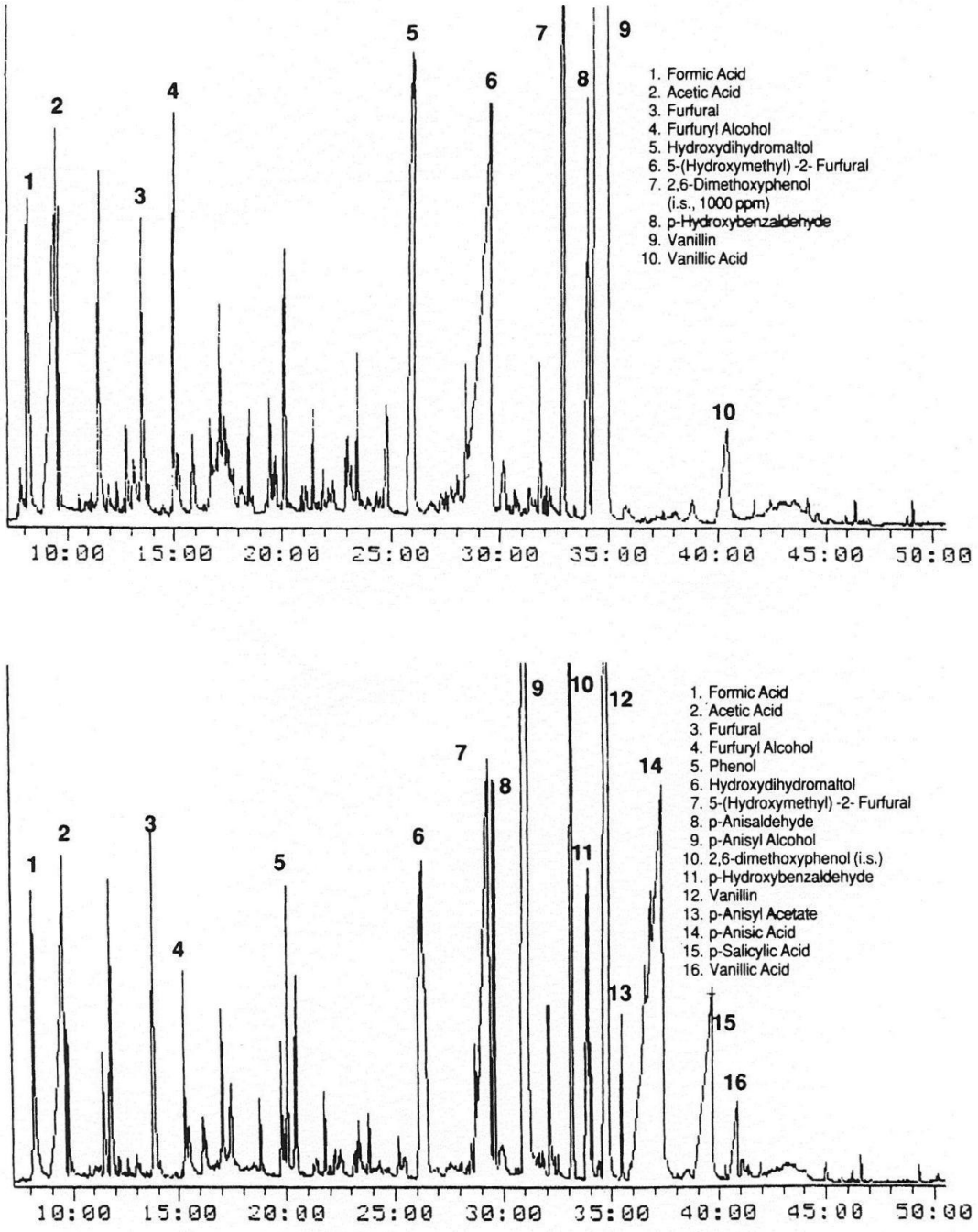

Figure 22. Short Path Thermal Desorption application — vanilla flavor study

Upper chromatogram is from Bourbon vanilla (Vanilla planifolia), lower trace is Tahitian variety (*Vanilla tahitensis*) (Hartman *et al.*, 1992)

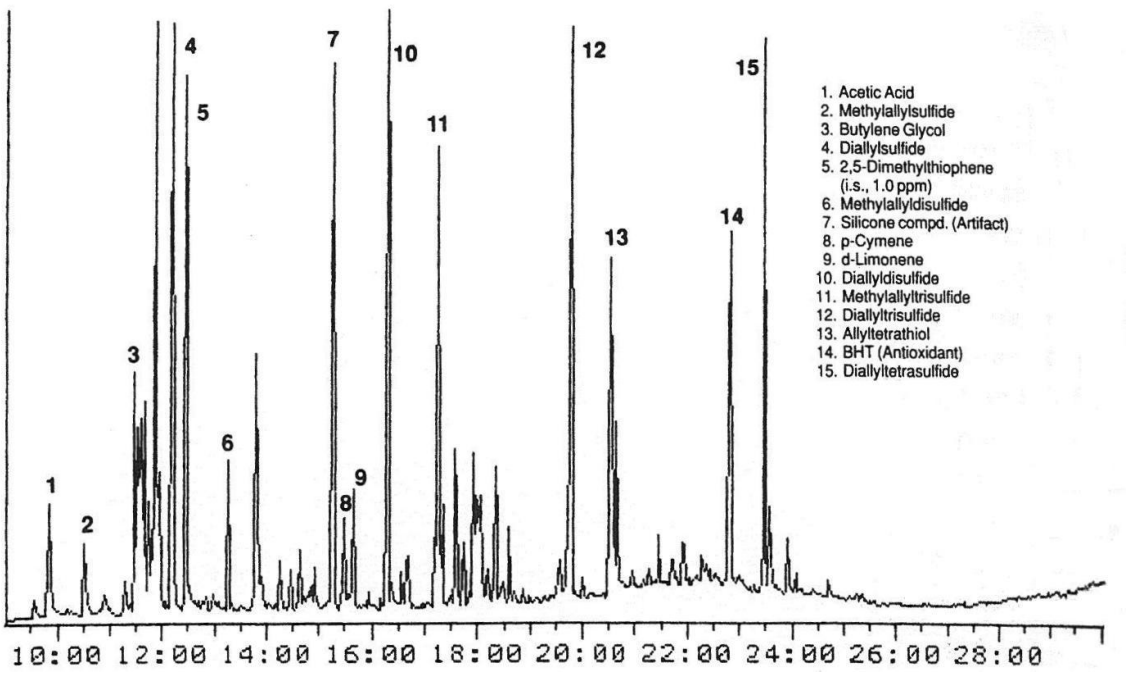

Figure 23. Short Path Thermal Desorption application — garlic flavor study

Aroma profile obtained by P&T-TD—GC-MS analysis of a Chinese dehydrated granular product (Hartman *et al.*, 1991)

III. HYPOTHESIS AND OBJECTIVE OF THE RESEARCH

A. Hypothesis

Integration of a pyrolysis probe into Short Path Thermal Desorption will remedy disadvantages associated with commercialized pyrolysis instruments, specifically the combined pyrolysis unit will be easily setup, not dedicated to GC, easily movable and transferable, not prone to injector contamination, and be accurate and precise.

B. Objective

Firstly, to integrate a pyrolysis probe into Short Path Thermal Desorption system to obtain an advanced pyrolysis unit that possesses the features from both Short Path Thermal Desorption and CDS Pyroprobe® while ensuring safety, cost efficiency and convenience.

Secondly, to test various model synthetic polymers such as polyethylene, polystyrene, polyethylene vinyl alcohol (EVOH), polyethylene vinyl acetate (EVA), and polyethylene terephthalate (PET) on the new pyrolysis unit and to evaluate its feasibility and performance in analytical pyrolysis study from the resulting polymer pyrograms.

IV. EXPERIMENTAL

A. Instrumentation Development

1. Engineering Requirements

Some engineering requirements must be fulfilled throughout the whole designing and building process for cost, safety, and function consideration.

- The pyrolysis attachment must be seamlessly integrated into existing short path thermal desorption system.
- All construction materials must be chemically inert and high temperature stable to 350-900°C range.
- Construction materials should use "shelf ready" parts to the extent possible to minimize complexity and expensive machining costs.
- For safety consideration, system must be electrically grounded, properly insulated, and operators must be protected from electrocution hazards, mechanical injury and burns.
- Need leak tight seals up to 100 psi across operation temperature range from ambient to 450°C.

2. Building Parts

A conceptual pyrolysis probe attachment configuration was illustrated in Figure 24. The major building parts were the modified connector tube and a desorption tube from Short Path Thermal Desorption system, a two-hole ceramic insulator, a two-hole Teflon®

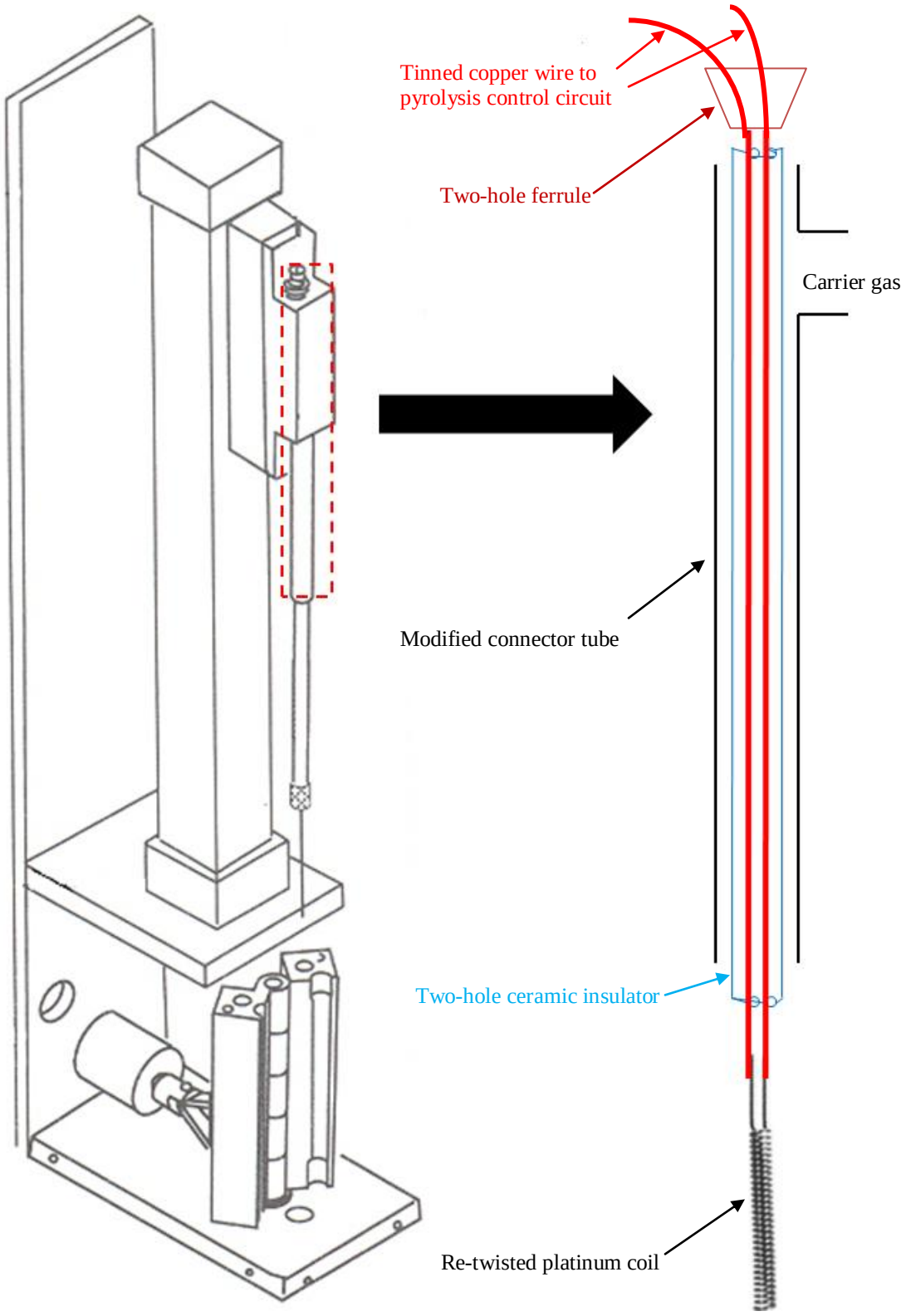

Figure 24. Conceptual configuration illustration of the new pyrolysis unit

ferrule, two pieces of tinned copper conducting leads, modified platinum coil for pyrolysis, and some connectors and insulators.

1) Platinum Coil Element

A prototype pyrolysis probe attachment was made out from CDS Pyroprobe® 100. Platinum coil was detached from the Pyroprobe® with metal wire pliers and was straightened and then re-twisted into a double-helix conformation around the sampling tube (quartz capillary tube with one end sealed) with both ending pointing upwards. The final shape of the coil element was 20mm in length and 2.0mm in internal diameter (Figure 25) and cold resistance was determined as approximately 0.2 ohm.

2) Two-hole Teflon® Ferrule and Ceramic Insulator

A two-hole Teflon® PTFE (polytetrafluoroethylene) ferrule was purchased from SIS (Scientific Instrument Services, Part No: TF1825H, OD=0.25”, ID=0.32mm, Length=0.25”) for fixing conducting wire and allowed for air-tight sealing. A two-hole ceramic insulator was purchased from Omega® (Part No: TRX-04018-12, Length=12”, OD= 1/8”, ID=0.04”) for holding electrical leads in place, providing insulation and protection. During operation the two-hole ceramic insulator provides flow path for carries gas which can also cool down the electrical leads within the ceramic insulator simultaneously. A Teflon® O-ring was machined to just fix the ceramic insulator inside connector tube without any slip (Graphite O-ring was ruled out for its instability at high temperature conditions).

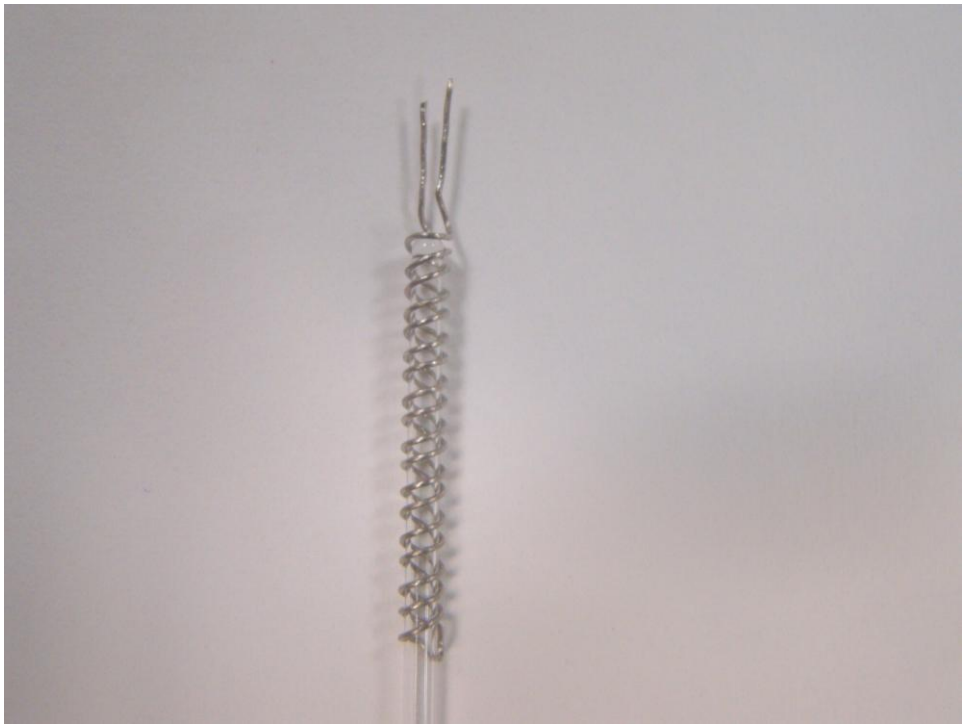

Figure 25 Re-twisted double helix platinum coil

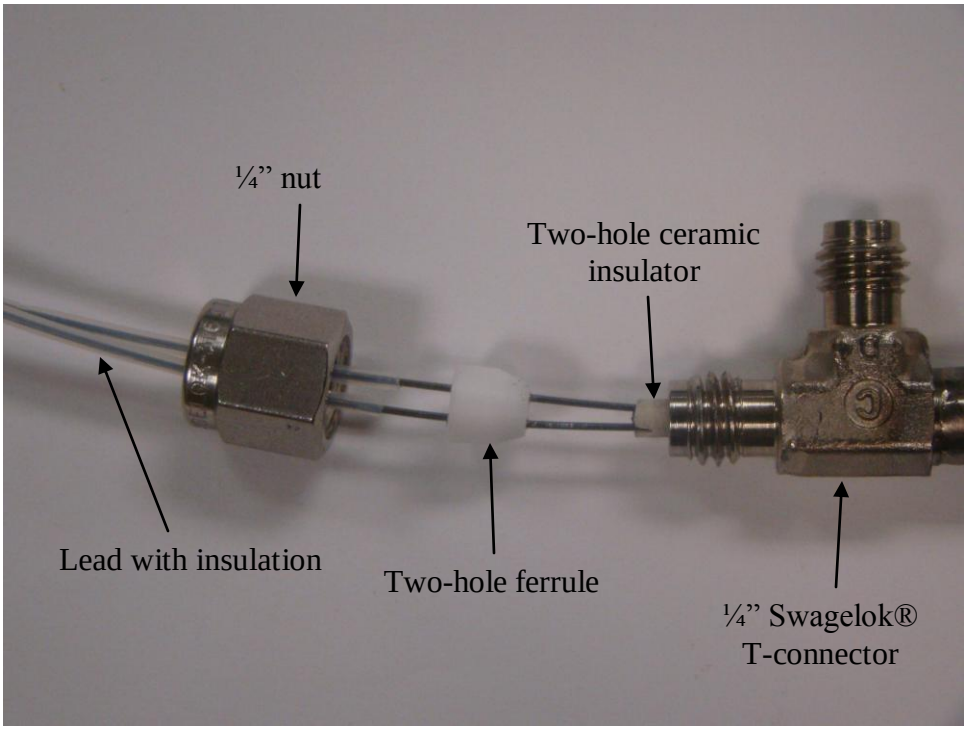

Figure 26. Close view at top of connector tube (including ferrule, nut, lead, and insulation)

3) Tinned Copper Electrical Leads

Two strands of tinned copper leads were adopted to provide DC current for the platinum coil. Tinned copper lead was chosen over other leads (stainless steel, copper) for its low heat generation on electricity due to its low resistance. The two strands of tinned copper leads were fed through the two-hole ceramic insulator with the bottom ends silver welded to the ends of the platinum coil prepared before. The upper ends were fed through the two-hole Teflon® ferrule and insulated by HPLC Teflon® tubing against each other and the nut on top of the connector tube (Figure 26).

4) Connector Tube

The connector tube was detached from the Short Path Thermal Desorption system and was re-engineered with a modified Swagelok® 1/4" T-connector. One side arm of the T-connector was cut off and polished until flat. The top threaded part of the connector tube was also chopped off, polished and welded together with the polished face on modified T-connector. The whole connector tube was completely insulated from the electrical current inside to eliminate any electrocution hazards. The final configuration of the connector tube was shown in Figure 27 with the top opening for electrical leads and the side opening for carrier gas flow. A ¼ to ½ turn beyond finger tight of the nut should be enough to provide air-tight sealing.

5) Electrical Leads Connection

The cord at the end of the Pyroprobe® 100 was stripped and cut open. Five strands of electrical leads were spotted and traced carefully for components they connected with and their functions. The five strands of leads were connected with the two tinned copper

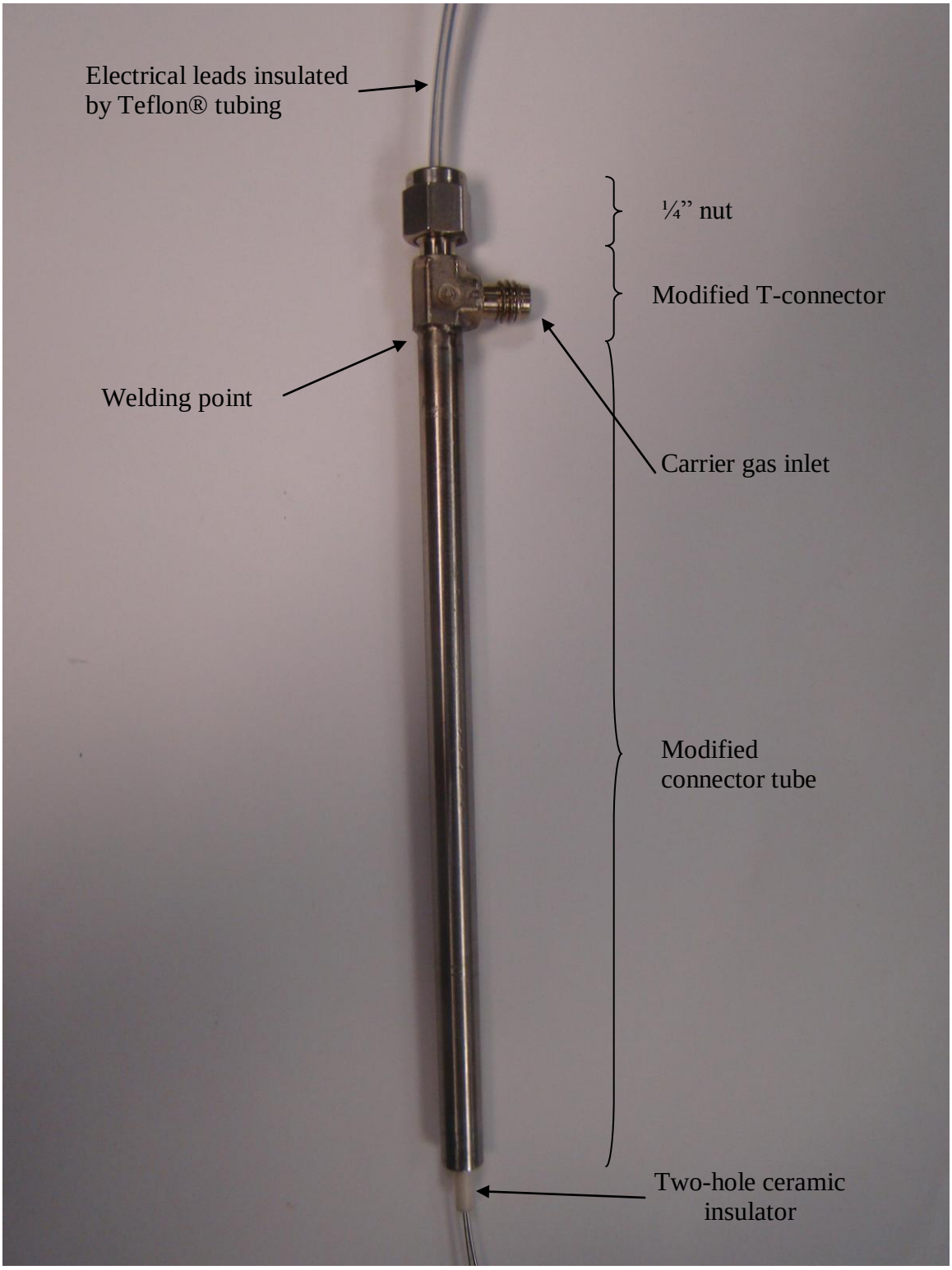

Figure 27. Modified connector tube

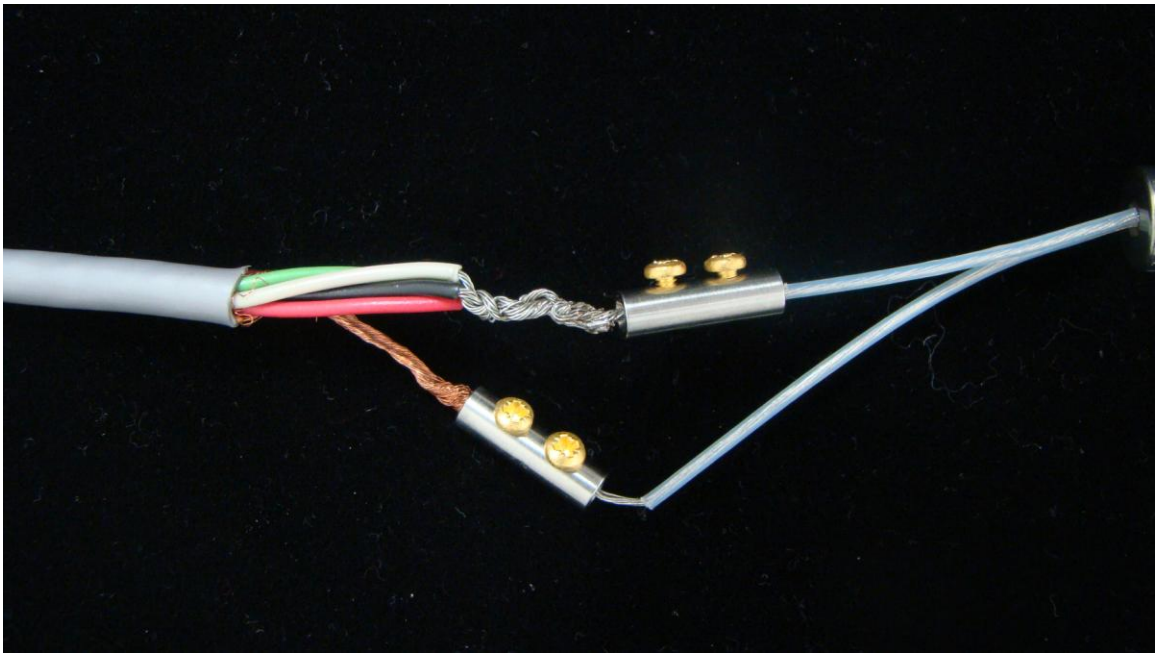

Figure 28. Wire connection zone before putting on heat-shrinking tubing
left wires lead to Pyroprobe® control module, right wires lead to platinum coil

leads mentioned above respectively via stainless steel connector and the connection zone was protected and insulated by heat-shrinking tube (Figure 28). The completed circuit was tested for conduction and insulation.

6) Desorption Tube

The pyrolysis platinum coil was shrouded inside a desorption tube connected to the bottom of the connector tube. The glass liner inside the desorption tube provides ideal insulation against the platinum coil. The desorption tube serves as carrier gas flow path, pyrolysis vessel, and injector for GC-MS analysis (with needle cap at the bottom end of the tube). The glass lined stainless steel desorption tubes are available in two inside diameters, i.e. 3mm and 4mm. Each tube is 4.0” long by ¼” diameter and is threaded on both ends.

B. Operation Procedures

Before taking off, the entire instrument should be set up with the Short Path Thermal Desorption on top of the GC injection port and the control units at a stable and safe place to prevent falling or stretching. Figure 29 was taken right after initial setup.

1. Sample Placement in Quartz Capillary Tube

The pyrolysis attachment constructed in this study is specially designed for solid polymers such as polyethylene, polystyrene, EVOH (ethyl vinyl alcohol), nylon family and so on. The polymer samples must be powered by file or grinder to fit into the quartz capillary tube (I.D.=1.4 mm). Quartz has a high melting point (>1600 ℃) that can withstand the pyrolysis temperature. Loading capacity is typically 50μg. Polymer powders should be tightly packed and open space be minimized to avoid any oxidation reactions during pyrolysis. Also make sure all the powder in tube is inside the heating zone of platinum coil. Sample tubes are changed every run to eliminate cross contamination.

2. Capillary Tube Placement in Platinum Coil

The capillary tubes should just fit in the platinum heating coil without slip and the sealed end of the capillary tube should point downward to keep sample powder from falling out. Adjust the capillary tube so that the sample powder area aligns to the heating coil. Any contact within the platinum coil will lead to short circuit and thus strictly prohibited. Figure 30 illustrated the loading position.

3. Shroud in Desorption Tube

Before shrouding in the desorption tube, make sure sample tube parallels to the connector tube to prevent any possible damage during this step. Glass liner inside every

Figure 29. Whole system view after setup with GC (bottom) and MS (right)

Figure 30. Capillary tube on platinum coil before pyrolysis

desorption tube provides insulation for the platinum heating coil from metal surface of the instrument. Fix the needle cap to the bottom end of the desorption tube and make sure the needle align to the GC injection port. All the tightening in this step only requires finger tight without aid of tools.

4. Pre-purge with Carrier Gas

The purpose of this step is to sweep out oxygen remaining in gas flow path especially inside the desorption tube. Helium is commonly applied as carrier gas at 100 ml/min and pre-purge lasts for 10 seconds. From this step until before the start of pyrolysis are automated by the electronic module of the Short Path Thermal Desorption system by

pressing “autostart” button on the control panel. Operation parameters are preset and rarely changed.

5. Sample Injection

This step is automatically initiated after the pre-purge. The air-powered solenoid drives the injection assembly to lower the needle into the injection port and place desorption tube right between aluminum heating blocks.

This whole injection procedure lasts 30 seconds, during which in-column carrier gas is switched from GC to SPTD at 20 second and re-equilibrated for 10 seconds. At the switch time point (20s) on-column pressure should stay or rise a little. Any noticeable pressure drop indicates leak within the SPTD gas transfer line and the SPTD must be shut down within the next 10 seconds and subject to leak check. Since the carrier gas flow is pressure-regulated, a constant column head pressure throughout the whole operation must be fulfilled.

6. Start Pyrolysis and Thermal Desorption

Pyrolysis process is controlled by the power switch on the CDS Pyroprobe® 100 control panel and should be pressed at the same time when thermal desorption starts (right after the 30 seconds injection step). Pyrolysis takes place within the quartz capillary tube when the platinum heating coil heats up to appropriate temperature and converts polymer powder into gaseous pyrolysates which escape from the top opening of the quartz tube into the desorption tube. In the meantime aluminum heating blocks close around desorption tube to provide ballistic heating to the desorption tube thus keep the pyrolysates volatile while being purged into the GC injection port by the carrier gas.

The 20-second pyrolysis and the simultaneous 5-minute thermal desorption process is enough to break down polymer samples and transfer pyrolysates onto the head of the GC column. Carrier gas is from the SPTD transfer line in this 5 minutes duration.

7. Start GC-MS Operation

In this study we used cryogenic trapping technique to concentrate pyrolysate vapors by placing dry ice into column oven to lower column oven temperature to -20°C before starting GC operation. Pyrolysate vapors were cold-trapped within a very limited length at the head of the capillary column and thus concentrated to improve resolution after the 5-minute thermal desorption process. GC operation is then started automatically by the SPTD on top of the GC injection port after the 5-minute thermal desorption and a pre-set GC temperature profile will be activated. The commencement of MS, unlike GC, is right after the 30-second injection step manually (at the same time when pyrolysis starts) in order to collect low molecular weight volatiles that would not be cold trapping in column. A total ion chromatogram (TIC) will be developed after each GC-MS run carrying all valuable information on the polymer under analysis.

On starting the GC, the GC carrier gas is simultaneous switched on to provide carrier gas onto the column, while the SPTD carrier gas will stay on for another 5 minutes for the purpose of cooling down the hot aluminum heating blocks, the thermal desorption tube, and the platinum coil within.

8. Cleanup

After obtaining the TIC for the polymer sample, the system must be cleaned and reset for next run.

Desorption tube after 30-40 min analysis time is cooled and can be detached. Quartz capillary tube is pulled out with a pick from the platinum coil and discarded (Figure 31). Check platinum coil for any possible deformation or short-circuit. The needle cap can be washed with methanol and then baked out for re-use. Each sample is assigned with its own quartz capillary tube and desorption tube to prevent any carry-overs. Press "reset" button on GC to cool down the GC oven to ambient temperature before putting in dry ice for next run.

Figure 31. Capillary tube after pyrolysis (black substance is carbonization residue)

C. Operation Condition and Methodology

GC: Varian GC 3400, 100:1 split injection, temperature program: -20-320°C at 15°C/min, hold at 320°C until run over.

Capillary column: Supelco Low Bleed SLB™-5ms capillary column, 30m x 0.32mm x 0.25μm film thickness. Carrier gas: helium, 1 ml/min on column.

Short Path Thermal Desorption: heating blocks temperature: 220°C, desorption duration: 5 minutes. Carrier gas: helium, 100 ml/min.

MS: (1) for virgin HDPE sample, Finnigan MAT TSQ-70 Quadrupole MS, EI mode, m/z scan: 10 to 750, run time: 45 minutes. (2) for other polymer samples (PS, EVOH, EVA, PET), Finnigan MAT 8230 High Resolution MS, EI mode, m/z scan: 35 to 650, run time: 35 minutes.

Sample amount: (1) for virgin HDPE, filled up the capillary sample tube. (2) for other polymer samples (PS, EVOH, EVA, PET), 50 μg.

Pyrolyzer control unit: temperature ramp: off, pyrolysis interval: 20s, set final temperature: 900°C.

Room temperature: 20°C.

V. RESULT AND DISCUSSION

A. Temperature Calibration

In most cases the set temperature displayed on the control panel of a pyrolyzer may not reflect the true temperature which a polymer sample within a capillary tube is exposed to. Thus calibration is necessary in order to determine the actual pyrolysis temperature. During calibration the carrier gas flow rate (100 ml/min) and current must be kept the same as under real pyrolysis condition since these variables can affect the temperature.

In our study, calibration was realized though directly thrusting a fine J-type thermocouple (Omega HH-26J, +: iron, -: constantan, 12" x 0.5mm) wire into a capillary sample tube loaded in position and the readings were directly read from the LCD on thermometer. In this way more sensitive and instant readings comparing to Kraton® 1107 method (Walker, 1977) can be acquired thus the resulting calibration curve is more reliable (Table 3 and Figure 32).

Table 3 Temperature calibration data*

Set temperature(°C)	500	550	600	650	700	750	800	850	900
Actual mean peak temperature(°C)**	428	472	510	569	594	660	685	749	788
Heating duration in seconds	22	22	22	22	22	22	22	22	22

*Calibration condition: 100 ml/min helium flow, 20°C room temperature.

**Peak temperatures were measured in triplicate.

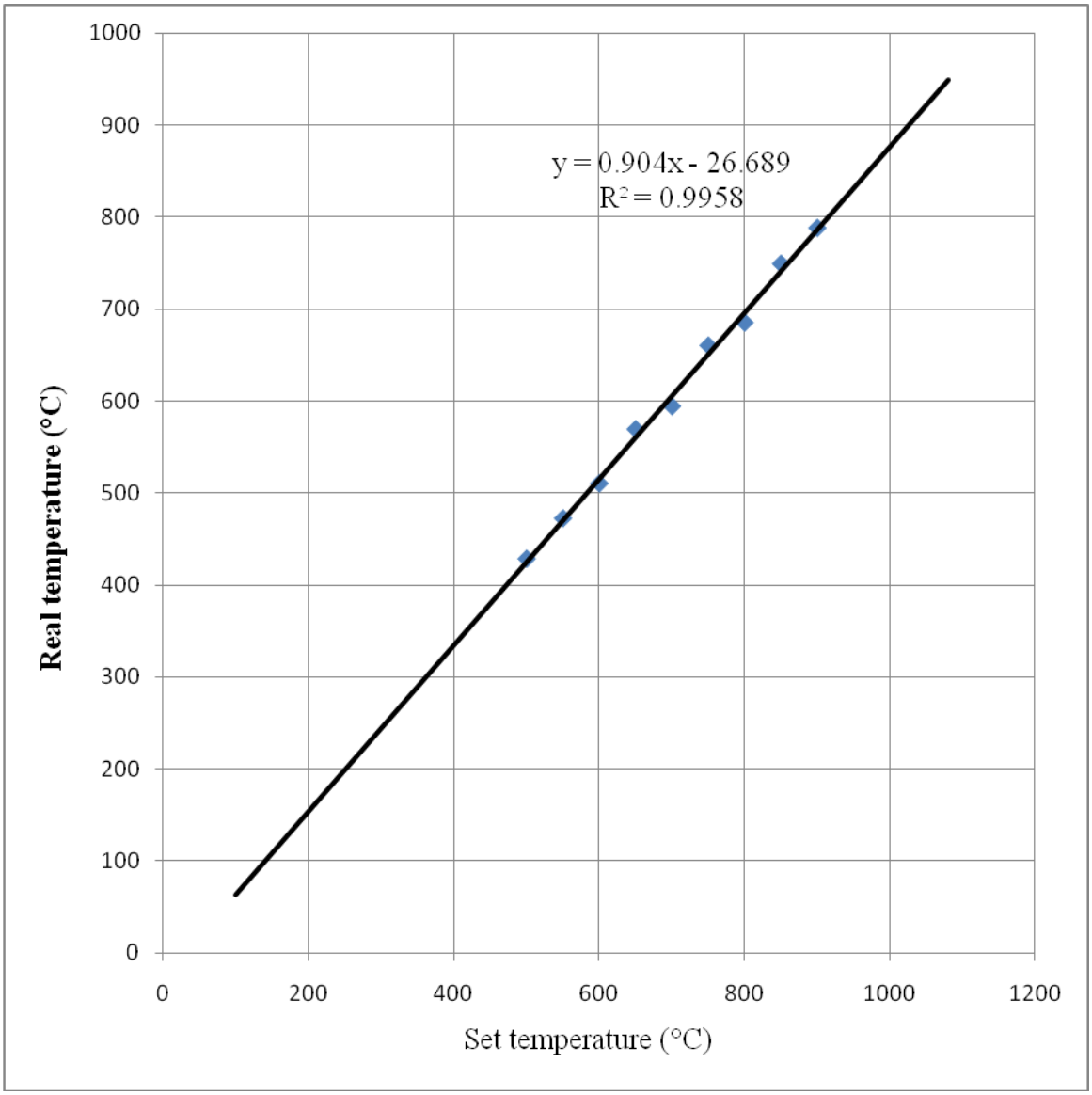

Figure 32. Temperature calibration curve (data from Table 3)

From the calibration curve actual mean pyrolysis temperature was 787°C when the pyrolyzer was set at 900°C.

B. Pyrolysis Results and Discussion

Five kinds of polymers were individually pyrolyzed to investigate the performance and feasibility of the Pyrolysis-SPTD-GC-MS system as described. The results are described below for each individual polymer.

1. Virgin High Density Polyethylene (HDPE)

Polyethylene is a thermoplastic polymer consisting of long chains of the monomer ethylene. HDPE has little branching, which endow it stronger intermolecular force and tensile strength than low density polyethylene (LDPE) characterized by more branching and thus weaker intermolecular bonds. Its applications can be readily found in food containers, storage bags, and supply pipes.

Pyrolysis of HDPE was carried out under the condition stated before and the resulting pyrogram is shown in Figure 33. A very strong peak of ethylene (the primary pyrolysis product) was seen in the pyrogram followed by a homologous series of oligomers up to C_{40}. Ethylene, the monomer building block of HDPE was released after severe pyrolysis at 787°C and evolved as the earliest peak in pyrogram due to its low boiling point. α-olefins were the most prominent peak in each peak clusters of same carbon number (RT=13.61, 14.72, 15.64 min…) evolved later as carbon number increased.

In each of the peak cluster between C_8 (RT=13.61 min) and C_{23} (RT=30.28 min), several peaks with very close retention times were observed (like in C_{16} cluster, peaks at 22.58, 22.69, 22.79, 22.87, 22.92, 22.97, 23.04, and 23.10 min were observed in Fig 34-A) among which a triplet stood out as major ones (peaks at 22.92, 23.04, and 23.10 min).

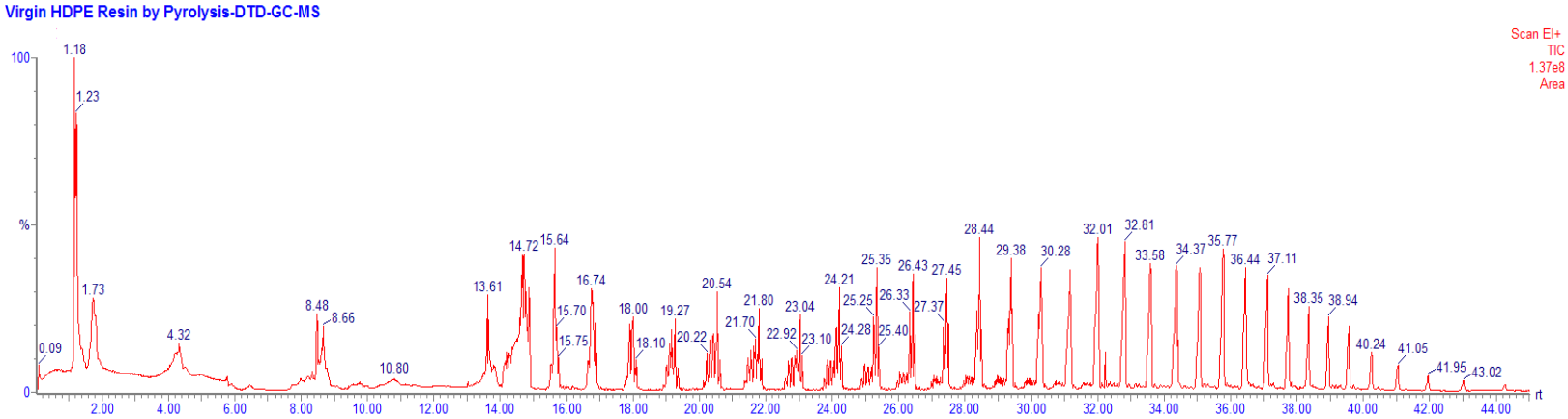

Figure 33. Virgin HDPE pyrogram

Peaks were identified as: 1.16:ethylene; 1.23:propene+propane; 1.73:1-butene; 4.32:1-pentene; 8.48:1-hexene; 10.80:1-heptene; 13.61:1-octene; 14.72:1-nonene; 15.64:1-decene; 16.74:1-undecene; 18.00:1-dodecene; 19.27:1-tridecene; 20.54:1-tetradecene; 21.80:1-pentadecene; 22.92:1,15-hexadecadiene; 23.04:1-hexadecene; 23.10:n-hexadecane; …27.45:1-eicosene;… 43.02:1-tetracontene mixed with other C_{40} hydrocarbons

Zoom-in view of C_{16} eluents in HDPE pyrogram

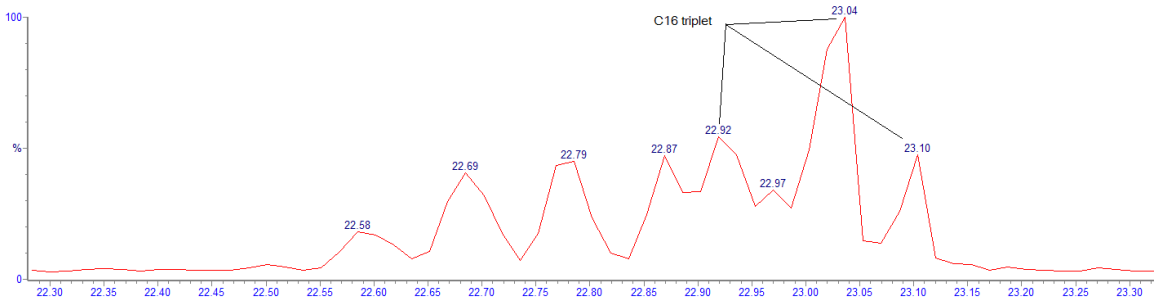

Mass spectrum at RT=22.92 min

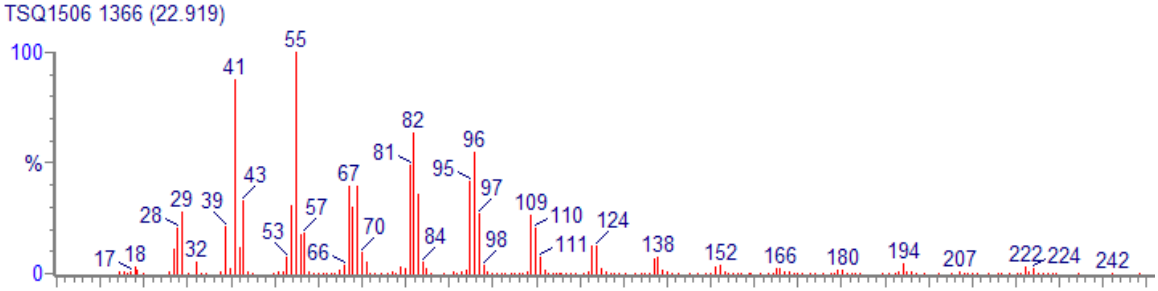

Mass spectrum of 1,15-hexadecadiene from NIST library

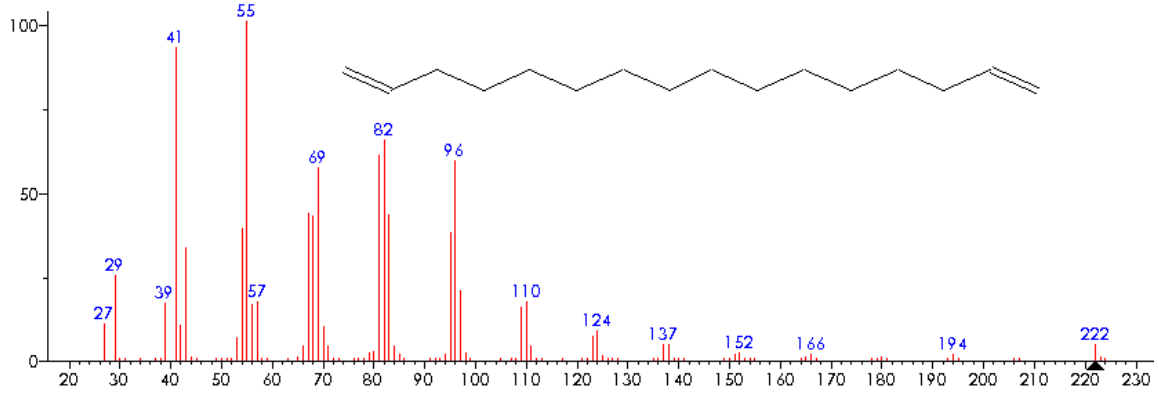

Figure 34-A. C_{16} triplet identification

Mass spectrum at RT=23.04 min

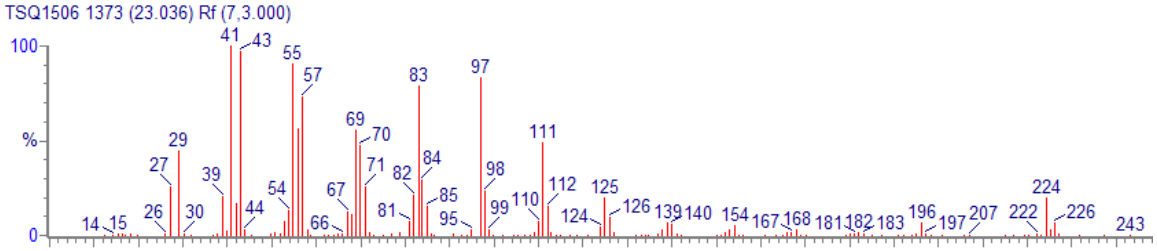

Mass spectrum of 1-hexadecene from NIST library

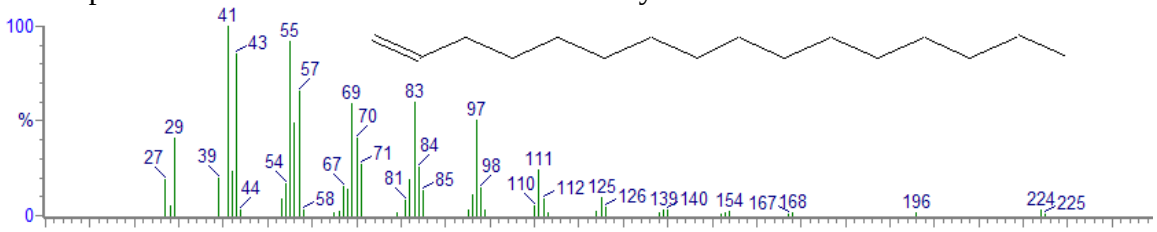

Mass spectrum at RT=23.10 min

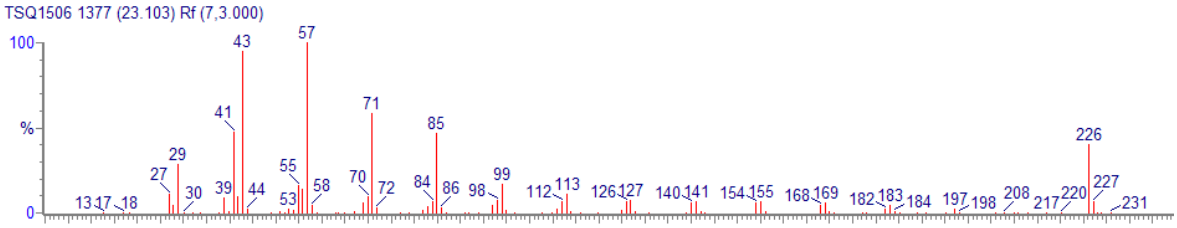

Mass spectrum of hexadecane from NIST library

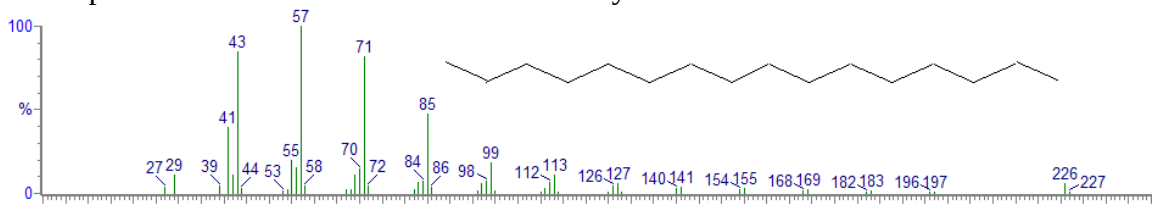

Figure 34-B. C_{16} triplet identification

Structural identification of C_{16} triplets was shown in Figure 34-A,B and peaks at 22.92, 23.04, and 23.10 min were assigned to 1,15-hexadecadiene (α, ω-diolefin), 1-hexadecene (α-olefin), and n-hexadecane (n-alkane) respectively. Similar pattern can also be found in other peak clusters from the pyrogram. Pioneer researchers (Sugimura *et al.*, 1979) has established the identity of the peaks in triplets as being the α, ω-diolefin, the α-olefin, and the corresponding n-alkane. The pyrolysis of HDPE proceeds by a free radical chain mechanism (Wall *et al.*, 1954) and hydrocarbon triplet series are resulted from intramolecular hydrogen abstraction (backbiting) followed by β-cleavage (Figure 35). The smaller peaks in each cluster between or proceeding the triplets (peaks at 22.58, 22.69, 22.79, 22.87, and 22.97 min) are believed related to branched olefins and diolefins because of their lower retention indices.

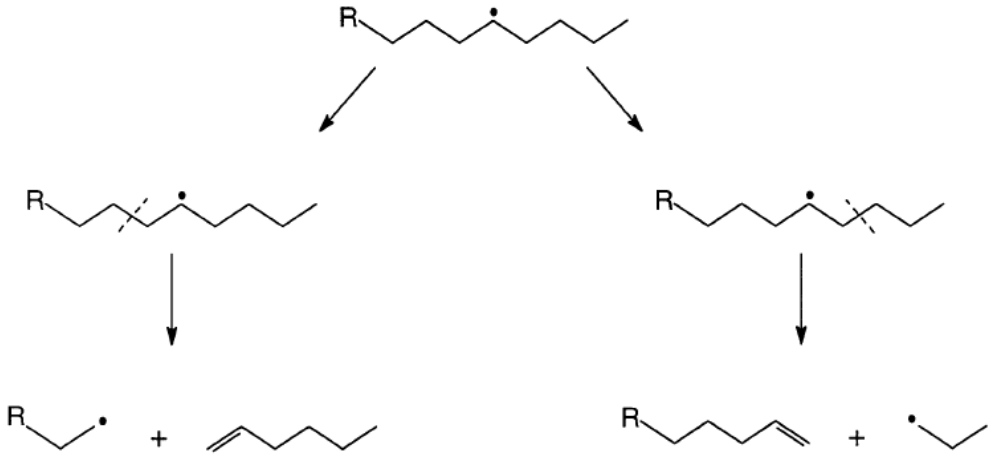

Figure 35. Olefin formation via β-scission of radical species (Favavelli *et al.*, 1999)

Mass spectrum at RT=43.02 min

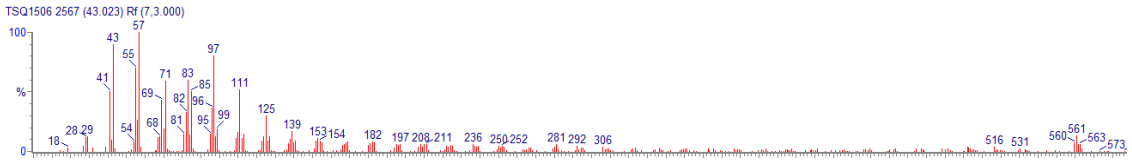

Figure 36. Mass spectrum of compound at 43.02 min

As column temperature went up, long chain hydrocarbons started to elute out until up to C_{40}. Meanwhile high temperature also raised the viscosity of carrier gas and in turn lowered carrier gas flow speed, which compromised the resolving power of column and causes each peak clusters above C_{24} (RT=31.17 min) merged into one uniform peak. Even though there is no way of distinguishing different hydrocarbons (alkane, olefins, diolefins) mixed into a single peak, general information can still be retrieved from the mass spectra (see Figure 36, the mass spectrum pattern strongly indicates hydrocarbon and a molecular ion around m/z 560 indicates $C_{40}H_{80}$).

Figure 37 was the total ion chromatogram (TIC) of the same HDPE sample from DTD-GC-MS analysis without pyrolysis. Difference in chromatograms between with pyrolysis and without pyrolysis is remarkable: (1) no ethylene peak was observed in the TIC without pyrolysis comparing to the strong ethylene peak at the front of the pyrogram, proving that thermal desorption alone at 300°C cannot break down the carbon-carbon bonds within HDPE polymer. (2) unlike the characteristic triplets peaks found in pyrogram, in TIC without pyrolysis only one peak corresponding to α-olefin was found for each carbon number, proving that during thermal desorption no free radical chain reaction took place at all, those α-olefin peaks were simply short-chain oligomer molecules

physically trapped within the polymer matrix and driven out by thermal desorption. (3) the hydrocarbons found in pyrogram had successive carbon numbers while in TIC without pyrolysis only even carbon number α-olefins were found, the absence of odd carbon number α-olefins proved again that thermal desorption along cannot provide sufficient energy to disrupt the carbon-carbon bonds within HDPE polymer.

Figure 30 and Figure 31 were taken before and after HDPE pyrolysis respectively. All HDPE powder sample were degraded and transferred onto column after the 20-second pyrolysis process, leaving only a trace amount of black residues resulted from carbonization.

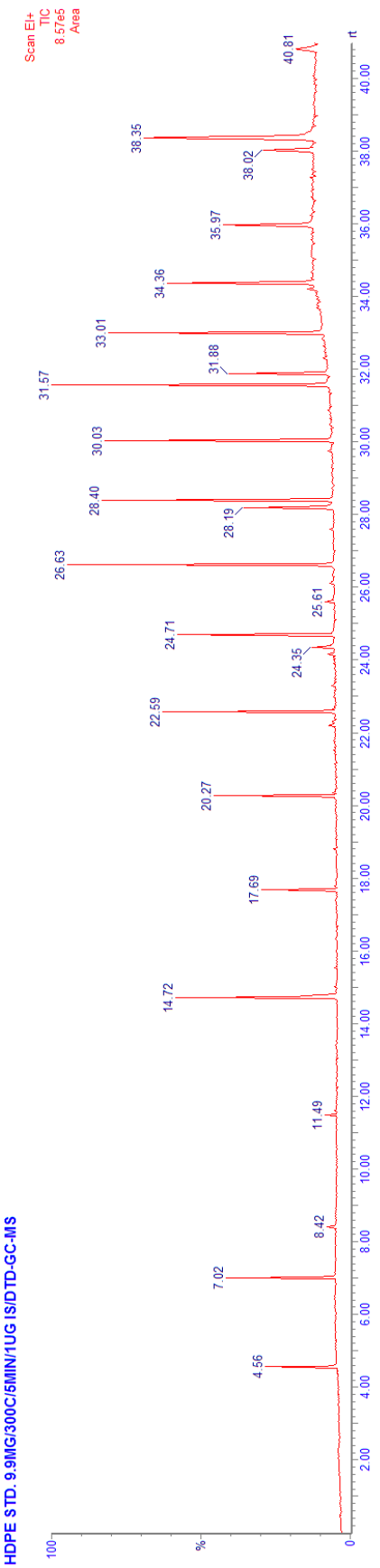

Figure 37. TIC of Virgin HDPE by DTD-GC-MS

Peaks were identified as: 4.56:benzene-D6; 7.02:toluene-D8, 14.72:naphthalene-D8; 17.69:1-tetradecene; 20.27:1-hexadecene; 22.59:1-octadecene; 24.71:1-eicosene; … 38.25:1-octatricontene

2. Polystyrene (PS)

PS (Figure 38) is an aromatic thermoplastic polymer that is commercially manufactured from petroleum and is one of the most widely used plastic. Solid PS is used in plastic models, CD/DVD cases, and disposable cutlery while foamed PS is used in packing materials, insulation and disposable cups and dishes.

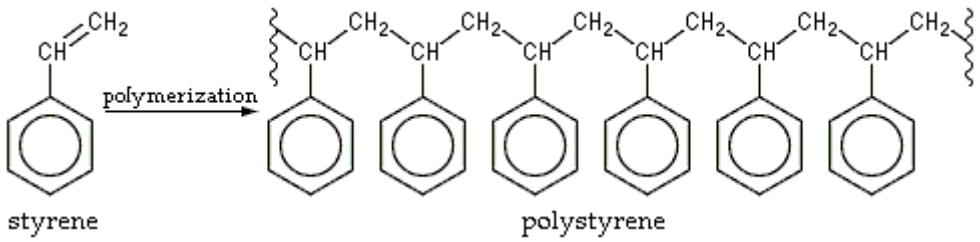

Figure 38. Polystyrene structure and synthesis (from Wikipedia)

The first noticeable peak showed up in the pyrogram in Figure 39 was at RT=2.09 min and was later identified as 2-methyl butane. 2-methyl butane is commonly applied as propellant as well as blowing agent in the polystyrene processing for foam development (sample for pyrolysis was a foamed PS for packing purpose). During the phase transition of polystyrene from solid phase into foamed phase 2-methyl butane helps to produce a cellular structure and was physically trapped within the matrix.

Monomer (styrene) was identified as expected from the pyrogram at 11.46 min. The peak ahead of styrene at 9.67 min was identified as toluene (C_7H_8), which indicated that toluene is, though less favorable to styrene, a noticeable pyrolysis product from PS (Lehmann *et al.*, 1961).

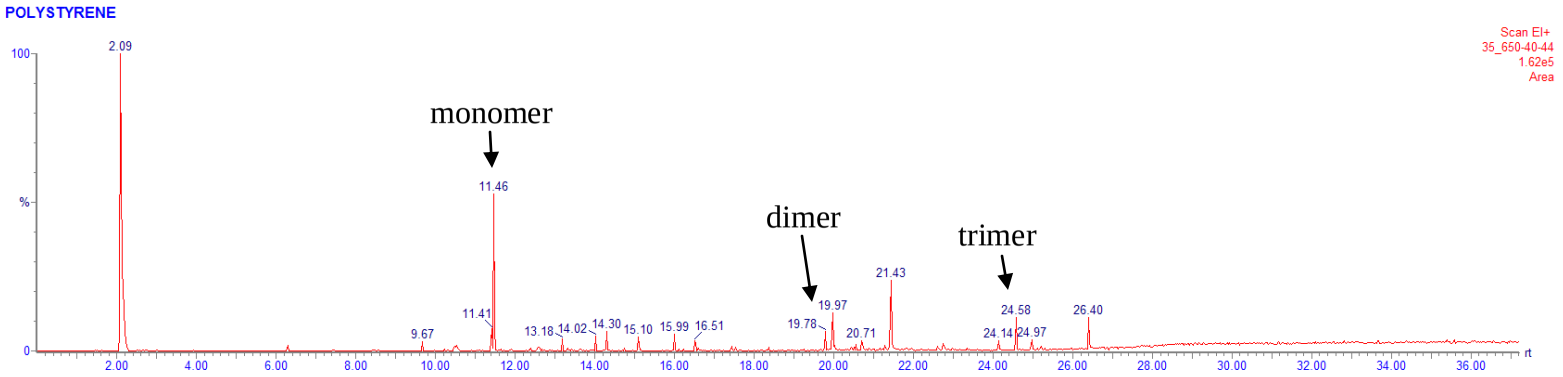

Figure 39. PS pyrogram

Peaks were identified as: 2.09:2-methyl butane; 9.67:2-propenylidene-cyclobutene; 11.46:styrene; 14.30:cyclopentasiloxane, decamethyl-(from column bleeding); 19.78:benzene ethenyl- dimer; 19.97:tetradecanoic acid; 24.14: hexanedioic acid, dioctyl ester ; 21.43:hexadecanoic acid; 24.58:benzene ethenyl- trimer; 24.97: phthalic acid, diisooctyl ester ; 26.40:squalene

Peak at RT=19.78 min was identified as ethenylbenzene dimer fraction (Figure 41) and it appeared to be a complex mixture of structural isomers. Noffz and his colleagues in 1968 have detected about 20 peaks corresponding to the molecular formula $C_{16}H_{16}$ among which six were successfully identified. The major dimer was generally regarded as 1-benzyl-2-methylbenzocyclobutene (Figure 40, Exner *et al.*, 1971). The composition and ratio in the ethenylbenzene dimer blends depends greatly on pyrolysis condition, sample amount, and microstructures of different PS polymers (level of chain branching, Jones *et al.*, 1967).

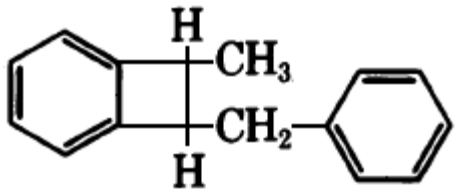

Figure 40. 1-benzyl-2-methylbenzocyclobutene

The structural elucidation for ethenylbenzene trimers is even more formidable than dimers because of increasing isomer possibilities and experimental variables. Figure 42 shows the mass spectrum at 24.58 min. The molecular ion at m/z 312 ($C_{24}H_{24}$) together with fragment peaks at m/z 207 (dimer), 104 (monomer), and 91 (toluene) all clearly indicate an ethenylbenzene trimer structure. Furthermore, the major fragment ion peaks and molecular ion peak found in the resulting pyrogram (m/z=92, 118, 208, 312) supports the pyrolysis field-ion MS (PFIMS) work from Hummel (Figure 43, Hummel in Polymer Spectroscopy).

Mass spectrum at RT=19.78 min

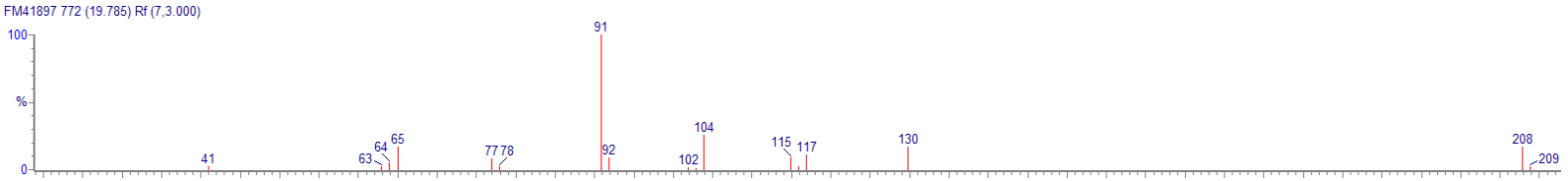

Mass spectrum of benzene ethenyl- dimer from NIST library

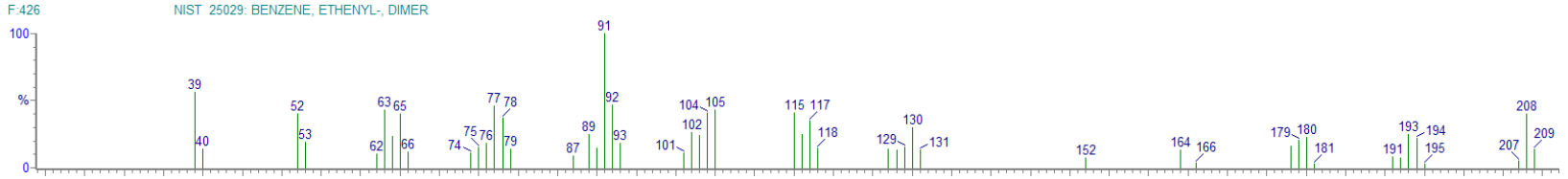

Figure 41. Benzene ethenyl- dimer identification

Mass spectrum at RT=24.58 min

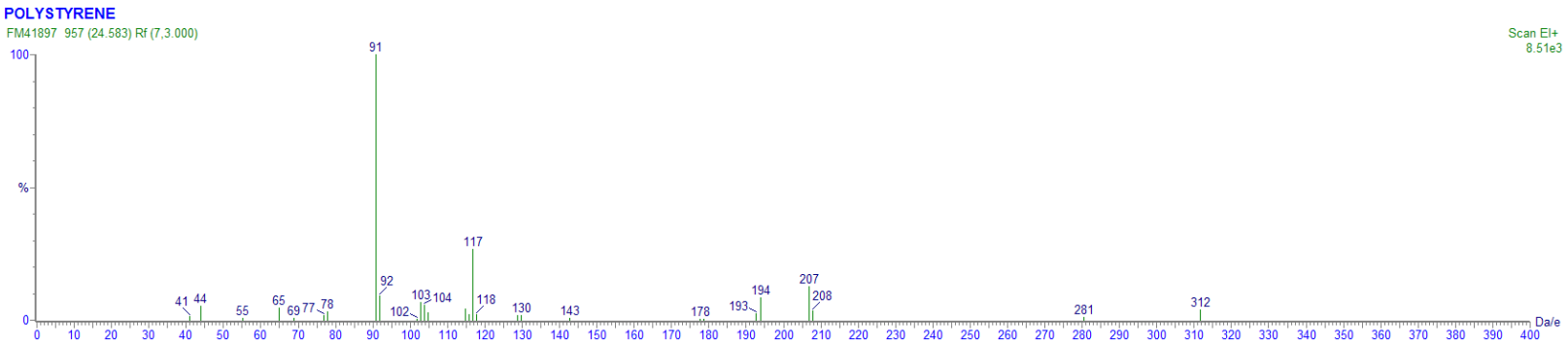

Figure 42. Benzene ethenyl- trimer identification

Fragment ions were: m/z=91:toluene; m/z=117:nMethylstyrene; m/z=207:styrene dimer; m/z=312:trimer molecular ion

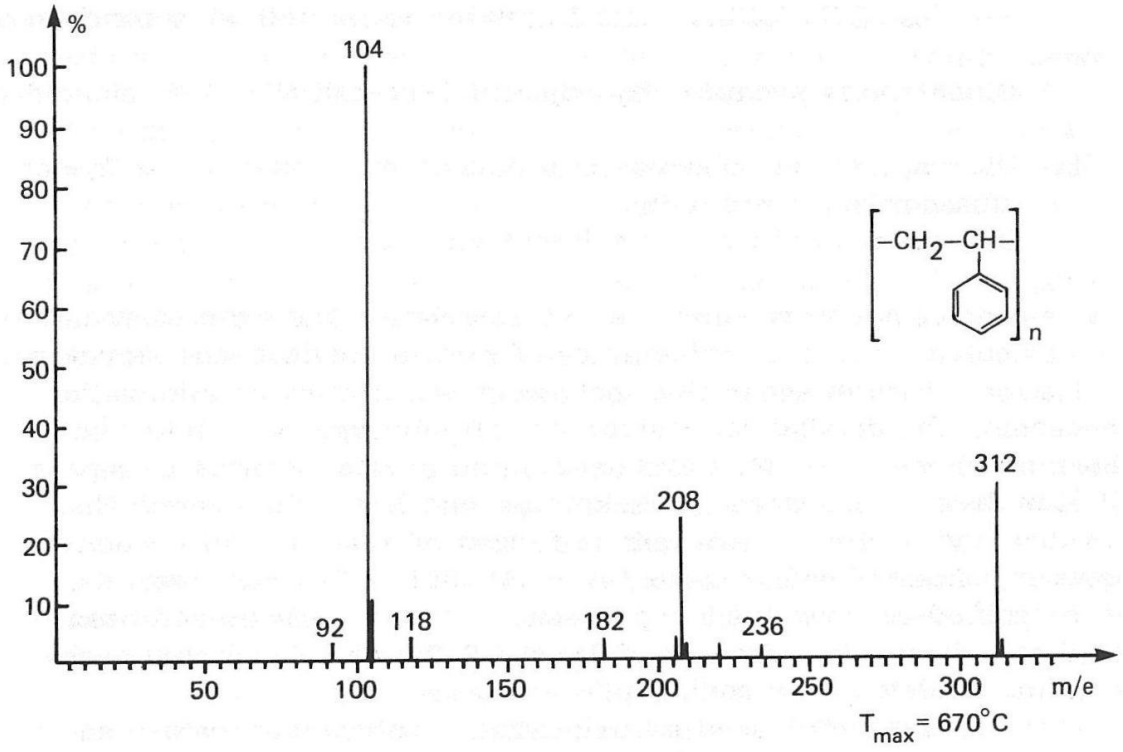

Figure 43. PFIMS of polystyrene (Hummel, D. O. in Polymer Spectroscopy)

The amount of PS sample pyrolyzed was around 50 μg, which was much less than the amount of HDPE sample in the previous run. Therefore the total ion current (TIC) in PS pyrogram (1.62e5) was 3 orders magnitude smaller than that in HDPE pyrogram (1.37e8). The definitive peaks for PS monomer, dimer, trimer, and other break down fragment on the TIC pyrogram from tiny little amount of sample proved excellent sensitivity of the new pyrolysis unit.

3. Ethylene Vinyl Alcohol (EVOH)

EVOH is a copolymer of ethylene and vinyl alcohol (Figure 44). Since vinyl alcohol mainly exists as its tautomer acetaldehyde, the copolymer is prepared by polymerization of ethylene and vinyl acetate followed by hydrolysis. EVOH resin is mostly applied to provide barrier properties, primarily as an oxygen barrier in food packaging to improve shelf life, or as a hydrocarbon barrier for gasoline tanks. EVOH copolymer is defined by the mole percentage ethylene content (x/(x+y) in Figure 44): lower ethylene content grades have higher barrier properties while higher ethylene content grades have lower temperatures for extrusion.

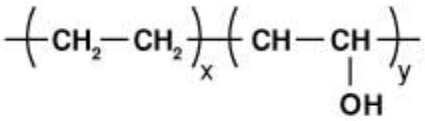

Figure 44. EVOH structure

In our study an EVOH resin (ethylene content unknown) was grinded to fine powder (50 μg) and subjected to pyrolysis at same condition stated before (flash pyrolysis at 787°C, 22s). Resulting pyrogram was shown in Figure 45 with identified compounds listed. Major pyrolysates can be classified as alcohols (peaks at 11.17 and 12.14 min); aldehydes (peaks at 1.23, 7.56, 11.50, 12.14, and 14.84 min, most of which were unsaturated); ketones (peaks at 2.74, 8.24, 9.17, 12.50, and 15.43 min most of which

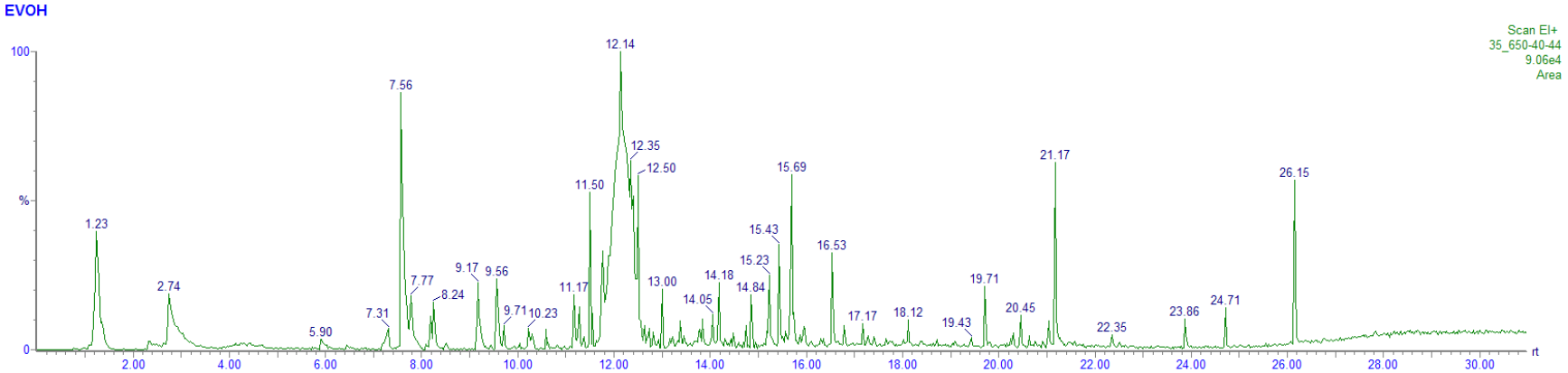

Figure 45. EVOH pyrogram

Peaks were identified as: 1.23:acetal aldehyde; 2.74:acetone; 7.56:(E)-2-butenal; 8.24:3-methyl-3-buten-2-one; 9.17:(E)-3-penten-2-one; 9.56:3,4-dihydro-6-methyl-2H-pyran; 11.17:2-butanol; 11.50:(E,E-)-2,4-hexadienal; 12.14:benzaldehyde; 12.14(base peak):3-hexene-2,5-diol; 12.50:4,4-dimethylcyclopent-2-en-1-one; 13.00:2,6-dimethyl-2,4-heptadiene; 13.33:2,6-dimethyl-2,4-hepadiene; 14.18:$C_{10}H_{18}O_2$; 14.84:nonanal; 15.43:7-octen-2-one; 15.69:4-methyl-2,6-octadiene; 16.53: 3-methyl-hexahydro-pyrano[3,2-b]pyran-2-one; 19.71:tetradecanoic acid; 20.45:pentadecanoic acid; 21.17:hexadecanoic acid; 23.86:hexanedioic acid, dioctyl ester; 24.71:phthalic acid, diisooctyl ester; 26.15:squalene

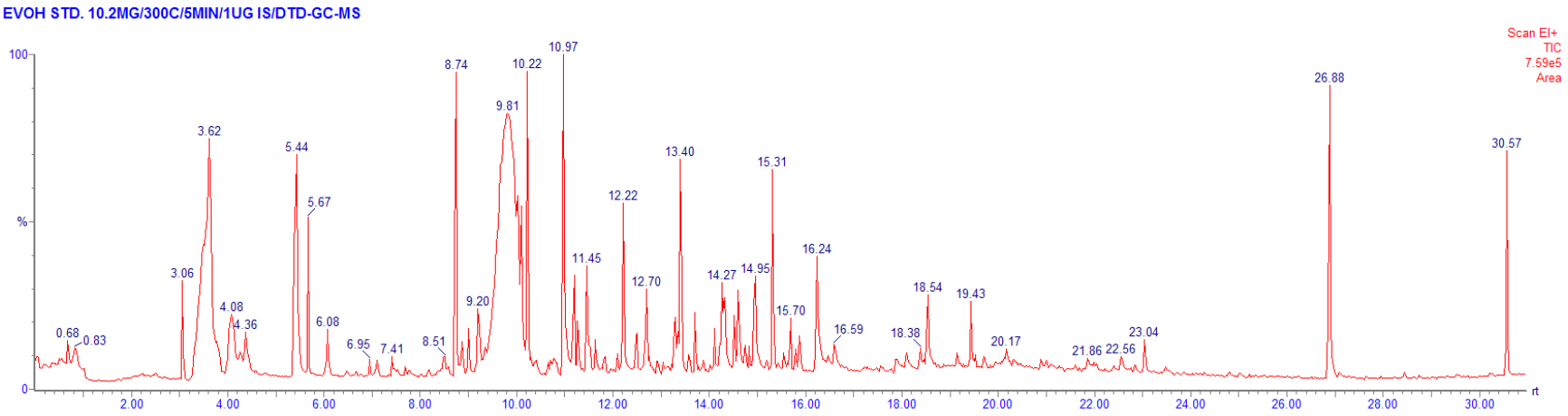

Figure 46. TIC of EVOH by DTD-GC-MS

Peaks were identified as: 0.68:acetone; 3.06:benzene D-6; 3.62: 1-hydroxy-1,3-butadiene; 4.08: 2,2,4,4-tetramethyl-1,3-cyclobutanediol; 4.36: 4-methyl-2-pentene; 5.44:3-penten-2-one; 5.67:toluene D-8; 6.08:3,4-dihydro-6-methyl-2H-pyran; 6.95:3-hepten-2-one; 8.74: (E,E-)-2,4-hexadienal; 9.81:3-hexene-2,5-diol; 10.22: 4,4-dimethylcyclopent-2-en-1-one; 10.97: 2,6-dimethyl-2,4-heptadiene; 11.45: 2,6-dimethyl-2,4-hepadiene; 12.22:ethanone, 1-(1-cyclohexen-1-yl)-; 12.70: $C_{10}H_{18}O_2$; 13.40:naphthalene D-8; 15.31: D-verbenone; 16.24: 3-methyl-hexahydro-pyrano[3,2-b]pyran-2-one; 19.43:$C_{14}H_{28}$; 23.04:hexadecanoic acid; 26.88(Z)-9-octadecenamide; 28.44: phthalic acid, diisooctyl ester; 30.57:squalene

were unsaturated); olefins (peaks at 13.00 and 15.69 min); and additives (peaks at 23.86 and 24.71 min).

Figure 46 showed DTD-GC-MS total ion chromatogram (without pyrolysis) from the same EVOH sample. Unlike the differences found from HDPE sample, the TIC of EVOH without pyrolysis was similar to its pyrogram in Figure 45. Major compounds were also classified as alcohols (peaks at 4.08 and 9.81 min); aldehyde (peaks at 8.74 min); ketones (peaks at 0.68, 5.44, 6.95, 10.22, 12.22, 15.31, and 16.24 min); olefins (peaks at 3.62, 4.26, 10.97, 11.45, and 19.43 min); and additives (peaks at 26.88 and 28.44 min). Table 4 listed compounds that were identified in both of the chromatograms.

It is reasonable and convenient to generalize the thermal degradation of copolymer (EVOH) from its corresponding homopolymers (polyethylene and polyvinyl alcohol, PVA). Studies (Tsuchiya *et al.*, 1969; Ballisteri *et al.*, 1980; Holland *et al.*, 2001) showed that thermal degradation of PVA comprised of two distinct stages: (1) side-chain elimination of H_2O, and (2) chain-scission reactions leading to the formation of volatile compounds, such as saturated and unsaturated aldehydes and ketones. The two stages can both take place at temperature around 300°C and the activation energy E_a was calculated as 148.35 kJ/mol in stage one and 129.4 kJ/mol in stage two (Shie *et al.*, 2002).

Figure 47 showed PVA thermal degradation schemes. Dehydration reaction in scheme (a) leads to the formation of polyenes and unsaturated alcohols. Tautomerization reaction in scheme (b) leads to the formation of ketone group within the main chain. Scheme (c), (d), and (e) leads to chain scission, particularly formation of aldehyde, alkene, and ester via six-membered transition states. These schemes can account for most of the

Table 4. Compounds present in both Figure 45 (EVOH pyrogram) and Figure 46 (EVOH DTD-GC-MS TIC)*

Compound	Structure	Retention time (min) in Figure 45	Retention time (min) in Figure 46
3,4-dihydro-6-methyl-2H-pyran	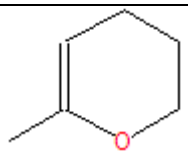	9.56	6.08
(E,E-)-2,4-hexadienal		11.50	8.74
3-hexene-2,5-diol	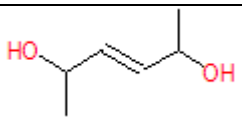	12.14	9.81
4,4-dimethyl-2-cyclopenten-1-one	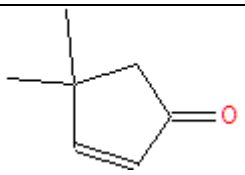	12.50	10.22
2,6-dimethyl-2,4-heptadiene	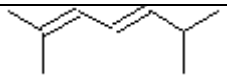	13.00	10.97
2,6-dimethyl-2-trans-6-octadiene	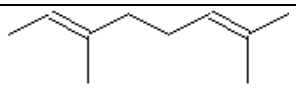	13.33	11.45
3-methyl-hexahydro-pyrano[3,2-b] pyran-2-one	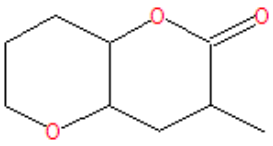	16.53	16.24

* Structural information obtained from NIST library.

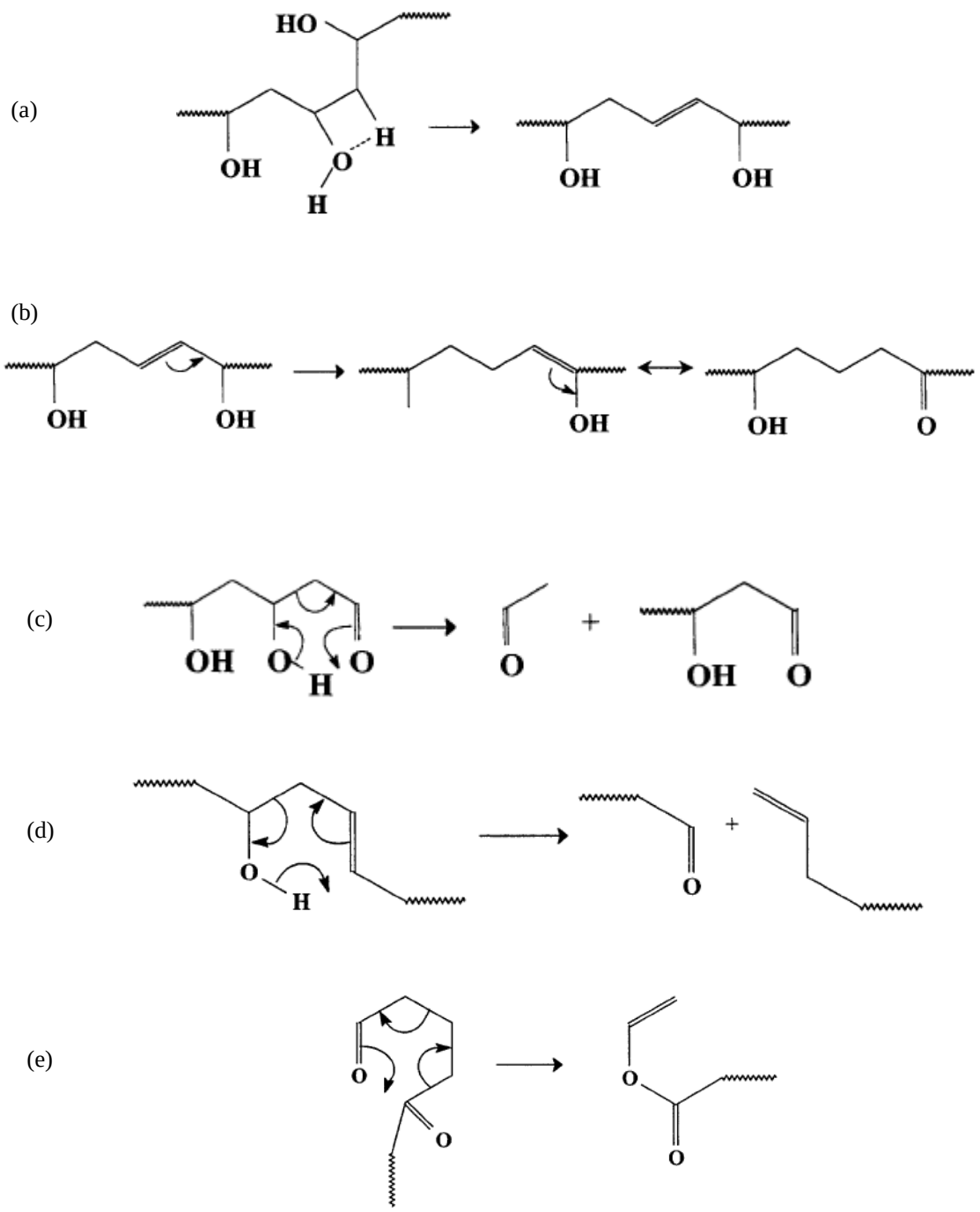

Figure 47. Thermal degradation scheme of PVA polymer (Holland *et al.*, 2001)

(a) side chain elimination (b) keto-enol tautomerization (c) hydrogen transfer leading to depropagation (d) leading to aldehyde and alkene end-group (e) leading to ester or lactone

thermal degradation products identified in Figure 45 and Figure 46.

Ethylene content varies in different EVOH copolymer and study (Alvarez *et al.*, 2003) showed that polyethylene acts as a thermal stabilizer of PVA in EVOH copolymers. This is because the bond dissociation energy for C-C bond in PE degradation (around 340 kJ/mol, according to Mita, 1978) is much bigger than the activation energy in PVA degradation (less than 150 kJ/mol, according to Shie *et al.*, 2002).

Low activation energy in PVA thermal degradation led to the similarity between the pyrogram (Figure 45) and the DTD-GC-MS TIC chromatogram without pyrolysis (Figure 46). The thermal desorption temperature (300°C) alone was sufficient to provide energy required to initiate EVOH thermal decomposition and generate characteristic breakdown products. The more thermally intensive pyrolysis at around 787°C would generate some of the same pyrolysates, and further led to the formation of pyrolysates that need higher activation energy like benzaldehyde found at RT=12.14 min (benzaldehyde formed as a result of cyclization of the intermediate polyene structure and require high temperature above 700°C (Peng *et al.*, 2007; O'Mara, 1970).

From both of the chromatograms diisoocyl phthalate and diocyl adipate (Figure 49) were identified. They are plasticizer additives added during plastic processing with the purpose of rendering flexibility and durability. Diisoocyl phthalate is an all-purpose plasticizer that usually applied to vinyl polymers while diocyl adipate was generally used for resistance to ultraviolet light (from Wikipedia). Another additive found in the chromatogram without pyrolysis was 9-octadecenamide (oleamide, Figure 49). It was added during plastic processing as a slip agent and provided surface lubrication as it

gradually migrated to the surface. Oleamide was not identified from the pyrogram probably because the unsaturated chain was broke down by pyrolysis.

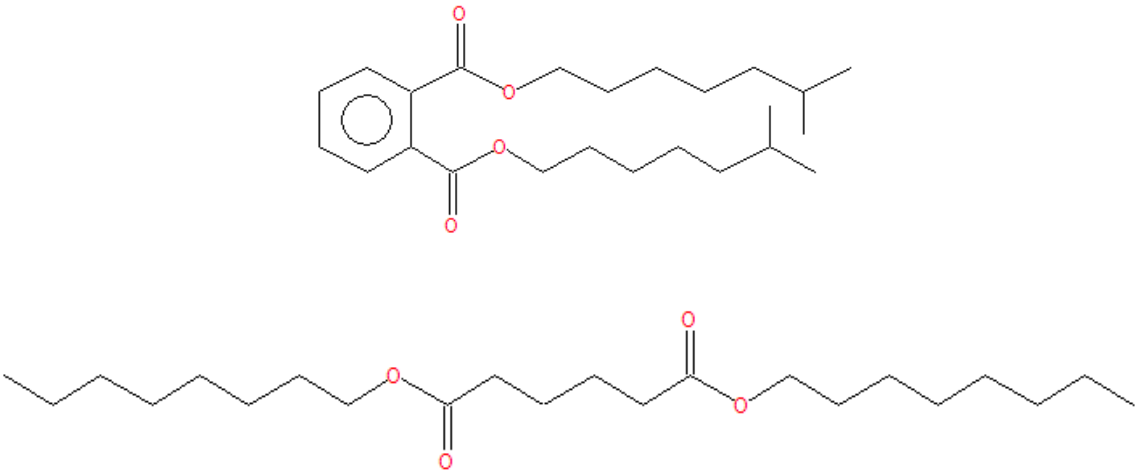

Figure 48. Phthalic acid, diisooctyl ester (DIOP, upper) and hexanedioic acid, dioctyl ester (DOA, bottom) structures (from NIST library)

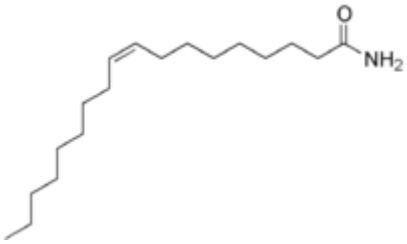

Figure 49. (Z)-9-octadecenamide (oleamide) structure (from Wikipedia)

4. Ethylene Vinyl Acetate (EVA)

Ethylene vinyl acetate (EVA, Figure 50) is the copolymer of ethylene and vinyl acetate and the weight percent of vinyl acetate usually varies from 10 to 40%. EVA copolymers represent the largest-volume segment of the ethylene copolymer market (Odian, 1991). The material has good hot melt adhesive property thus used to make hot glue sticks. EVA foam is used to as padding in equipment for various sports, typically as shock absorber in sports shoes. It is also used in biomedical engineering applications as a drug delivery device for its solubility in organic solvent and inertness.

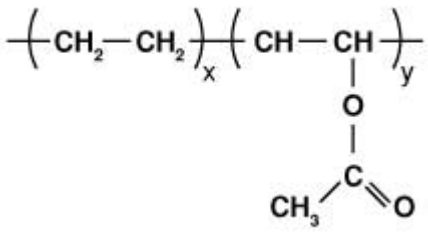

Figure 50. EVA structure
(http://www.polysciences.com/SiteData/poly/assets/product_images/24763.jpg)

The pyrogram of EVA polymer was shown in Figure 51 and Figure 52 (after ten times magnification). In Figure 51 the three most prominent peaks were acetic acid (RT=8.44 min), vinyl acetate (monomer, RT=9.15 min), and butylated hydroxytoluene (BHT, antioxidant additive, RT=17.93 min). On the ten times magnified pyrogram (Figure 52) more peaks showed up and most of them were hydrocarbons such as alkanes and alkenes.

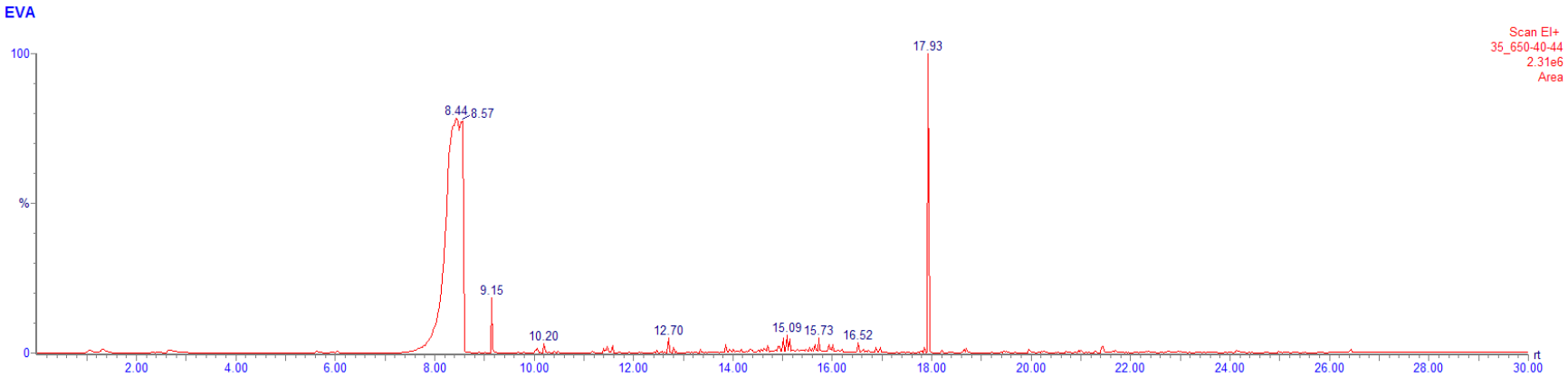

Figure 51. EVA pyrogram

Peaks were identified as: 8.44:acetic acid; 9.15:acetic acid, vinyl ester; 16.52:2-(1,1-dimethylethyl)-4-methyl-phenol (BHT fragment); 17.93:butylated hydroxytoluene (BHT)

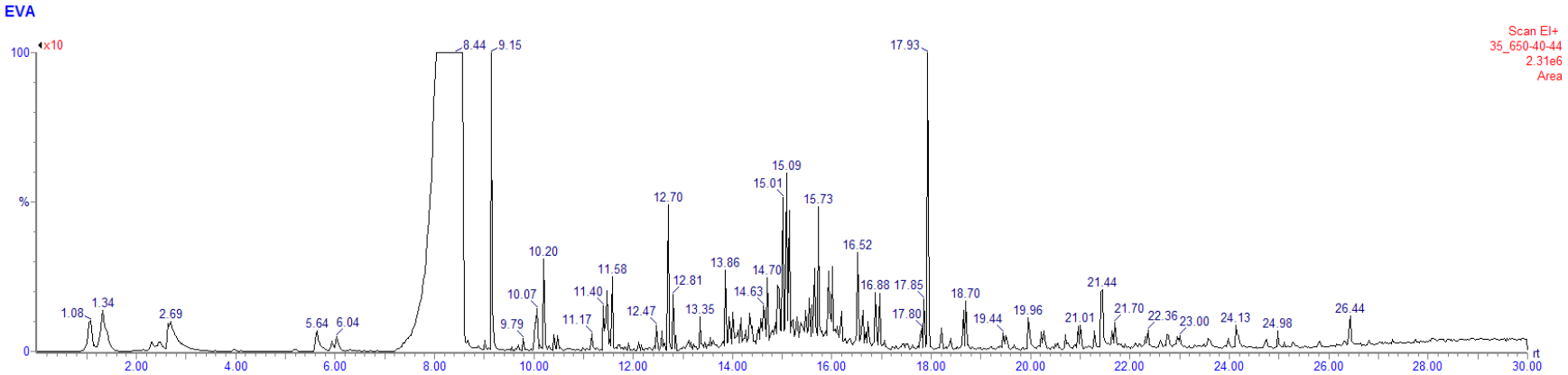

Figure 52. EVA pyrogram (10 X magnified)

Peaks were identified as: 1.08:acetal aldehyde; 1.34:2-butene; 2.69:acetone; 5.64:cyclohexane isomers; 6.04:3-methyl-2-pentene; 7.55 benzene; 10.07:1-octene; 10.20:octane; 11.53: 1-nonene; 11.58:nonane; 12.70:1-decene; 12.81:decane; 13.86:1-undecene; 14.70:undecanal;15.01:dodecane; 15.09:dodecanal; 15.73:7-methyl-tridecane; 16.96:tetradecane; 18.70:hexadecane; 19.96:tetrahexadecanoic acid; 20.95: phosphonic acid, dioctadecyl ester; 21.44:hexadecanoic acid; 26.44:squalene

Similar to the other ethylene copolymer EVOH discussed in the previous section, the thermal decomposition of EVA copolymer is composed of two steps: (1) side chain elimination, or deacetylation by way of a six-membered ring transition state (Figure 53, Edward *et al.*, 1963) and leaves an acetylene-ethylene copolymer p(AC-E) (Figure 53, Marcilla *et al.*, 2005) and (2) decomposition of the p(AC-E) leads to formation of alkanes, alkenes, and mononuclear aromatic compounds (Figure 54, Marcilla *et al.*, 2005, Camino *et al.*, 2000). The pyrolysates identified from pyrogram, including acetic acid, short chain alkanes (octane, nonane, decane, dodecane, *etc*.), alkenes (2-butene, 1-octene, 1-nonene, 1-decene, 1-undecene, *etc*.), and benzene, provided strong support to this two-step thermal decomposition theory.

Chain scission reaction in the unsaturated p(AC-E) chain is different for that in saturated polyethylene chain. The existence of C=C bond in the p(AC-E) chain lowers the C-H bond dissociation energy (via the formation of resonance structures in Figure 54) thus facilitates the formation of radical series. Activation energy studies showed the same conclusion. Angela *et al.*, in 2003 found that the activation energy of the deacetylation step in EVA copolymer (18% vinyl acetate percentage) decomposition was around 156 kJ/mol and for the chain scission step activation energy was around 265 kJ/mol, which is much smaller than the 340 kJ/mol of bond disassociation energy for C-C bond in polyethylene chain (Mita, 1978). The difference in activation energy may also indicate that the temperature required for PVA pyrolysis would not be as high as the temperature required for polyethylene pyrolysis.

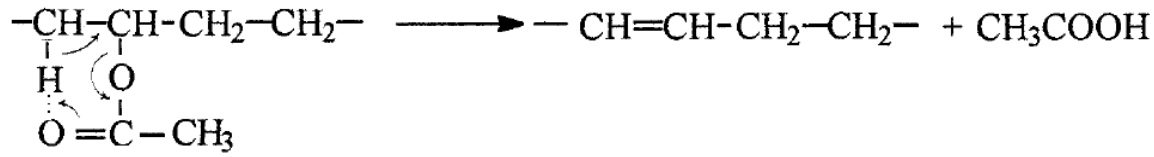

Figure 53. Scheme for the first step of EVA decomposition-deacetylation (Edward *et al.*, 1963)

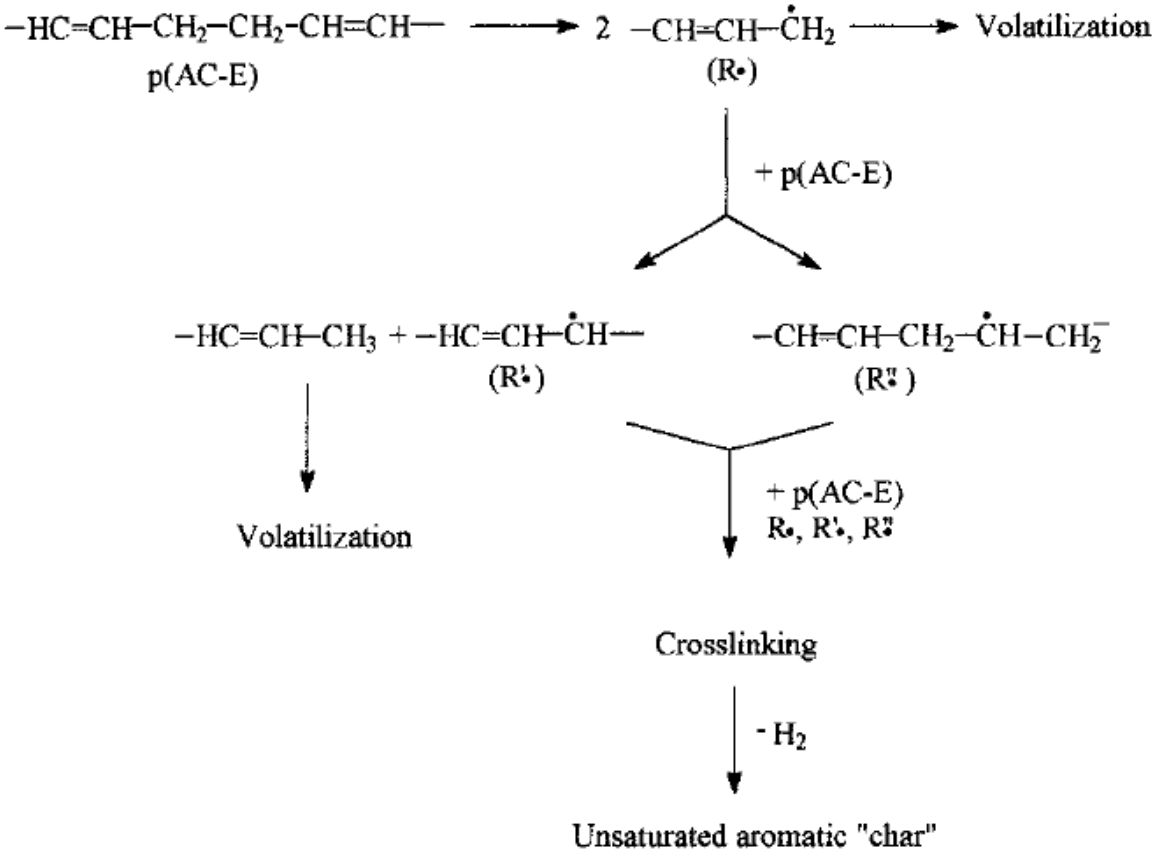

Figure 54. Scheme for the second step of EVA decomposition-chain scission (Camino *et al.*, 2000)

Dioctadecyl phosphite (Figure 55) was identified in pyrogram at RT=20.95 min. It is an essential stabilize used in synthetic polymers to improve polymer hydrolytic stability against high humidity or temperature, particularly used in PVA polymers in our study to prevent conversion to polyethylene vinyl alcohol via hydrolysis. A large amount of BHT (butylated hydroxytoluene, Figure 56) was identified at RT=17.93 min, which was added as a resin stabilizer.

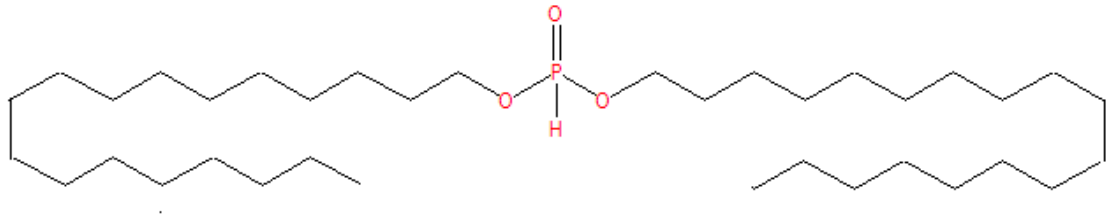

Figure 55. Dioctadecyl phosphite structure (from NIST library)

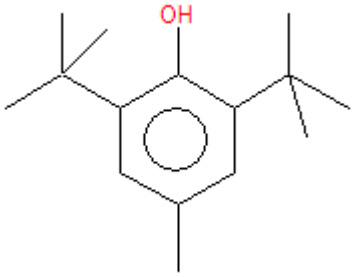

Figure 56. BHT (butylated hydroxytoluene) structure (from NIST library)

5. Polyethylene Terephthalate (PET)

Polyethylene Terephthalate (PET) is a thermoplastic polyester resin and is used in food and beverage containers and synthetic fibers. PET can be synthesized by the esterification reaction between terephthalic acid and ethylene glycol with water as a byproduct (Figure 57), or by transesterification reaction between ethylene glycol and dimethyl terephthalate with methanol as a byproduct. The PET industry makes up about 18% of world polymer production and is third after polyethylene and polypropylene.

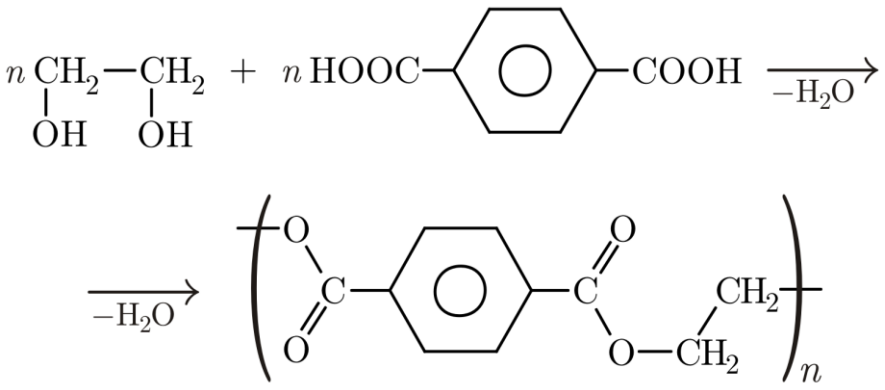

Figure 57. PET structure and synthesis
(http://upload.wikimedia.org/wikipedia/commons/a/a4/PETreakcia.png)

The pyrogram of PET was shown is Figure 58. Among all those identified peaks benzoic acid vinyl ester (RT=14.37 min, Figure 59-a), benzoic acid (RT=14.68 min, Figure 59-b), terephthalic acid divinyl ester (RT=18.43 min, Figure 59-c), terephthalic acid monovinyl ester (RT=18.77 min, Figure 59-d), and the dimer (RT=27.45 min, Figure 59-e) were of structural importance.

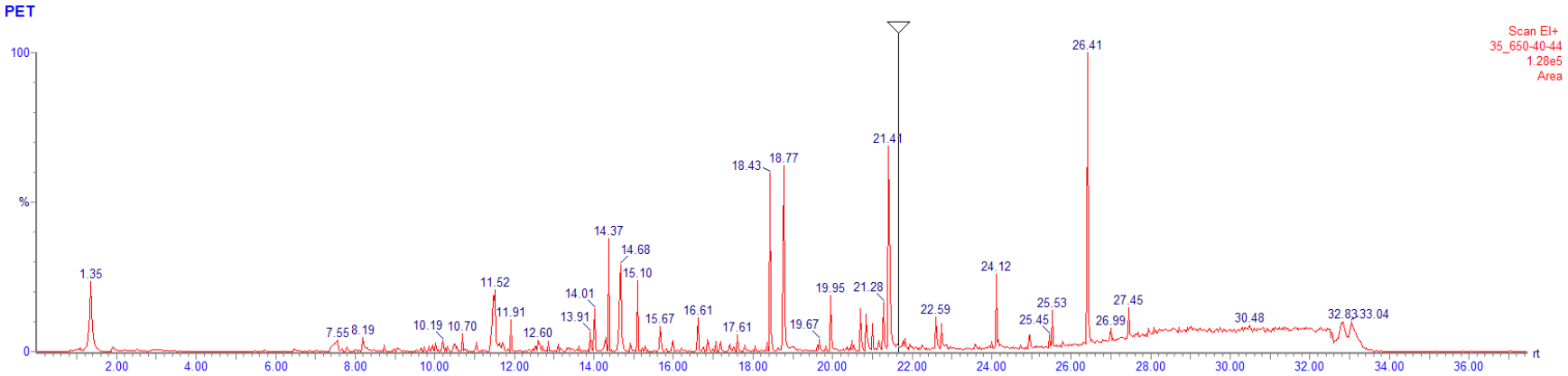

Figure 58. PET pyrogram

Peaks were identified as: 1.35:acetal aldehyde; 7.55:acetic acid; 10.70:3-furaldehyde; 11.52: butanediol isomers; 14.01:nonanal; 14.37:benzoic acid vinyl ester; 14.68:benzoic acid; 15.10:decanal; 18.43:terephthalic acid divinyl ester; 18.77: terephthalic acid monovinyl ester (monomer); 19.95:tetradecanoic acid; 21.41:hexadecanoic acid; 24.12:hexanedioic acid, dioctyl ester; 24.96:phthalic acid, diisooctyl ester; 26.41:squalene; 26.99:cholesterol; 27.45: CH_2=CH-O-CO-Ph-CO-O-CH_2-CH_2-O-CO-Ph-CO-OH, (dimer, MW=384)

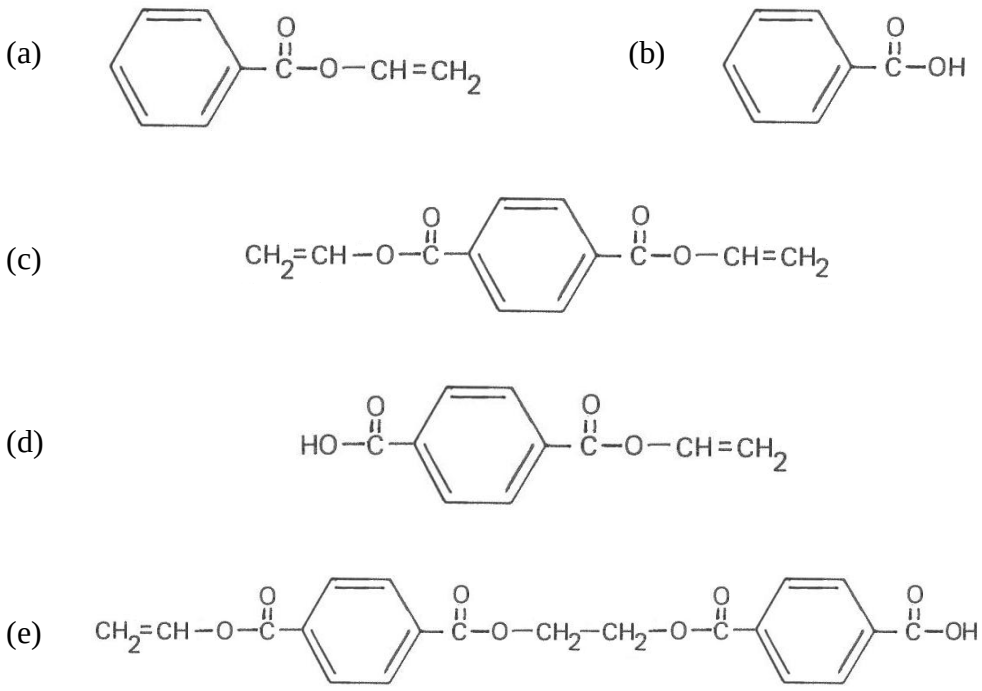

Figure 59. PET pyrolysates of structural importance

(a) vinyl benzoate (b) benzoic acid (c) divinyl terephthalate (d) monovinyl terephthalate, monomer (e) dimer

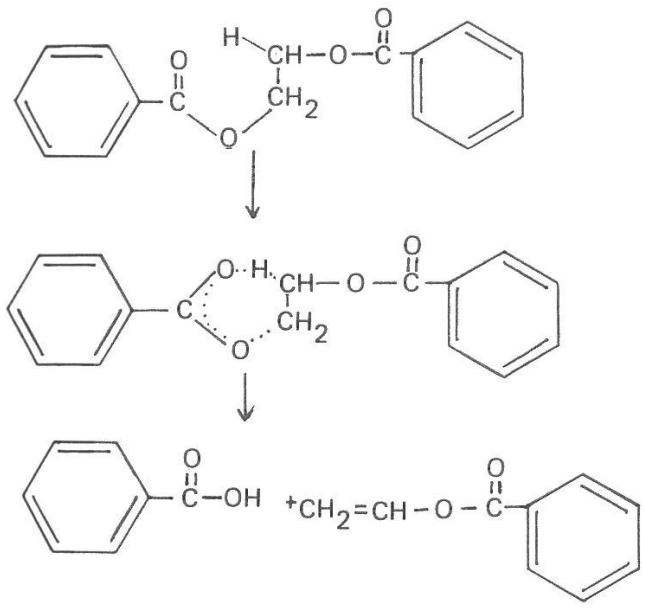

Figure 60. PET decomposition mechanism (Liebman *et al.*, 1982)

Thermal decomposition of PET polymer follows a mechanism shown in Figure 60 (Liebman *et al.*, 1982) to give acids and olefins which involves a cyclic transition state. Luderwald in 1977 carried out a PEIMS (pyrolysis-electron ionization MS) experiment to study the degradation of PET and products were shown in Table 5. All the positive molecular ions Luderwald obtained were in line with Liebman's decomposition mechanism.

Table 5 Pyrolysis products of PET (Luderwald *et al.*, 1977)

m/z	Fragment ion
917	HO(-CO-Ph-CO-O-CH_2-CH_2-O)$_4$-CO-Ph-C≡O
725	HO(-CO-Ph-CO-O-CH_2-CH_2-O)$_3$-CO-Ph-C≡O
577	HO(-CH_2-CH_2-O-CO-Ph-CO-O)$_2$-CH_2-CH_2-O-CO-Ph-C≡O
533	HO(-CO-Ph-CO-O-CH_2-CH_2-O)$_2$-CO-Ph-C≡O
489	Ph(-CO-O-CH_2-CH_2-O-CO-Ph)$_2$-C≡O
445	Ph-CO-O-CO-Ph-CO-O-CH_2-CH_2-O-CO-Ph-C≡O
385	HO-CH_2-CH_2-O-CO-Ph-CO-O-CH_2-CH_2-O-CO-Ph-C≡O
367	CH_2=CH-O-CO-Ph-CO-O-CH_2-CH_2-O-CO-Ph-C≡O
341	HO-CO-Ph-CO-O-CH_2-CH_2-O-CO-Ph-C≡O
297	Ph-CO-O-CH_2-CH_2-O-CO-Ph-C≡O
193	HO-CH_2-CH_2-O-CO-Ph-C≡O
175	CH_2=CH-O-CO-Ph-C≡O
149	HO-CO-Ph-C≡O
132	O=C-C_6H_4-C≡O
105	Ph-C≡O

In our study the structure identification of the five listed PET pyrolysates were shown in Figure 61 to Figure 63. Vinyl benzoate and benzoic acid were confirmed by comparing structure with the data in NIST library (Figure 61), while divinyl terephthalate, monovinyl terephthalate, and dimer structures were confirmed from their fragment ions (Figure 62 and 63). The identified pyrolysates structures all possessed acid groups or vinyl ester groups and confirmed the thermal decomposition theory proposed by Liebman.

Plasticizers (hexanedioic acid, dioctyl ester and phthalic acid, diisooctyl ester) were found in the PET polymer sample. These two plasticizers are generally added to polyethylene copolymers during processing.

Mass spectrum at RT=14.37 min

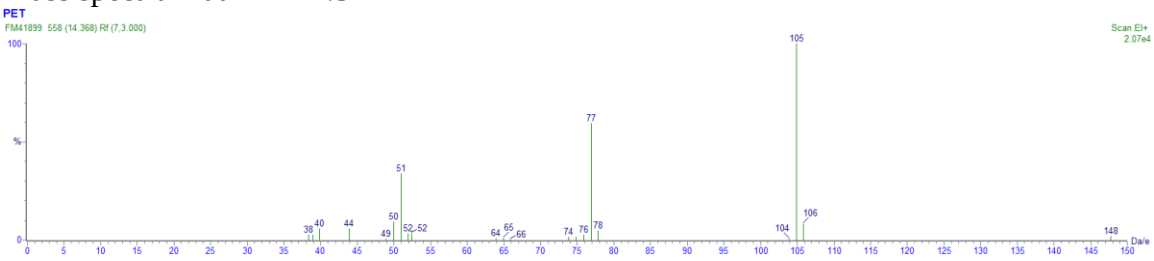

Mass spectrum of vinyl benzoate from NIST library

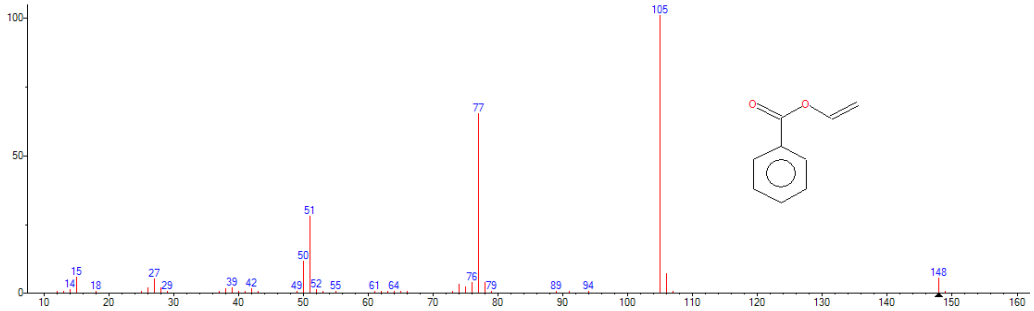

Mass spectrum at RT=14.68 min

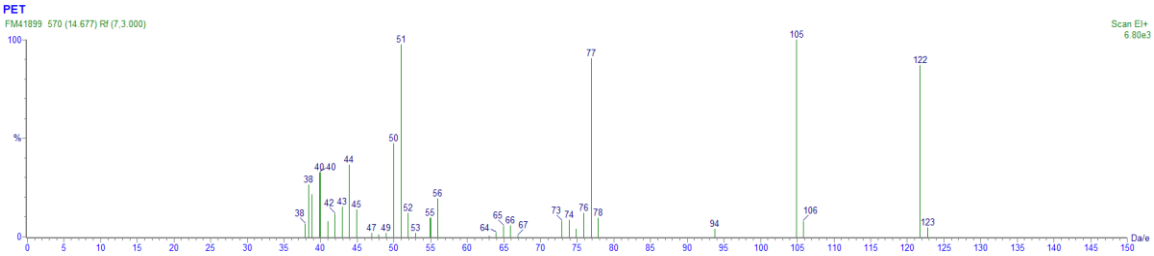

Mass spectrum of benzoic acid from NIST library

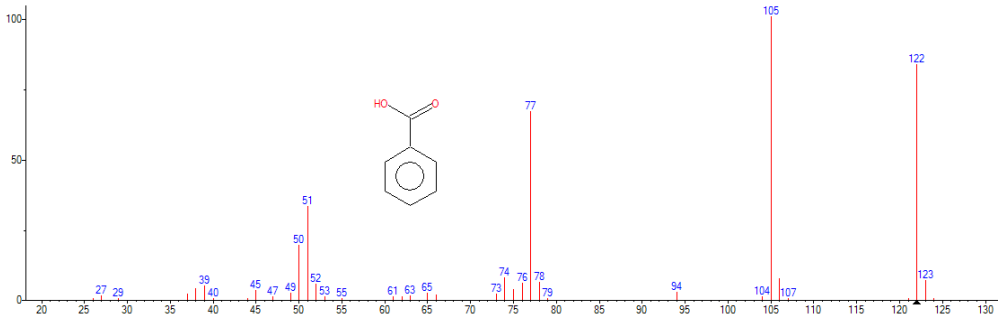

Figure 61. Structure identification of vinyl benzoate (upper) and benzoic acid (bottom)

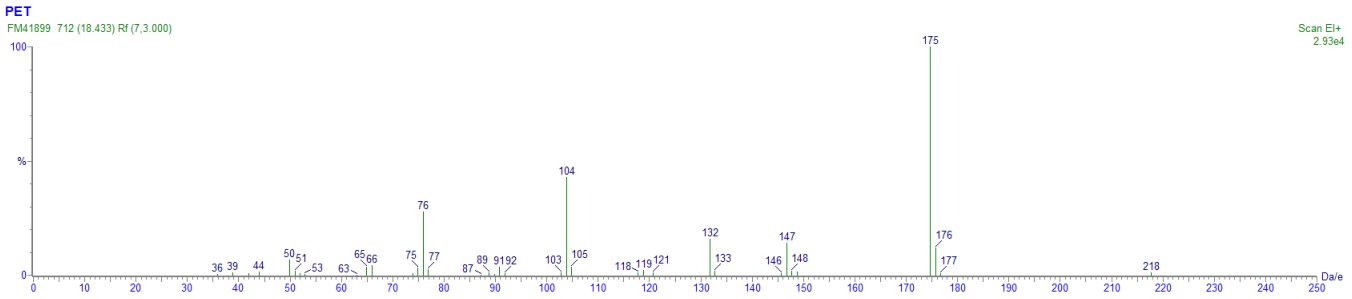

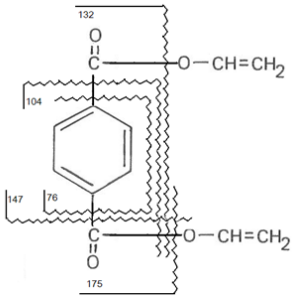

MW=218

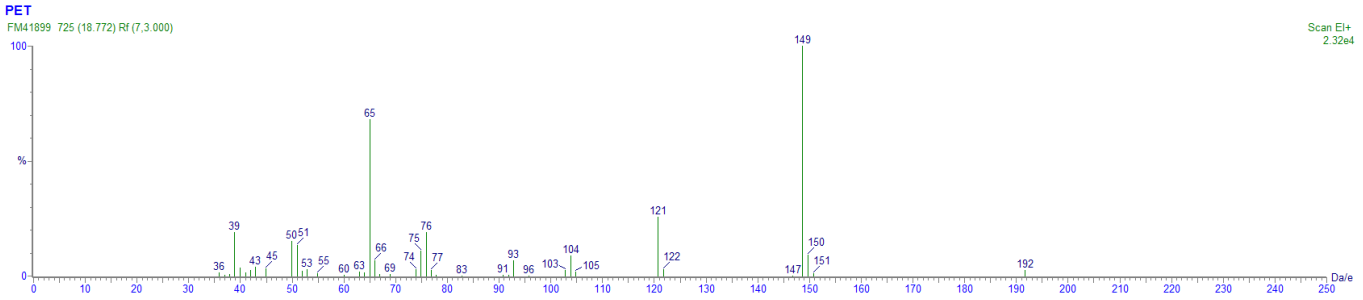

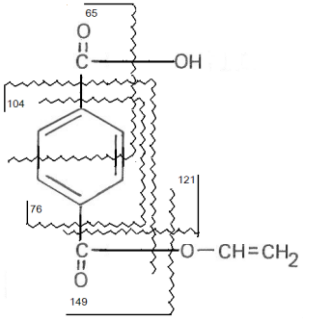

MW=192

Figure 62. Structure identification of divinyl terephthalate (upper) and monovinyl terephthalate (bottom)

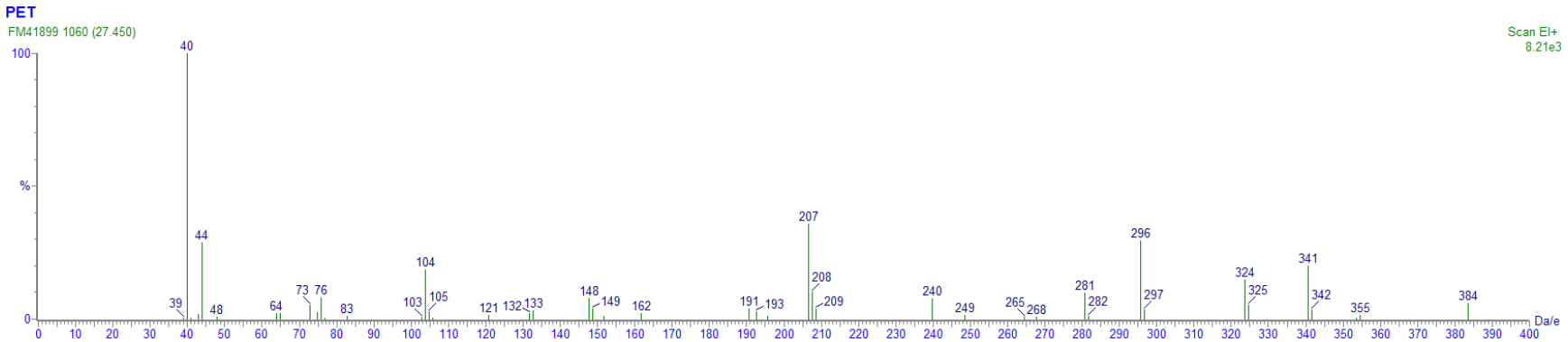

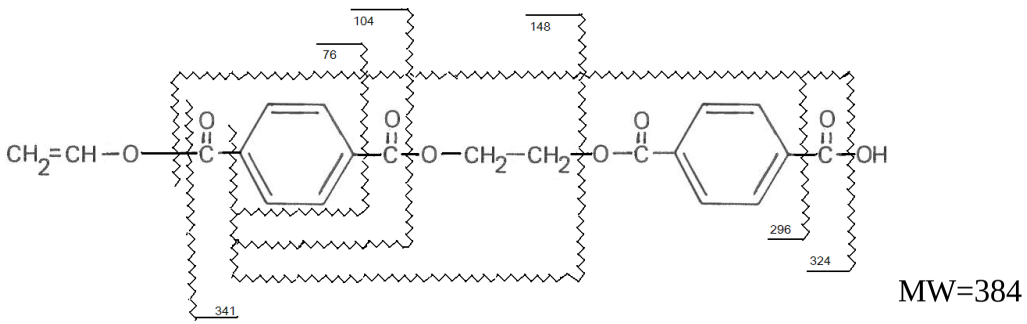

MW=384

Figure 63. Structure identification of PET dimer

VI. CONCLUSION

A new pyrolysis unit was built in our study by integrating the pyrolysis probe from an existing Pyroprobe® 100 pyrolyzer to a Short Path Thermal Desorption system. Engineering requirements on safety, function, and cost efficiency was fulfilled through the entire design and development process. The new pyrolysis unit is expected to demonstrate superiority over its predecessor Pyroprobe® 100, particularly it should combine the features of Short Path Thermal Desorption, have a quick setup, not be prone to injector contamination, be easily moveable and transferable, accurate and precise.

Five model polymers (virgin HDPE, PS, EVOH, EVA, and PET) were subjected to pyrolysis-GC-MS study for validation of the new pyrolysis unit. Conclusion from the study can be drawn as following:

- Setup of the new pyrolysis-GC-MS system took less than 10 minutes and no tools or connectors were involved, proving the new pyrolysis unit is easy to setup and not dedicated to GC injection port.
- From the resulting pyrograms monomers, dimers, and other thermal decomposition products were clearly identified (Table 6) and can be properly explained by prevailing thermal degradation mechanisms, proving the feasibility of the new unit in carrying out polymer microstructure study.
- From the resulting pyrograms different additives were also identified, proving the ability of the new unit in recycled resin analysis.
- No carryovers were found between injections, proving the new pyrolysis unit is free from sample to sample cross contamination.

- Peaks on pyrograms were all needle-sharp and well-resolved at very low sample amount (50 μg), proving the new pyrolysis unit is extremely sensitive and has excellent sample transfer ability.
- Disassembly process after pyrolysis study was equally effortless as setup, proving the new pyrolysis unit is easily removable and transferable.

In summary, the new developed pyrolysis unit has inherited all the excellent features from Short Path Thermal Desorption system yet retaining pyrolysis functionality from Pyroprobe®. The instrumentation development is proved successful and should promote analytical pyrolysis study in synthetic polymers.

Table 6 Polymer pyrolysis study summary

Polymer	Important pyrolysates	Additives
Virgin HDPE	Ethylene, hydrocarbon triplets	N/A
PS	Styrene, benzene ethenyl-dimer, benzene ethenyl-trimer	2-methyl butane[1], DIOP[2], DOA[3]
EVOH	Acetaldehyde, acetone, benzaldehyde,	DIOP, DOA, oleamide[4]
EVA	Acetic acid, vinyl acetate, benzene, alkanes, alkenes	DNOP[5], BHT[6]
PET	Vinyl benzoate, benzoic acid, monovinyl terephthalate, divinyl terephthalate, PET dimer	DIOP, DOA

1. Blowing agent
2. Phthalic acid, diisooctyl ester, plasticizer
3. Hexanedioic acid, dioctyl ester, plasticizer
4. (Z)-9-octadecenamide, slip agent
5. Dioctadecyl phosphite, stabilizer
6. Butylated hydroxytoluene, stabilizer

VII. REFERENCES

Alvarez, V. A., Ruseckaite, R. A., Vazquez, A. Kinetic analysis of thermal degradation in poly(ethylene-vinyl alcohol) copolymers. *Journal of Applied Polymer Science*, 2003, 90, 3157-3162.

Anderson, E. M., Ericsson, I. Samples from ng to mg in pyrolysis—gas chromatograph. *Journal of Analytical and Applied Pyrolysis*, 1980, 2(2), 97-107. (From Liebman, 1984)

Angela, N. G., Rafael, F. Thermogravimetric kinetic model of the pyrolysis and combustion of an ethylene-vinyl acetate copolymer refuse. *Fuel*, 2004, 83, 1165-1173.

Ballisteri, A., Foti, S., Montaudo, G., and Scamporrino, E. Evolution of aromatic compounds in the thermal decomposition of vinyl polymers. *Journal of Polymer Science Part A-Polymer Chemistry*, 1980, 18, 1147. (From Liebman, 1984)

Bayer, F. L. *Pyrolysis Gas Chromatography Investigations of Enzymes, Hemoglobins, and Steroids*. Ph. D. Dissertation, Emory University Atlanta, GA, 1976. (From Liebman, 1984)

Berezkin, V. G., Alishoyev, V. R., Nemirouskaya, I. B. *Gas Chromatography of Polymers*. Elsevier, Amsterdam, Netherland, 1977, 223p.

Camino, G., Sgobbi, R., Zaopo, A., Colombier, S., and Scelza, C. Investigation of flame retardance in EVA. *Fire and Materials*, 2000, 24, 85-90.

Edward, M. B., Roger, S. P., and Julian, F. J. Gas chromatographic analysis of poly(ethylene ethyl acrylate) and poly(ethylene Vinyl Acetate) pyrolyzates. *Analytical Chemistry*, 1963, 35, 73-76.

Exner, J., Seeger, M., Cantow, H. J. Macromolecular colloquium. *Angewandte Chemie, International Edition*, 1971, 10, 345. (From Liebman, 1984)

Faravelli, T., Bozzano, G., Scassa, C., Perego, M., Fabini, S., Ranzi, E., and Dente, M. Gas product distribution from polyethylene pyrolysis. *Journal of Analytical and Applied Pyrolysis*, 1999, 52, 87-103.

Freeman, R. R. *High Resolution Gas Chromatography, 2nd Edition*. Hewlett-Packard Company. 1981, 197p.

Giacobbo, H., Simon, W. Methodik zur pyrolyse und anschlie benden gaschromatographischen analyse von probemengen unter einem mikrogramm. *Pharmaceutica Acta Helvetiae,* 1964, 39, 162. (From Liebman, 1984)

Hanson, R. L., Vanderborgh, N. E., Brookins, D. G. Characterization of coal by laser pyrolysis gas chromatography. *Analytical Chemistry*, 1977, 49, 390. (From Liebman, 1984)

Hartman T. G., Karmas, K., Chen, J., Shevade, A., Deagro, M., and Hwang, H.-I. Determination of vanillin, other phenolic compounds and flavors in vanilla beans by direct thermal desorption-gas chromatography and gas chromatography-mass spectrometry. In *Phenolic Compounds in Food and Health I*, C.-T. Ho, C. Y. Lee, and M.-T. Huang(Ed.). ACS Symposium Series. Washington, DC. 1992.

Hartman, T. G., Lech, J., Fukuda, E., and Rosen, R. T. Methodologies for the quantification of purge and trap thermal desorption and direct thermal desorption analyses. *Mass Spectrometry Source,* 1991, XIV (3), 18-23.

Hartman T. G., Lech, J., Karmas, K., Salinas, J., Rosen, R. T., and Ho, C.-T. *Flavor characterization using adsorbent trapping-thermal desorption or direct thermal desorption-gas chromatography and gas-chromatography-mass spectrometry* in Ho, C.-T., Manley, C. H. *Flavor Measurement*. M. Dekker, 1993, Chapter 2, 37-60.

Hartman, T.G., Lech, J., and Rosen, R. T. Breath analysis of garlic-borne phytochemicals in human subjects by combined adsorbent trapping, short path thermal desorption GC-MS. In *Proceedings of the 39th ASMS Conference on Mass Spectrometry and Allied Topics*, 1991, 641-642.

Hartman, T. G., Overton, S., Manura, J., Baker, C. W., and Manos, J. N. Short path thermal desorption: Food science applications. *Food Technol*ogy, 1991, 45(7), 104-105.

Holland, B. J. and Hay, J. N. The thermal degradation of poly(vinyl alcohol). *Polymer*, 2001, 42, 6775-6783.

Hummel, D. O. *Polymer Spectroscopy*. Hummel, D. O., Editor, Verlag Chemie. (From Liebman, 1984)

Jones, C. E. R., and Reynolds, G. E. J. The contribution of integrated pyrolysis/gas chromatography to the elucidation of polymer microstructure. *Journal of Gas Chromatography*. 1967, 5, 25.

Liebman, S. A., Ahlstrom, D. H., Starnes, W. H., Schilling, F. C. *Journal of Macromolecular Science – Chemistry*, 1982, A-17(6), 935. (From Liebman, 1984)

Liebman, S. A., and Hassan, A. "Microstructure and analysis" in *Plastics Polymer Science & Technology*, Ed. M. Baijal, John Wiley & Sons, 1982. (From Liebman, 1984)

Liebman, S. A., Levy, E. J. *Pyrolysis and GC in Polymer Analysis*. Oxford, Pennsylvania: Marcel Dekker, Inc. 1984, 557p.

Luderwald, I., Urrutia, H. *Analytical Pyrolysis* (C. E. R. Jones, and C. A. Cramers, Editors) Elsevier Scientific Publishing Co., Amsterdam, 1977. (From Liebman, 1984)

Marcilla, A., Gonez, A., Menargues, S. TG/FTIR study of the thermal pyrolysis of EVA copolymers. *Journal of Analytical and Applied Pyrolysis*, 2005, 74, 224-230.

Merritt, C., Robertson, D. H. The analysis of proteins, peptides and amino acids by pyrolysis-gas chromatography and mass spectrometry. *Journal of Gas Chromatography*, 1967, 5, 96.

Meuzelaar, H. L. C., Haverkamp, J., Hileman, F. D. *Curie-Point Pyrolysis Mass Spectrometry of Recent and Fossil Biomaterials*, *Compendium and Atlas*, Elsevier, Amsterdam, Netherland, 1982.

Mita, I., In Aspects of Degradation and Stability of Polymers (H. H. G. Jellinek, ed.), Elsevier, Amsterdam, 1978, 248p. (From Liebman, 1984)

Noffz, D., Benz, W., Pfab, W. Untersuchung yonhochpolymeren mittels pyrolyse--gas-chromatographie. *Z. Analytical Chemistry*, 1968, 235, 121. (From Liebman, 1984)

Odian, G. *Principles of Polymerization*, 3rd ed. John Wiley & Sons, New York, 1991. 812p

O'Mara, M. M. High-temperature pyrolysis of poly(vinyl chloride): Gas chromatographic-mass spectrometric analysis of the pyrolysis products from PVC resin and plastisols. *Journal of Polymer Science*, 1970, 8, 1887. (From Liebman, 1984)

Peng, Z., Kong, L. X. A thermal degradation mechanism of polyvinyl alcohol/silica nanocomposites. *Polymer Degradation and Stability*, 2007, 92, 1061-1071.

Raghavan, S. K., *Characterization and differentiation of food proteins by pyrolysis-gas chromatography/mass spectrometry*. Thesis (Ph. D.)--Rutgers University, 1985.

Schomburg, G., Behlau, H., Dielmann, R., Weeke, F., and Husmann, H. Sampling techniques in capillary gas chromatography. *Journal of Chromatography*, 1977, 142, 87. (From Liebman, 1984)

Shie, J. L., Chen, Y. H., Chang, C, Y., Lin, J. P., Lee, D. J., and Wu, C. H. Thermal pyrolysis of poly(vinyl alcohol) and its major products. *Energy & Fuels*, 2002, 16, 109-118.

Simon, W., Giasccobbo, H. Thermal fragmentation and the determination of the structure of organic compounds. *Angewandte Chemie, International Edition*. 1965, 4, 938. (From Liebman, 1984)

Smith, R. M., Shawkat, S. A., Hayes, W. P. Pyrolysis-gas chromatography of proline, hydroxyproline and related peptides. *Analyst*, 1980, 105, 1176. (From Liebman, 1984)

Stern, N. J., Kotula, A. W., and Pierson, M. D. Differentiation of selected enterobacteriaceae by pyrolysis-gas-liquid chromatography. *Applied and Environmental Microbiology*, 1979, 12, 1098-1102.

Stern, N. J., Kotula, A. W., and Pierson, M. D. Virulence prediction of *Yersinia enterocolitica* by pyrolysis gas-liquid chromatography. *Applied and Environmental Microbiology*, 1980, Sept, 646-651.

Steward, W. D. Jr., Pyrolysis-gas chromatographic analysis of automotive paints, *Journal of Forensic Science*, 1974, 19, 121-129. (From Liebman, 1984)

Sugimura, Y., Tsuge, S. Pyrolysis-hydrogenation glass capillary gas chromatographic characterization of polyethylenes and ethylene-α-olefin copolymers. *Macromolecules*, 1979, 12, 512.

Tsuchiya, Y., Sumi, K. Thermal decomposition products of polyisobutylene. *Journal of Polymer Science Part A-Polymer Chemistry*, 1969, 7, 813. (From Liebman, 1984)

Vollmin, J., Kriemler, P., Omura, I., Seible, J., Simon, W. Structural elucidation with a thermal fragmentation—Gas chromatography—Mass spectrometry combination. *Journal of Microchemical*, 1966, 11, 73. (From Liebman, 1984)

Walker, J. Q. Pyrolysis gas chromatographic correction trials of the American society for testing and materials. *Journal of Chromatographic Science*, 1977, 15, 267.

Walker, J. Q., Jackson, M. T., Maynard, J. B. *Chromatographic system maintenance and troubleshooting.* Academic Press, NY, 1972, Chapter 9. 359p. (From Liebman, 1984)

Wall, K. A., Madorsky, S. L., Brown, D. W., Straus, S., Simka, R. The depolymerization of polymethylene and polyethylene. *Journal of American Chemistry Society*, 1954, 76, 3430. (From Liebman, 1984)

Wolf, C. J., Levy, R. L., Fanter, D. L. Temperature rise time and true pyrolysis temperature in pulse mode pyrolysis gas chromatography. *Analytical Chemistry*, 1972, 44, 38. (From Liebman, 1984)